STREAM NETWORK ANALYSIS AND GEOMORPHIC FLOOD PLAIN MAPPING FROM ORBITAL AND SUBORBITAL REMOTE SENSING IMAGERY

APPLICATION TO FLOOD HAZARD STUDIES IN CENTRAL TEXAS

by

Victor R. Baker[1]
Robert K. Holz[2]
Steven D. Hulke[1]
Peter C. Patton[1]
Margarida M. Penteado[3]

1
Department of Geological Sciences, The University of Texas at Austin, Austin, Texas 78712

2
Department of Geography, The University of Texas at Austin, Austin, Texas 78712

3
Faculdade de Filosofia, Ciencias e Letras, Rio Claro, Sao Paulo, Brazil

Final Project Report for the National Aeronautics and Space Administration
EREP No. 064B; NASA Contract No. 9-13312
30 April 1975

Acknowledgements

The Water Resources Research Center, Purdue University, made available computer programs for watershed analysis. J. Boone and R. M. Looney assisted with the field mapping of drainage basins. Martin L. Miller and Victor Mazade greatly aided the research on this grant by solving numerous administrative problems and by showing a general cooperative spirit and willingness to help with certain technical problems. This final report would not have been ready nearly so soon without their hard work and help.

CONTENTS

Page

ILLUSTRATIONS

TABLES

INTRODUCTION

Flood hazard evaluation can be approached from two viewpoints. An "upstream" approach would consist of evaluating the interaction of rainfall inputs and physiographic factors in producing flood responses on small watersheds. A "downstream" approach would map flood hazard zones in the broad alluvial valleys which rivers develop after collecting the flow of numerous tributaries. In this report, we have attempted to apply remote sensing imagery to both aspects of the flood hazard evaluation problem.

This report has two general parts. The first part concerns upstream controls through a discussion of the adjustment of stream network geometry to climatic and geologic factors. Morphometric attributes of drainage basins are used to compare probable flood responses. The objectives of this aspect of the study included the following: (1) evaluation of various remote sensing imagery formats for interpretation of watershed drainage networks, (2) determination of quantitative geomorphic parameters for several small central Texas drainage basins to find the effect that rock and soil type have on drainage network development, and (3) correlation of quantitative geomorphic parameters with estimates of flood peak discharge and other indices of runoff.

The second part of the report concerns downstream flood problems through a discussion of flood plain mapping techniques. This aspect of the study was not embodied in the original work plan. Rather, it developed when we discovered that both the orbital and suborbital remote sensing imagery were very useful for the mapping of certain flood susceptibility indicators. When used for this purpose, even orbital remote sensing imagery was found

to possess many advantages over large-scale topographic maps.

Location and Physiography

Austin is situated in central Texas at lat 30°15' N.; long 97° 42' W., or almost at the nadir of ground track 34 of the orbiting skylab workshop. The city occupies a more or less central position in the vaguely defined geographic region of the state known as central Texas. Austin is the focal area for this study (Figure 1).

Central Texas includes parts of two major physiographic provinces (Hunt, 1967). Physiographically it grades from the gently sloping and undulating Gulf Coastal Plains in the south and southeast to the uplifted and dissected Edwards Plateau in the north and northwest. The plateau, which is underlain by interbedded, soft limestone, dolomite and marl, has been deeply eroded to produce the steep slopes of the "Texas Hill Country," which physiographically is the southeastwardmost extension of the Great Plains. The boundary between these two physiographic provinces is marked by a sharp change in elevation at the 500 foot contour line (Atwood, 1940). This topographic break is the surface expression of an old and inactive fault which stretches in an arcuate curve from near Del Rio, Texas on the border with Mexico, through San Antonio, Austin, and Dallas to the Red River and beyond into Oklahoma (Weeks, 1945). This escarpment marks the Balcones Fault Zone (Deussen, 1924). Regionally then, the topographic slope in central Texas is from the northwest to the south, and southeast. Precipitation falling on the "Hill Country" to the north and west collects in basins which discharge across the escarpment into the major drainage channels of the Gulf Coastal Plain, such as the Guadalupe, Colorado, Brazos, and Trinity.

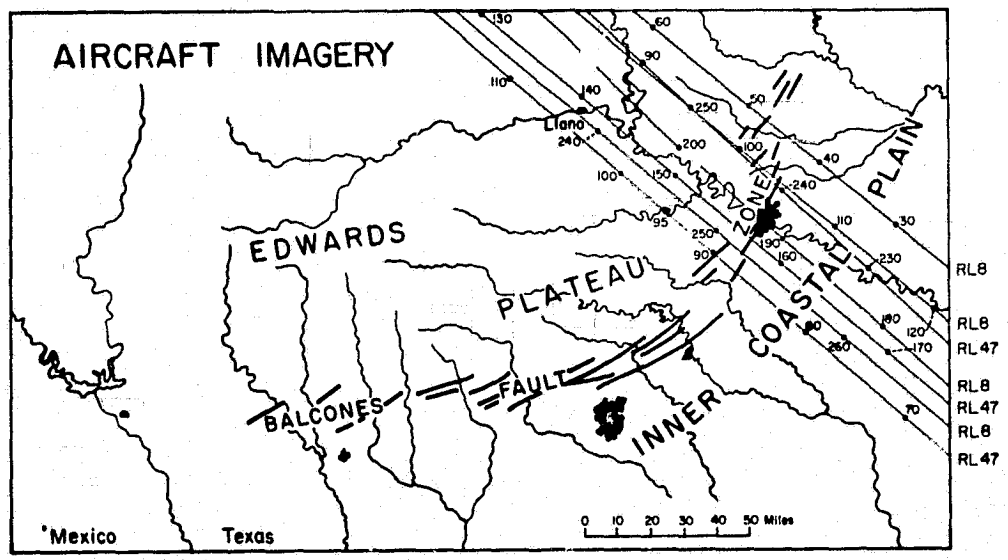

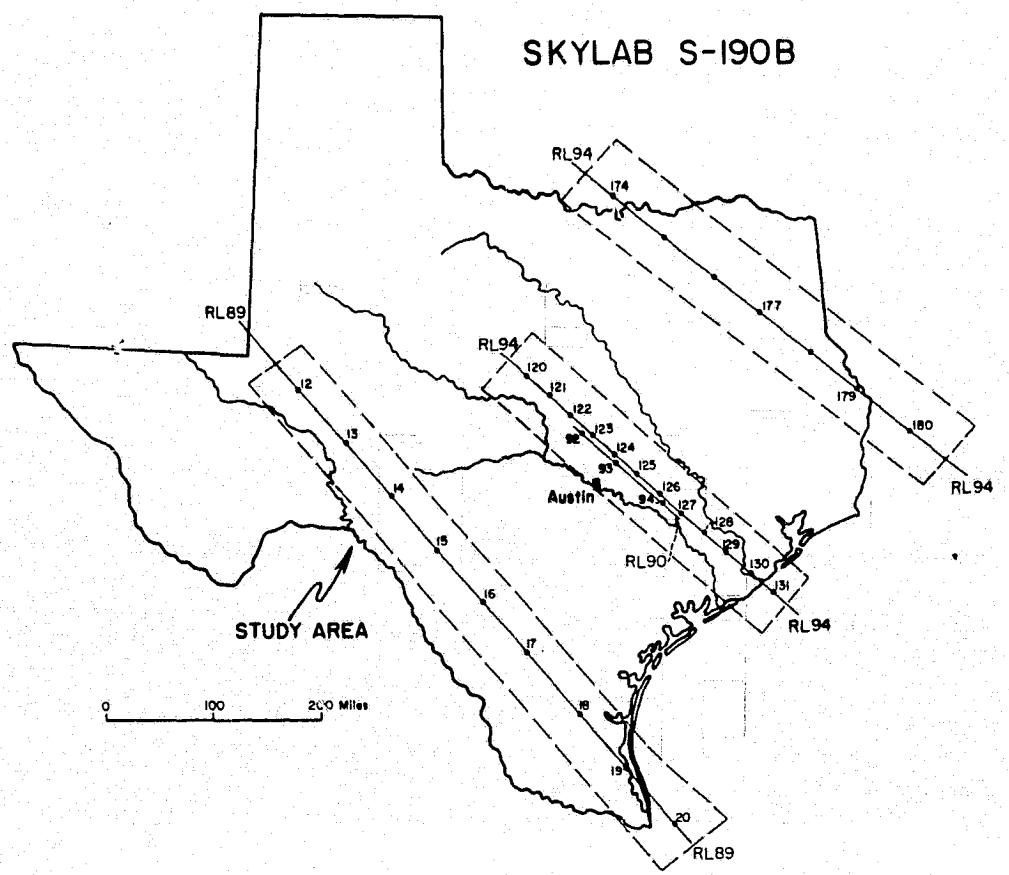

Figure 1. Map of Texas showing location of study area and approximate coverage of Skylab and suborbital imagery used in the investigation.

Drainage basins developed to the north and west of the Fault Zone in the Edwards Plateau have steep slopes, ridge-like interfluves, sparse, generally shallow-rooted brushy vegetation, and thin lithosols, over consolidated limestone and marl bedrock (Figure 2). There is considerable bedrock exposure at the surface, both on valley sides and in the bottom of stream channels. Because of the increased elevation, stream gradients on the uplifted plateau are steeper and channels are undergoing rapid headward erosion. The "Hill Country" is used primarily for grazing of cattle, sheep, and goats. There is little farming except on small areas of relatively flat stream terraces. Overgrazing, cutting of cedar (juniper) burning brush, and construction practices have enhanced hillslope erosion processes. Dense, brushy vegetation may grow to the edges of active stream channels and overhanging branches may obscure the channels on remote sensing imagery (Figure 3). The physical and land use characteristics of the basins promote rapid runoff under the best of conditions, and major, damaging flooding can occur during periods of heavy precipitation. Later in this section we will document that the topographic rise of the Balcones Escarpment serves as an orographic triggering device which can produce unusual amounts of precipitation in very short periods of time.

The drainage basins which have developed on the Coastal Plains are much different from those in the "Hill Country." Coastal Plain basins have gentle to flat slopes, low, rounded interfluves, dense, deeply-rooted grass and brushy vegetation, and deep soils, generally of a black, waxy, clay nature. While bedrock is covered by a relatively deep weathered mantle, fluvial processes, especially in stream channels, may excavate down to it. Even relatively low order stream channels have bedrock exposed, but only in the narrow portion of the active stream channel (Figure 4). Land use in the

Figure 2. Oblique aerial photograph of the Bee Creek area on the Edwards Plateau near Austin, Texas. Features shown include: B - Bee Creek, T - Tom Miller Dam, R - Bee Cave Road.

Figure 3. Vegetation along Blieders Creek near New Braunfels, Texas. The overhanging branches reduce recognition of channel alluvium and bedrock exposure on remote sensing imagery.

Coastal Plain basins is primarily agricultural cultivation and grazing. The major streams with their irregular sinuous courses and the bordering galeria tree and brush vegetation stand out in sharp contrast to the surrounding rectilinear pattern of cultivation. This sharp change in land use makes it easy to determine the higher ordered streams on remote sensing imagery (Figure 5). Because of deeper soils, denser vegetation, and more gentle stream gradients, basins on the Coastal Plain, in contrast to those in the "Hill Country," do not have such devastating floods except where major channels issue from the plateau.

Climate

Central Texas is subject to irregular, but chronic flooding of sometimes extraordinary magnitude in the frequency range of 10 - 50 years (Baker, 1975). The controlling factors in this pattern of flooding are climate and physiography with land use practices adding a dimension of acceleration. As pointed out earlier, the dominant topographic element of the region is the Balcones Escarpment. Mean annual precipitation along the escarpment varies from 32.58 inches at Austin to 22.0 inches at Bracketville (Figure 6), in Kinney County, near the border with Mexico (U. S. Army Corps of Engineers, 1964). In general, isohyets in Texas have a north-south vector with only two minor exceptional areas (Arbingast and others, 1973). One of these areas occurs along the western end of the Balcones Escarpment where this topographic rise, bending to the west, produces a westward bulge in the isohyets. When a more detailed set of isohyets is plotted they exhibit close spacing along the escarpment indicating the orographic effect of the increased elevation (Carr, 1967; Figure 2). Average monthly precipitation figures show that maxima occur

Figure 4. Oblique aerial photograph of the Inner Coastal Plain ("Blackland Prairie") just east of Austin, Texas. Features shown include: C - Travis County Landfill, H - U. S. Highway 290, W - Channel of Big Walnut Creek.

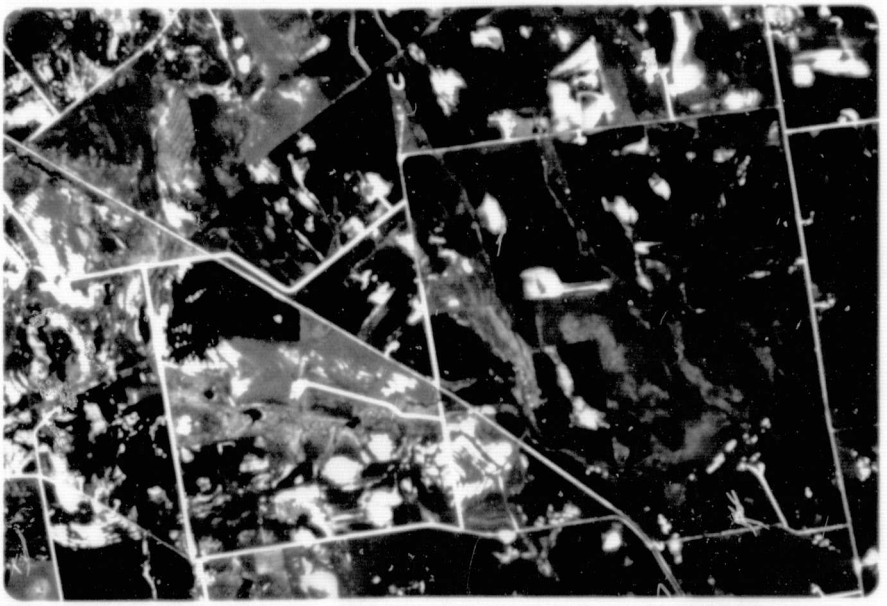

Figure 5. Color aerial infrared type 2443 imagery of Wilbarger Creek. Photograph shows an area approximately 5 x 4 km. Note the relationship of the stream channel (arrow) to land use patterns.

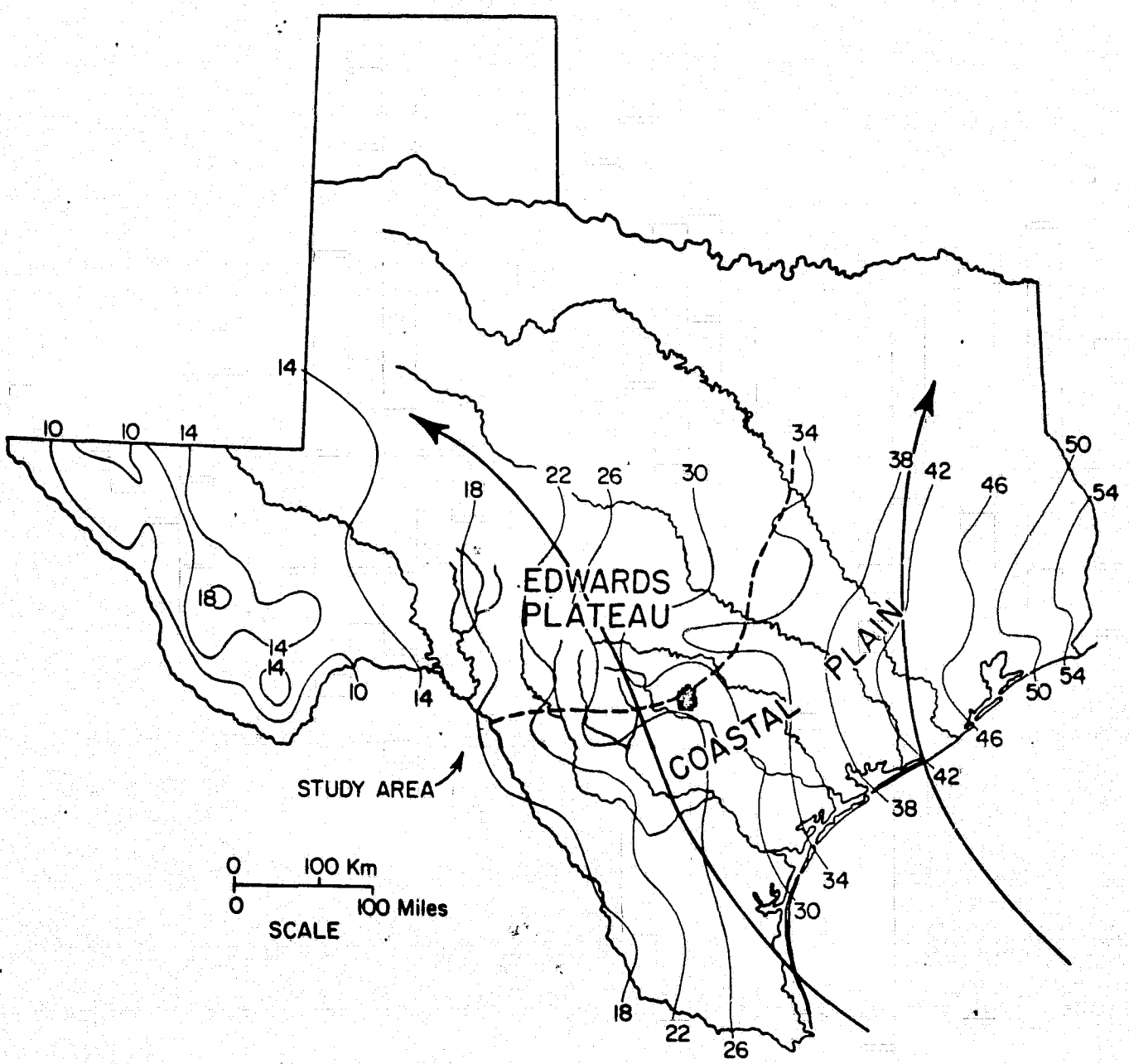

Figure 6. Isohyets of mean annual precipitation for Texas (Carr, 1967). Large arrows show major tropical storm tracks from the Gulf of Mexico. The dashed line shows the general location of the Balcones Fault Zone.

in May and September with lows in both winter and summer (Carr, 1967). The maxima are closely related to the seasonal period when the region undergoes a wind vector shift. For example, throughout the summer, which is normally hot and dry, there is a strong, almost monsoon-like current of hot, humid, maritime tropical air which crosses the escarpment from the south and southeast from its source region in the Gulf of Mexico (Arbingast and others, 1973). The winds will blow from these directions more than 80 percent of the time throughout the summer months at both Austin and San Antonio. As this strong flow breaks up in late summer and early fall, the prospects of frontal and convectional instability and turbulence increase and more precipitation occurs. In winter the wind pattern is more variable but there is a strong component from the north, north-northwest, and northwest. This air flow is generally cool to cold, dry continental polar air from a source area over the interior of the North American continent. When this pattern weakens in the spring, the possibility for atmospheric instability and resulting precipitation again increases, and heavy rains usually occur in April and May (Arbingast, 1973).

Topographically, central Texas is open to the Gulf of Mexico in the south and, except for the low Mid-Continent rise, there is nothing to prevent an Arctic air mass from penetrating into the region along the eastern edge of the Rocky Mountain front (Thornbury, 1965). A continental polar air mass can displace a marine tropical air mass very rapidly, but the region is close to a reservoir of warm, moist air which can produce great amounts of precipitation in any month of the year providing the proper atmospheric conditions exist for triggering it.

Climatically the area is located in that zone where the middle-latitude,

humid subtropical climate of the east grades into the middle-latitude steppe climate to the west (Strahler, 1965). Humid air masses can penetrate the area at any time of the year, but lack of triggering devices may lead to very dry conditions, over extended periods. In any one year the border between humid subtropical climate and middle-latitude steppe may shift completely across the region. As a result annual rainfall is highly variable, ranging from over 50 inches to less than 15 inches. Even in the dry and hot summers tropical disturbances can bring very heavy rainfall and rapid runoff from high gradient "Hill Country"streams flowing on bedrock. Great variation in stream flow is characteristic seasonally and annually.

The rainfall maxima, mentioned earlier, which occurs in May and September, result primarily from convective thunderstorm activity and the movement of moisture-laden air along the tropical Gulf storm track. Historically these storms have produced some astonishing amounts of rainfall which include both national and world records for a given period (Figure 7). The rain is concentrated over relatively small areas (Figure 8).

The western end of the Balcones Fault Zone is characterized by a steep, relatively high escarpment which is situated at right angles to the general direction of the Gulf tropical storm track. This joint topographic and climatic situation is ideal for giving an air mass an upward vector which can be strengthened by convection into what Dorroh (1964, p. 6) has described as a lift-convection thunderstorm. He further states, "at or near sudden changes in topography the characteristic rainfall intensities will far exceed those normally experienced in the vicinity." The most violent form of atmospheric convection is the thunderstorm, which occurs when thermally unstable air is lifted along orographic barriers, weather fronts and isobaric convergences.

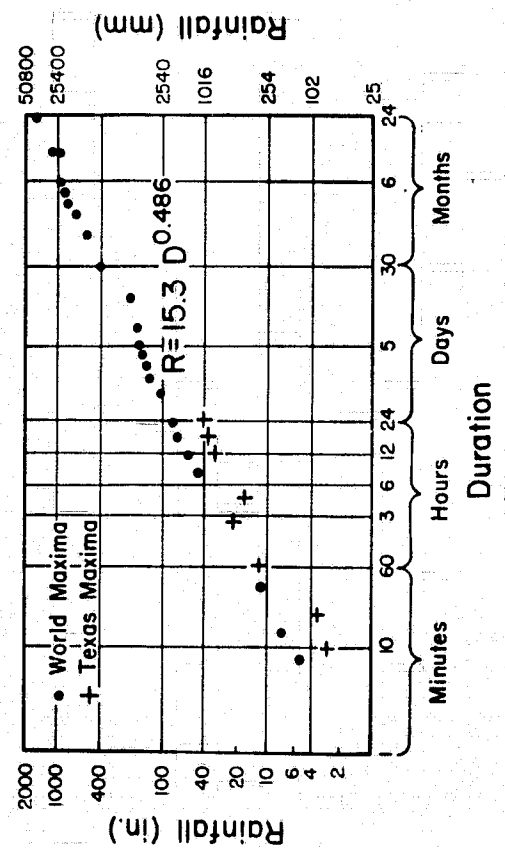

Figure 7. Magnitude-duration relationships for the largest rainfalls of the World and Texas. World data are from Jennings (1950) and Paulhus (1965). Values for the New Braunfels storm (May 11, 1973) are as reported by Colwick and others (1973).

Figure 8. Location of selected major rainstorms in central Texas. Rainfall amounts are given in inches. Storm duration is given in days and shown in parentheses after the month and year of the event. The map is biased toward the depiction of tropical storms with large areal extent rather than short-duration, local thunderstorms, which are generally one day or less in duration. Data were summarized from Breeding and Montgomery, 1954; Colwick and others, 1973; U. S. Army Corps of Engineers, 1964; U. S. Soil Conservation Service, 1954, 1958; Williams and Lowry, 1929.

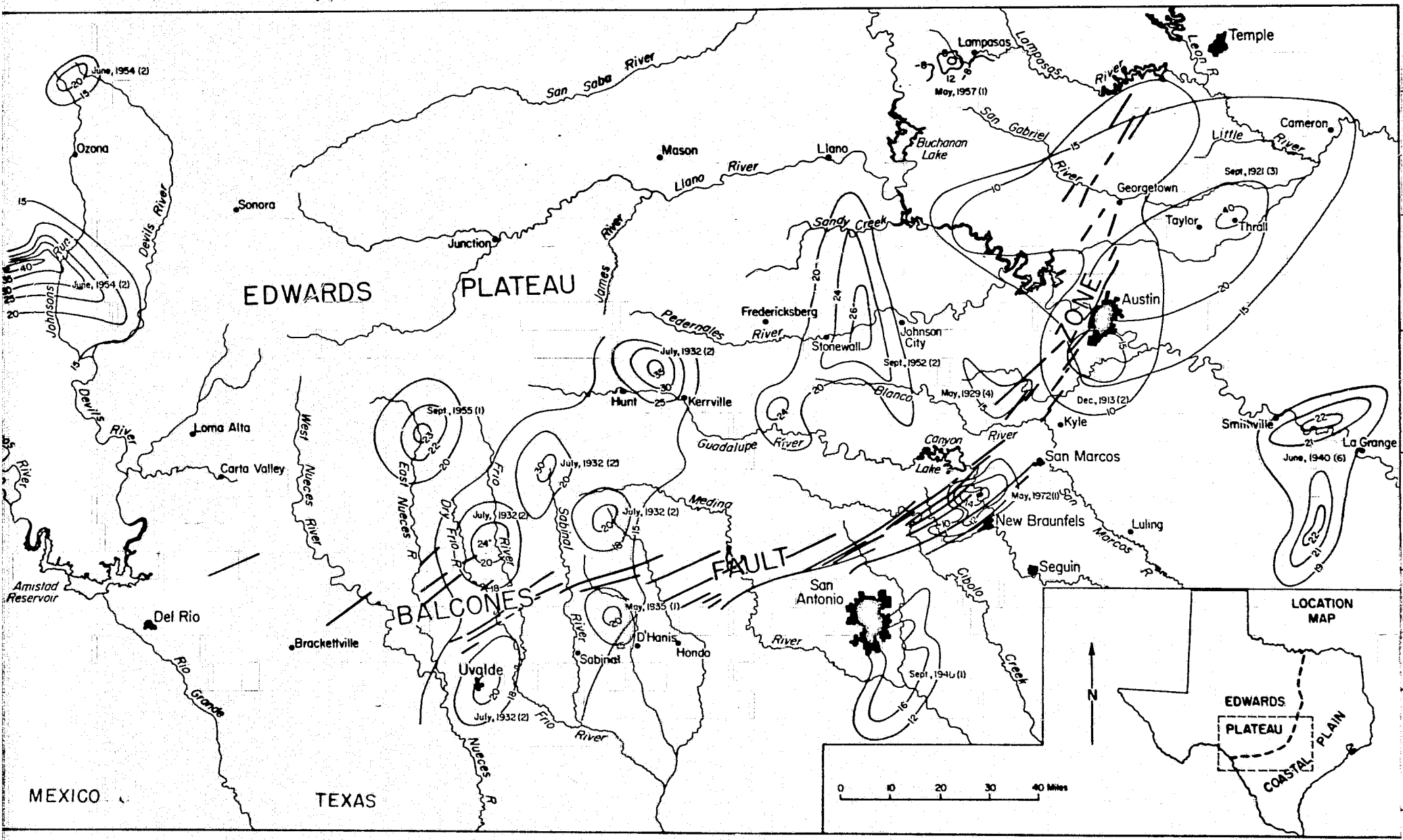

A spectacular example of this type of "cloud burst" thunderstorm occurred on May 31, 1935 near D'Hanis, Texas. A tongue of unusually moist, warm air protruded from the Gulf of Mexico into this area (Morgan, 1966). The orographic effect of the Balcones Escarpment on this unstable air produced 22 inches of rainfall in two hours and 45 minutes.

Air masses of marine tropical origin are responsible for the greatest flood-producing storms in Texas. These storms result from easterly waves which develop along the Intertropical Convergence Zone that extends into the Gulf of Mexico in summer. The air masses in these waves are warmed and they pick up great quantities of moisture during passage over thousands of kilometers of warm tropical seas (Orton, 1966).

Meteorological conditions in the Caribbean make the development of easterly waves most likely to occur throughout the summer months (Hurricane Season) but especially in September. If one of these unusually vigorous waves reaches the orographic barrier of the Balcones Escarpment, long-duration, heavy rains may result. This happened in the great storm at Thrall, Texas, on September 9-10, 1921. In this storm 36.4 inches of rain fell in 18 hours and 38.2 inches was recorded for the 24-hour period. For a 24-hour period, this storm is considered, by the U. S. Weather Service, to be the greatest which has ever occurred over the continental United States.

On September 9-10, 1952, almost simultaneously over central Texas, a pressure surge from the northeast came into contact with an easterly wave trough. The warm moist tropical air of the trough was lifted over the combined barriers of the Balcones Escarpment and the steep pressure gradient from the northeast (Orton, 1966). Rainfall totals of 20-26 inches were recorded in a localized area (Figure 8) over the upper Pedernales and Guadalupe Rivers

although generally heavy rains fell throughout the entire area (Lott, 1952). A particularly intense cell located between Stonewall and Johnson City produced a peak flood stage at the Johnson City bridge on the Pedernales of 48 feet as recorded by local residents. Later hydraulic calculations (Breeding and Montgomery, 1954) indicated a peak discharge of 441,000 cfs at that bridge location. Water depths of up to 60 feet and flow velocities exceeding 20 fps were recorded for smaller streams in the Guadalupe Basin. The advancing flood wave of the Colorado River drainage was stopped by Mansfield Dam, but it is estimated that the flood stage at Austin, Texas, would have been at least 47 feet (750,000 cfs). This would have exceeded all flows since at least 1833 (Orton, 1966).

The meteorologic factors that affect the magnitude and intensity of precipitation are the keys to forecasting the temporal occurrence of floods. Once that precipitation reaches the ground, the conversion to flow in stream channels depends mainly on the physical characteristics of the drainage basins and stream channels (Rodda, 1969). As pointed out earlier in this section, very rapid runoff from the Edwards Plateau is intensified by sparse vegetation, thin soils, and exposed bedrock that is often clay sealed (Tinkler, 1971). Drainage density measured from 1:24,000 scale topographic maps averages 10 miles/miles^2. Even more significant in concentrating overland flow are the many surface gullies on hill slopes which may not show up on topographic maps. Analysis of remote sensing imagery of the Bee Creek drainage basin (3.25 mi.^{2}) near Austin revealed over 1,000 such gullies.

The flood peak discharges that result in central Texas are known to exceed those recorded from similar-sized drainage basins elsewhere in the United States (Figure 9). By examining the relationship between the magnitude

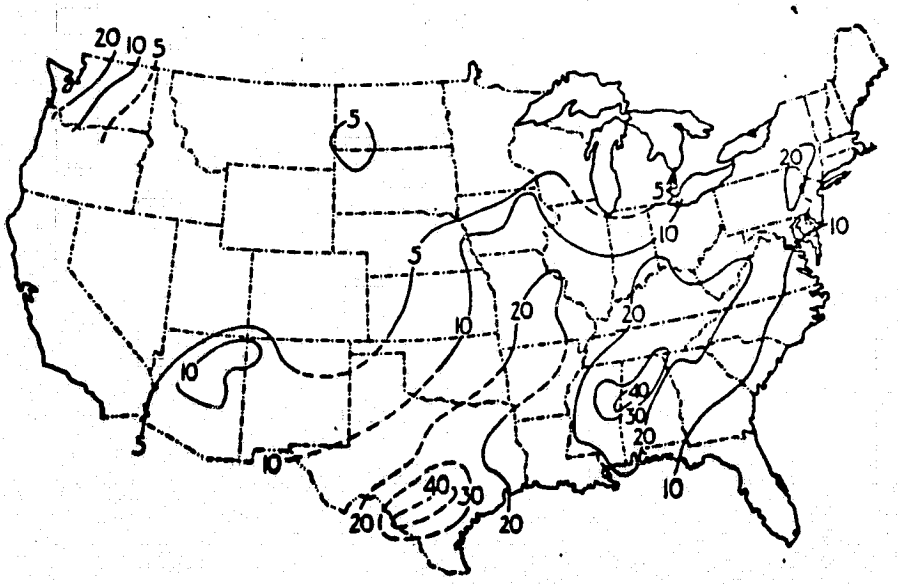

Figure 9. Regional interpretation of the magnitude of the 10-year flood in thousands of cubic feet per second from drainage basins of 300 square miles in area (from Leopold, Wolman, and Miller, 1964). Note the local maximum attained in central Texas and equalled only by a small area in the southern Appalachians.

of flood discharge and contributive drainage basin area, it is possible to define an envelope curve for the greatest floods in the region (Figure 10). Many of the flood peaks that define this relationship arose from the individual storms discussed earlier. It is impossible to predict the occurrence of such storms or even measure accurately their frequency. But by careful analysis of the morphology of the drainage basins developed in the area we can predict probable peak discharges and suggest economic and cultural development of the basins which would reduce the magnitude of flooding and insure human activities are assigned to topographic positions which are safe from floods.

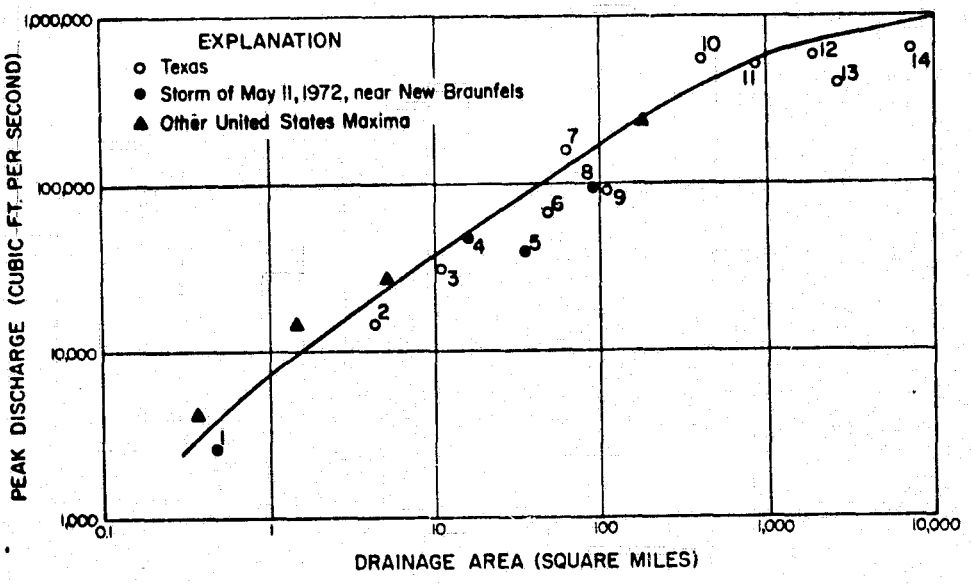

Figure 10. Maximum flood discharges recorded in central Texas in relation to contributing drainage area. The trend line represents the U. S. national maximum determined by Hoyt and Langbein (1955). Texas data are identified by number as follows: (1) Trough Creek near New Braunfels (1972), (2) Bunton Creek near Kyle (1936), (3) Little Red Bluff Creek near Carta Valley (1948), (4) Blieders Creek (1972), (5) Purgatory Creek near San Marcos (1972), (6) Sink Creek near San Marcos (1972), (7) Mailtrail Creek near Loma Alta (1948), (8) Guadalupe River at New Braunfels, contributive drainage area only (1972), (9) Hondo Creek near Hondo (1919), (10) West Nueces River near Kickapoo Springs (1935), (11) West Nueces River near Bracketville (1935), (12) Nueces River below Uvalde (1935), (13) Devils River near Del Rio (1932), (14) Little River at Cameron (1921). Data are from Colwick and others, 1973; Dalrymple, 1964; and Patterson, 1963.

DATA FORMATS FOR STREAM NETWORK ANALYSIS

All quantitative drainage basin analysis depends upon the initial interpretation of a basin's drainage network. In this study eight sources of graphic information (Table 1) were examined to determine their usefulness in delineating stream networks. These sources may be divided into three broad groups: topographic maps, suborbital imagery (aircraft), and imagery generated from space by Skylab and ERTS. These groups will be discussed in the order listed.

Topographic Maps

The largest scale topographic maps normally available in the United States are U.S.G.S. seven-and-a-half minute quadrangles at a scale of 1:24,000. In central Texas these maps cover an earth surface area of approximately 60 square miles and have a contour interval which varies from 5 feet on the Coastal Plain to 20 feet in the dissected "Texas Hill Country" (Figure 11). On American topographic maps at this scale, contour lines are printed in brown and streams in blue. A solid blue line indicates a perennially flowing stream. A dash and dotted blue line indicates a seasonal or ephemeral stream. When drafting these lines, the cartographer must exercise a good deal of subjective judgment in selecting the number and determining the length of these broken blue lines which will be printed on the map. Often the stream network developed from the pattern formed on large scale topographic maps by blue lines is not detailed enough to make accurate quantitative measures for geomorphic analysis of the drainage network or basin morphology.

The "method of V's" (Strahler, 1952) is usually used to derive a detailed drainage network from topographic map sources. This is accomplished

Table 1. Characteristics of the sources of drainage network information used in this study.

SOURCE	SCALE [1]	DATE	SPECIAL CHARACTERISTICS
A. Topographic Maps	1:24,000	Variable (1960's)	1:62,500 scale maps were used in 2 cases
B. Suborbital Imagery			
1. U.S.D.A. Air Photographs	1:20,000 & 1:13,000 9"x9"	1967	Standard B/W
2. U.S.A.F. Air Photographs	1:20,000, 9"x9"	1968	Standard B/W
3. N.A.S.A. Low Altitude	1:48,000, 9"x9" 70 mm	12-1-73	Color IR and multi-spectral
4. N.A.S.A. High Altitude	1:116,000, 9"x9" 70 mm	12-1-73	Color IR and multi-spectral
C. Other Imagery			
1. ERTS	1:500,000, 7"x7"	3-17-73	Multispectral
2. Skylab S-190A	1:750,000, 9"x9"	1-29-74	Multispectral
3. Skylab S-190B	1:500,000, 9"x9"	1-29-75	Hi-resolution color

[1] The imagery scale and sizes listed here are for the original data formats. Generally, imagery was optically enlarged in order to extract data from it and the working size varied according to basin size and complexity. All formats provided by NASA are not listed here.

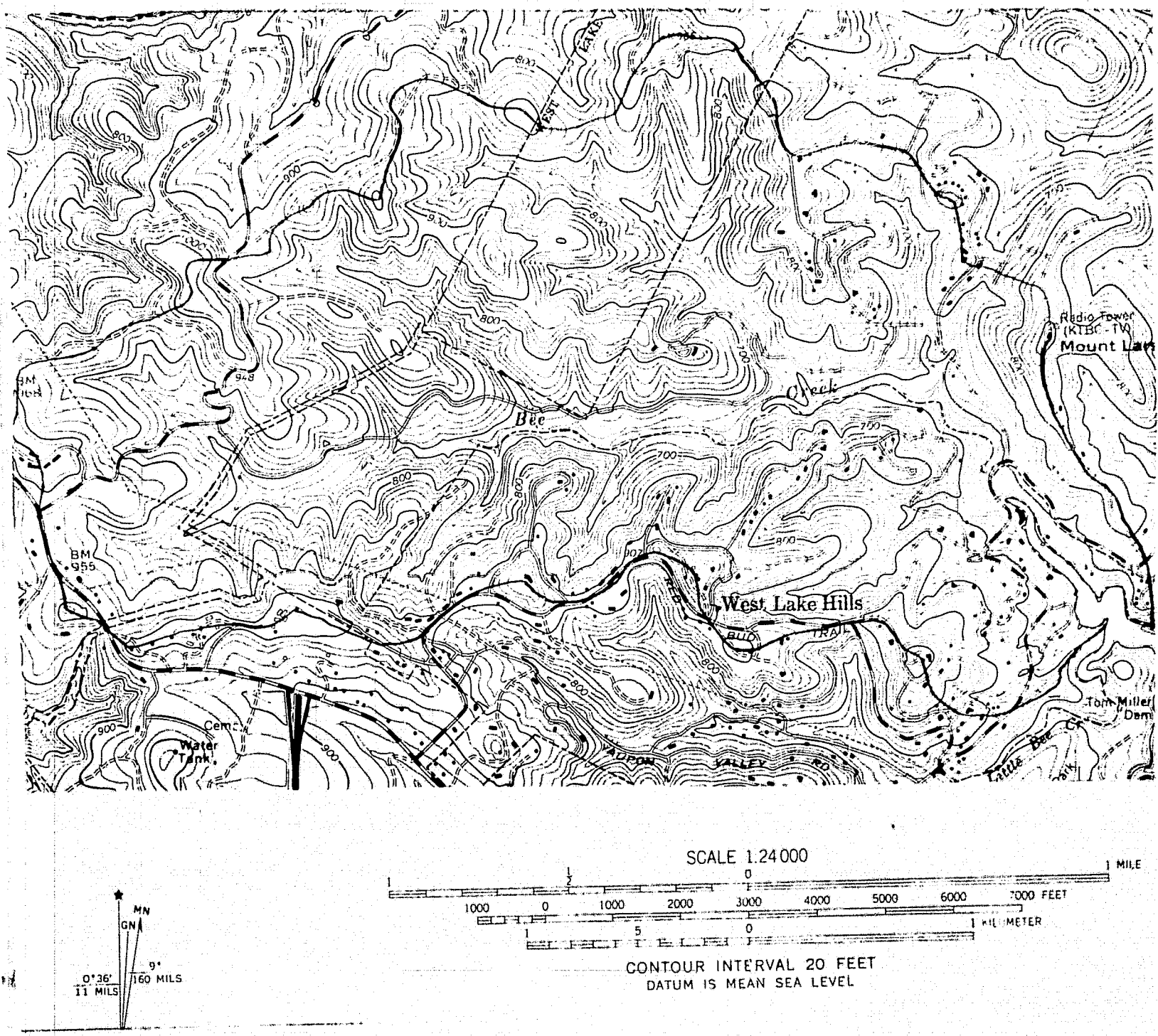

Figure 11. Topographic map of the Bee Creek study basin.

by extending lower order stream segments up-valley using the crenulations in contour lines (Figure 11). This method of extension takes advantage of the characteristic of contour lines in bending up-stream or up-valley when they cross a valley. The cartographic expression of this characteristic is often a series of interspersed "v's" in the contour lines, with the apex of each "v" pointing up-stream. Frequently, when these "v's" appear on a map, the blue line indicating a perennial or seasonal stream will not be extended through them. In this study we standardized interpretation by extending stream channels only where at least two adjacent contour lines indicated a drainage way. The channel was extended through the last contour line crenulation in a series of "v's" but stopped before it reached the first uncrenulated line.

The problems with this method for accurate measurements in small drainage basins is obvious. Many first order streams go unrecorded and determination of their length is at best an "educated guess." Failure to record all first order streams or measuring their length incorrectly leads to the following problems: (1) reduction of the total number of stream segments recorded, (2) reduction of the mean lengths of stream lengths, (3) reduction of basin Shreve magnitude, and (4) underestimation of drainage density. These observations will be documented quantitatively later in the report by a comparison of the topographic map data to the more detailed and accurate data derived from stereo pairs of air photographs (Table 6).

It is evident then from this comparison that remote sensing imagery is more useful and accurate in recording basin drainage characteristics. The questions then arise what type, scale and quality of imagery are best used in recording these characteristics? We will attempt to answer these questions in later sections of this report.

Suborbital (Aircraft) Imagery

For this study three scales of aircraft photography were available from three sources. First, low altitude (about 10,000 feet above terrain) black and white contact prints from the U.S. Department of Agriculture and U.S. Air Force were available for some of the basins studied. The cameras used to generate these photographs had a six inch focal length and from this aircraft altitude produced photographs at a scale of 1:20,000 with minor anomalies depending upon aircraft and terrain variation. The U.S.D.A. photographs used in this study were about eight years old; those from the U.S.A.F. about six years old; and in the rapidly changing area of Austin, and surrounding Travis County, they did not provide a temporal handle on major land use and other basin changes. Although these black and white photographs provided little vegetation contrast in the "Hill Country" basins, and strong shadows frequently obscured portions of drainage net, they were flown with a 60 percent forward over-lap and stereoscopic coverage was provided. This three dimensional view was very useful in determining low order stream channels, especially in the "Hill Country" where first order streams have high channel gradients. From these photographs the lower order channels can be observed, or inferred and measured accurately.

A second source of air photographs for this study was the medium altitude (24,000 feet) aircraft support program provided by N.A.S.A. in several different camera and film formats. Because of planning and mission constraints no forward overlap was obtained on the medium or high altitude N.A.S.A. suborbital photographs. Research on this project now proves that forward overlap is mandatory in areas of steep or rough terrain such as the Texas Hill Country.

Forward overlap is of little value in plains areas such as the Texas Gulf Coast. A point should be made that for future aircraft missions on projects studying terrain problems and especially drainage networks, thirty to forty percent overlap should be provided for rough or steeply sloping topography. Stereo overlap is very important in delineating first order stream channels which are critical to drainage system network analysis. In a small portion of one basin (Bee Creek) we were able to observe some stereographic coverage from side lap provided by adjacent flight lines. While stereographic coverage would undoubtedly have aided in photo interpretation of the basin networks, we were still able to extract more information from these photographs than from topographic maps. Further, they provided up-to-date information on land use and other basin changes, and the color photographs were especially valuable in assessment of vegetation characteristics. A single photographic frame of a drainage basin contains more usable information than a large scale topographic map of the same area. This is true because of the different nature of maps and photographs. A map is a cartographic abstraction, with detail selected by the cartographer. The cartographer chooses what to add or leave off the map. It is cartographic judgement which decides important statistical abstractions such as contour interval. On the final topographic map the only information available to the hydrologist studying a drainage basin is the blue lines of the stream channels, the contour lines, often with too large a contour interval, and perhaps, but not always, some indication of forest or brushy vegetation. A researcher studying drainage systems from topographic maps has to guess at the number and length of first order streams. A photograph, on the other hand, displays all objects reflecting light in the dynamic range of the film emulsion. Current land use practices are visible as well as

other cultural changes induced by man. Vegetation can be mapped and the drainage system can be defined in more detail and more accurately than by the educated guesses made from maps. As a final constraint the photographs are usually more recent than maps and they document recent land use, vegetation and stream morphology changes which would not be indicated on older maps.

Mission 259, over Test Site 213, was accomplished on December 1, 1973 using the NP3A/NC130B aircraft at a radar determined elevation of approximately 25,000 feet. The photographic imagery was generated between 16:00 and 20:30 Greenwich Mean Time or between 10:00 a.m. to 12:30 p.m. local time. There were three camera groups used. Two of these were RC8, six inch cameras with a 9 x 9 inch film size. The film in camera one was black and white High Resolution 3400, while camera two was loaded with color infrared, 2443 film. The third camera group was a multispectral array of six, 70 mm Hasseblad cameras, which were fitted with 80 mm lens. Cameras one and two were loaded with black and white 2402 film, but were filtered differently. Cameras two and three were loaded with black and white infrared 2424 film, filtered differently. Camera five was loaded with color infrared 2443 film and camera six contained SO 397 color film. Although we found that this film format was excellent for certain purposes, such as determining land use, we found it less valuable for measuring drainage nets. It seemed harder to distinguish land/water interfaces on the normal color film and shadows from vegetation and steep banks obscured some portions of stream channels. The larger format provided on the 9 x 9 inch film from the RC-8 cameras was much more valuable in delineating stream channels. Using this camera format from an elevation of 25,000 feet it is possible to resolve an object approximately 5 x 5 feet on the ground. As documented by Simmonett and Henderson (1969) and Holz and Boyer (1972),

it is frequently possible to resolve linears on the landscape such as roads, pipelines, streams and canals which are apparently below the minimum resolution capabilities of the sensor system. Using this larger format and without stereo overlap we were able to work out basin drainage networks more thoroughly than could be accomplished from large scale topographic maps and smaller scale imagery formats.

On the 1 December, 1973 Mission 261 was flown over test site 213. This high altitude (approximately 60,000 feet) flight was made by the WB57F aircraft, using two photographic camera arrays. The first of these consisted of two RC-8, six inch focal length camera arrays. One of these cameras was loaded with color infrared 2443 film and filtered so that light waves shorter than 510 nanometers were attenuated. The other RC-8 was loaded with black and white panchromatic film and used a W-3 filter. The second camera array was a six channel camera system with forward motion compensation. Cameras one and two of this system contained black and white infrared 2424 film, but filtered differently. Camera three was loaded with color infrared 2443 film, screened with an EE filter. Camera four had a normal color film with an FF filter. Cameras five and six were loaded with black and white panchromatic SO-022 film, but each was filtered differently.

Because of the high altitude involved and the corresponding reduction in scale we found the 70mm photographs to be of little value in discerning first and second order streams. The drainage basins examined in this study cover such a small area and their drainage networks are so intricate that even with considerable enlargement the 70mm format proved to be of very little value, other than assessing gross land use changes in the basins. We found the color and color infrared films, in combination, to be most useful

in determining land use. No systematic study was done on why these films worked better in combination. It must be remembered that our study basins were generally in rural areas. On infrared film it was easy to distinguish healthy, especially newly sprouted, vegetation which is highly reflective in the near infrared (about 700-1000 nanometers). It was easier on the infrared film to outline land/water interfaces,and there seemed to be better penetration capabilities of some shadowed area. The color film on the other hand gave more color variation in agricultural fields of varying type and age and this allowed better classification. In many cases, it was possible to make these same sortsof color discriminations in the more uniform brushy vegetation of "Hill Country" drainage basins. In many cases of identifying signatures on imagery it was possible to check an object or area on one photograph and verify it by examination of the photograph of contrasting film type. It was then the juxtaposition of the two film types which made possible object signature identification.

Using the larger RC-8 camera in the 9 x 9 inch data format, it is possible to do detailed drainage analyses from the altitude of 60,000 feet. Enlargements were made from the 9 x 9 inch transparencies for two drainage basins, Bee Creek and Wilbarger. Generally, the enlargements added little to our ability to measure drainage networks. We did find them of specific value in identifying ground objects or land use in certain small areas. The quality of these enlargements was not as good as the products which originate in the N.A.S.A. photographic laboratory.[2]

---

[2] The first set of enlargements were printed by a commercial firm in mirror image and proved difficult to work with although one could still measure

Space Imagery

For this study we had one ERTS frame which covered the area under investigation (Figure 12). This particular frame is not a good example of ERTS' capabilities or imagery, but it does point out conclusively that imagery of this scale and resolution capabilities is of little value for detailed drainage analyses of small stream basins.

Skylab imagery was available from SL-2 and SL-4. We received some 12 frames of S-190A imagery from SL-2. The SL-2 imagery provided information on only a small part of one basin (Baker, Holz, and Hulke, 1974). The other basins in the study area and our smoke experiment were obscured by clouds.[3] We gained little usable information from SL-2 imagery.

Skylab 4 imagery was excellent; it was almost cloud free and we were able to distinguish most of our study basins on the photographs. However, while the basins could be located, the spatial resolution of the S-190A photographs provided us with little usable data on stream networks within the basins.

Our experiences in this study indicate that the spectral resolution of the various film and filter combinations used, both in the aircraft support program and on-board Skylab, had a dynamic response sufficiently great to resolve all of the objects or phenomena necessary to complete our research.

---

basin networks on them.

[3] In an attempt to carefully locate a series of first order streams we triggered two smoke devices in the headward tributaries of Wilbarger Creek. A careful study of the SL-2 photographs, generated at this time did not reveal the ground smoke plume.

Figure 12. ERTS frame showing a portion of the central Texas study area. Location of Bee Creek is indicated by the letter "B." (Band 7, Frame E-1237-1637-701).

Spatial resolution, or the ability to resolve objects based on their size, is another matter. It is easy to confuse spatial resolution and scale. Imagery scale is the ratio between distance or area on the imagery compared to that same distance or area on the ground. The farther a sensor is from the earth or object being sensed the smaller will be the scale of the imagery produced. There is of course a close relationship between and scale and spatial resolution. As scale gets smaller, the resolving power of a sensor must increase in order to record an object of similar size at that greater distance. In this study the critical factor was to be able to identify stream channels on the imagery, especially first order channels. This is more a problem of spatial than spectral resolution. Because of their small scale and corresponding lack of increased spatial resolution we were unable to delineate, on S-190A photographs, a stream network detailed enough to do a meaningful analysis.

The best hope for drainage network analysis from space appears to be the S-190B or Earth Terrain Camera. This camera had a ground coverage of approximately 59 nautical miles on a side. Although the camera used a 5 inch film base, we eventually received the imagery as enlarged 9 x 9 inch transparencies. On the S-190B imagery the smallest area we attempted to identify on the original unenlarged imagery was a dot in Bee Creek basin. This area was approximately square on the ground, roughly 21 x 22 meters, and it was a high albeado white limestone and gravel surface recently cleared of brush. The surrounding vegetation was quite dark in tone and so the area provided a very strong target to background ratio which may have enhanced the resolving powers of camera system. The poor quality of the commercially prepared enlargements of S-190B imagery we had prepared was probably not a fair test of resolving power of this imagery. Examples of S-190A and S-190B imagery for

central Texas are illustrated in Figures 13, 14, and 15. Maps of drainage basins measured from the orbital imagery will be presented later in the report.

Discussion of Imagery Interpretation

In this study we attempted numerous methods of interpreting images for stream network analyses. On the large scale topographic maps we were able to digitize directly from the maps themselves or in some cases, from overlay tracings made directly from the maps at the same scale. On the large scale imagery formats, such as the 9 x 9 inch aircraft generated photographs, it was possible to digitize directly from the imagery, although stream channels were often hard to see because of shadows, both from vegetation and topography, and small scale. We found it more valuable to project the photographic transparencies onto a sheet of opaque white tracing paper and draw in the basin networks on paper. After scale calculations were made, it was possible to digitize from the tracing. We feel it would have been more valuable and probably more accurate if we could have developed the "Hill Country" basin networks from stereo pairs of air photographs. Where there is more relief the vertical exaggeration of steep sided slopes on stereographic air photographs makes it easier to delineate the drainage networks especially the critical level first order streams. Unfortunately the lack of stereo-overlap on the aircraft imagery made this impossible. Useful projection of the single image transparencies was accomplished by two methods. For the 70 mm format it was possible to mount the transparencies in a slide mount and project them with a "lantern slide" projector. This was an excellent method of projection and the enlargement and strong light source made it relatively easy to trace the networks which were resolved. The second method of projection used was a

13 A

13B

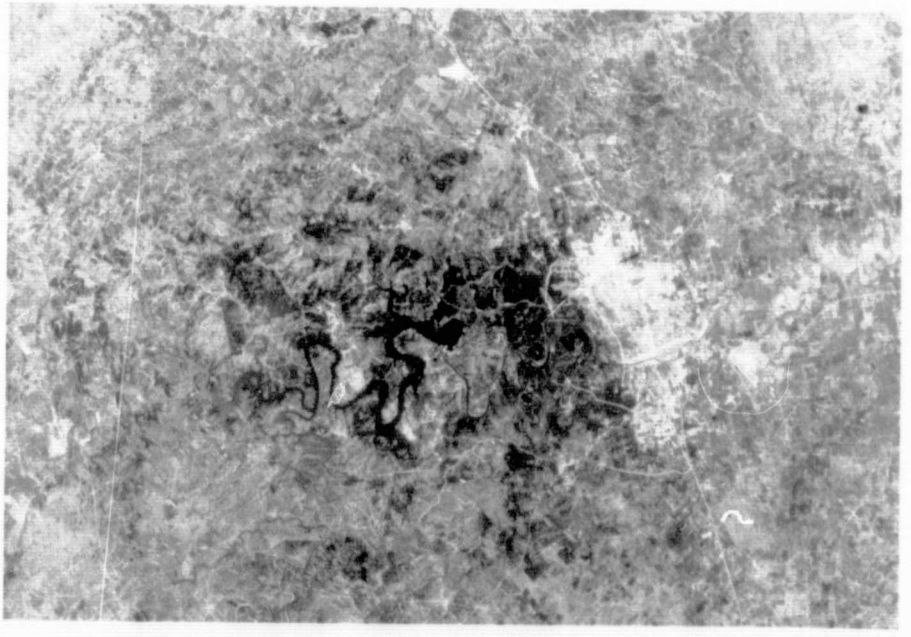

Figure 13. Skylab S-190A multispectral photography of the Austin, Texas area. A - Black and white infrared, Film EK 2424, Filter DD, 0.8-0.9μ. (SL4-74-371). B - Panatomic-X Black and white, Film SO-022, high resolution, Filter BB, 0.6-0.7μ. (SL4-77-371). Bee Creek is indicated by the "V."

14 A

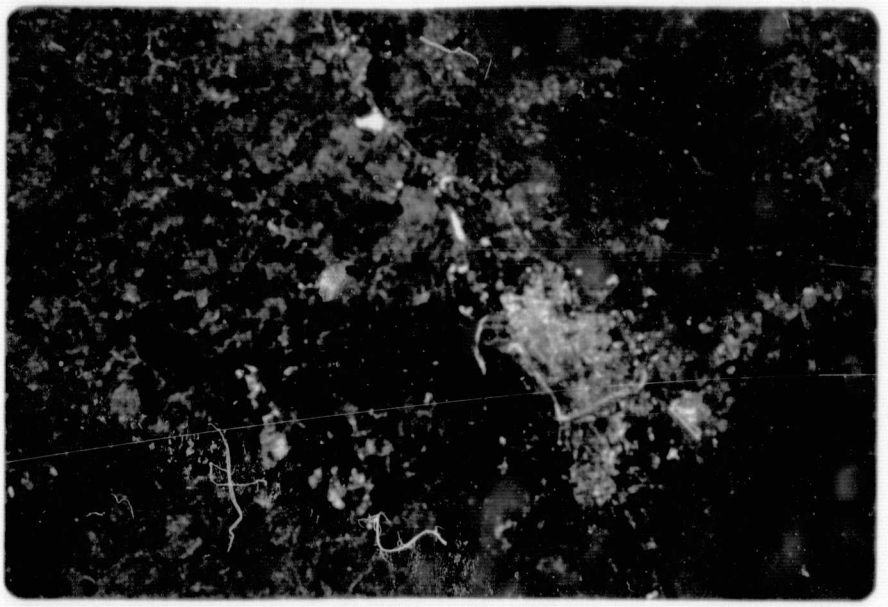

14 B

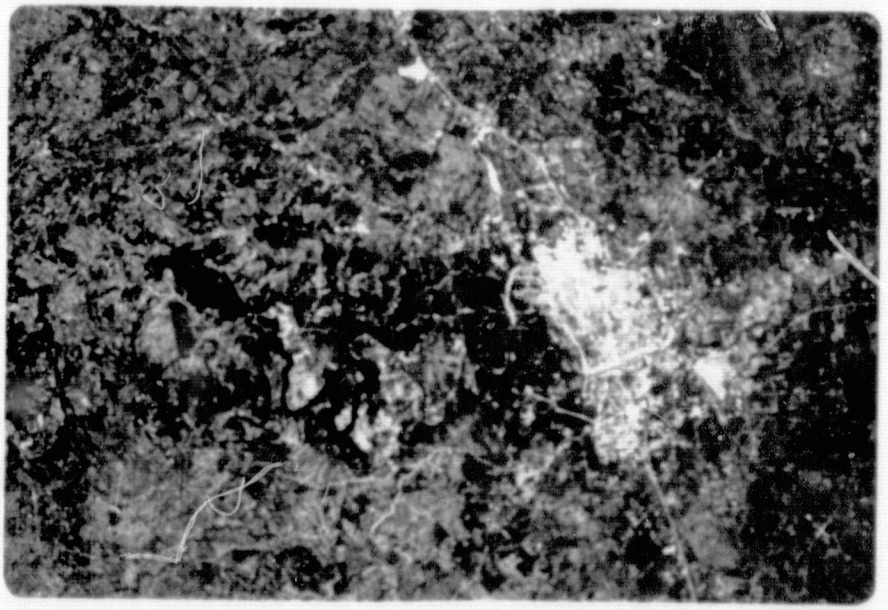

Figure 14. Skylab S-190A color multispectral photography of the Austin, Texas area. A - Color infrared, Film EK 2443, Filter EE, 0.5-0.88 , (SL4-75-371). B - High resolution color, Film SO-356, Filter FF, 0.4-0.7 , (SL4-76-371). Both frames cover scenes approximately 60 by 36 miles (96 x 58 km.).

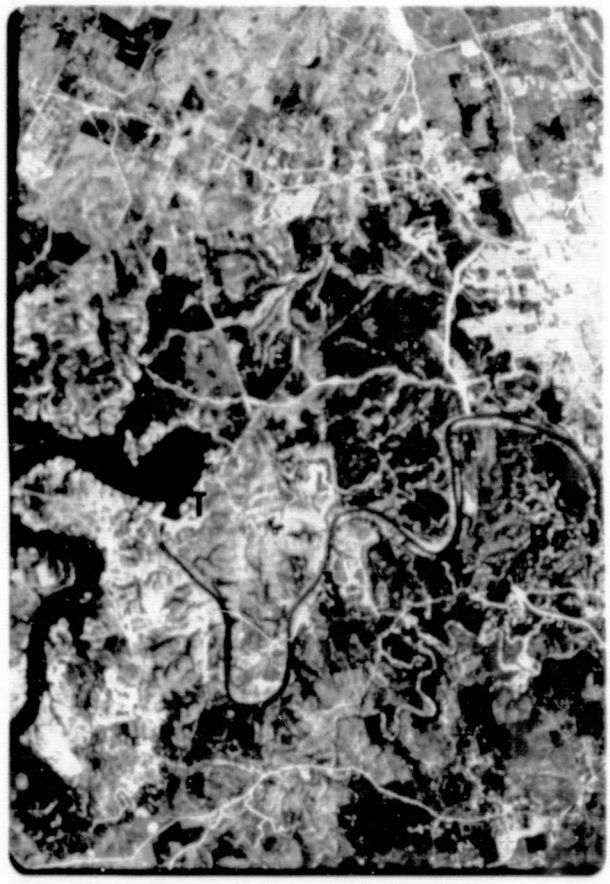

Figure 15. Skylab 4 S-190B imagery of the Bee Creek area near Austin, Texas. Features shown include: B - Bee Creek, D - Tom Miller Dam, T - Lake Travis. (Roll 94, Frame 124, hi-resolution SO-242 color film, 29/1/74). Frame depicts a scene approximately 20 by 12 miles (32 x 19 km).

high resolution overhead projector, for the larger transparencies. Although this system of projection is less desirable because the light source and resolution of the lens drops off rapidly, it did offer the draftsman using a hand lens the opportunity to check the actual imagery on the projector for selected stream segments. The draftsman could then correctly delineate any stream channels which were hard to resolve on the tracing.

Recognizing some of the weaknesses of this method of enlargement we had selected frames of aircraft and SL-2 and SL-4 imagery photographically enlarged. These enlargements were not of greater value in our study (they were fuzzy, indistinct, in two cases printed in mirror image) because they were poorly prepared by the commercial printer contracted to do the enlargements. They were not anything like the quality of contact prints produced by the N.A.S.A. photographic facility. Comparisons of digitized data generated from the projected and enlarged imagery proved conclusively that better data could be developed by projection. The enlargements were expensive, time consuming, and in one case printed incorrectly. In the latter case reversing the photographs did not really change the stream network values obtained; it did make it harder for the person digitizing the data to orient himself when working with the imagery.

Factors Used in Identifying Stream Channels

There was no problem in locating on the imagery the drainage basins selected for this study. This was true for low and high altitude aircraft generated imagery and for imagery generated from SL-2 and SL-4. Main channels in even the smallest basins (1.9 km^2) could be recognized on all imagery, although clouds, shadows and lack of contrast sometimes made recognition difficult

on space imagery. A detailed examination of stream reaches in the basins under study revealed the following diagnostic features:

1) Water - There was little ponded water in the stream channels under investigation. Stock tanks and the lower portion of Bee Creek where the main channel is drowned by water backed-up by the damming of the Colorado River to form Lake Austin are examples of the response of ponded water in the study area. Water does not always show up well on black and white photographs, either panchromatic or infrared, although water was easier to interpret on black and white infrared than on normal panchromatic film. The basins we examined generally were not large and did not have permanent flowing streams except along their extreme lower reaches. Channels were generally not large; therefore, there are few large areas of open water in the stream channels. On the colored infrared photography exposed water stands out in sharp contrast to surrounding land or vegetation. Farm ponds (stock tanks) show up clearly. But even in some of the larger exposed stream channels, which contained ponded water, the water could be observed on color infrared photography--but not always on normal color or black and white films generated simultaneously. In part this was due to shadow, background contrast and the reflectivity of surrounding signatures in the environment.

2) Land use and vegetation change - Sharp changes in land use are useful for locating and ordering streams on black and white, and infrared color photography. Where land use or vegetation changed sharply, for example, the brushy vegetation along stream courses transecting agricultural fields makes it easy to delineate stream courses. On the Edwards Plateau in the steep sloping "hill country," the more or less uniform tall, brushy, vegetation cover

effectively masks some stream courses. This is less true where micro environments on sloping hillsides lead to vegetation changes. For example, Bee Creek is in an area of relatively dense, brushy vegetation with little agriculture or grazing activities. The uniformity of the vegetation pattern is changed only where limited suburban development has removed vegetation. Wilbarger Creek, on the other hand, located on the Blackland prairie is in an area of intensive agricultural cultivation. The stream channels except for the first order streams are not ploughed, and the denser brush and tree vegetation along these courses clearly delineate the stream channels, even though the channel itself and exposed water can seldom be observed. In many places in the Coastal Plain basins, this sinuous galeria forest belt can be traced across unploughed pasture land (Figure 16). In Central Texas, where much of the vegetation especially in the "Hill Country" is evergreen (both needle and broadleaf), seasonality plays a minor role in the observational effects of drainage basin studies from remote sensing imagery.

3) Bare alluvium - Throughout much of the study area the general nature of the underlying bedrock is light colored limestone interbedded with shale. This countryrock has a very high albedo, especially when it is freshly disturbed. For example, mining or road cuts, which expose unweathered rock faces, are easily identifiable on remote sensing imagery (Figure 17). In stream channels freshly worked alluvium also shows up with a high reflectivity. It is possible to trace channels by the signature of discontinuously exposed, deposited alluvium, grading from gravel to coarse textured sand of predominantly limestone composition. In many cases the high albedo of the alluvium allows the channels of a basin drainage network to be traced through dense shadow or vegetation on suborbital and space photography.

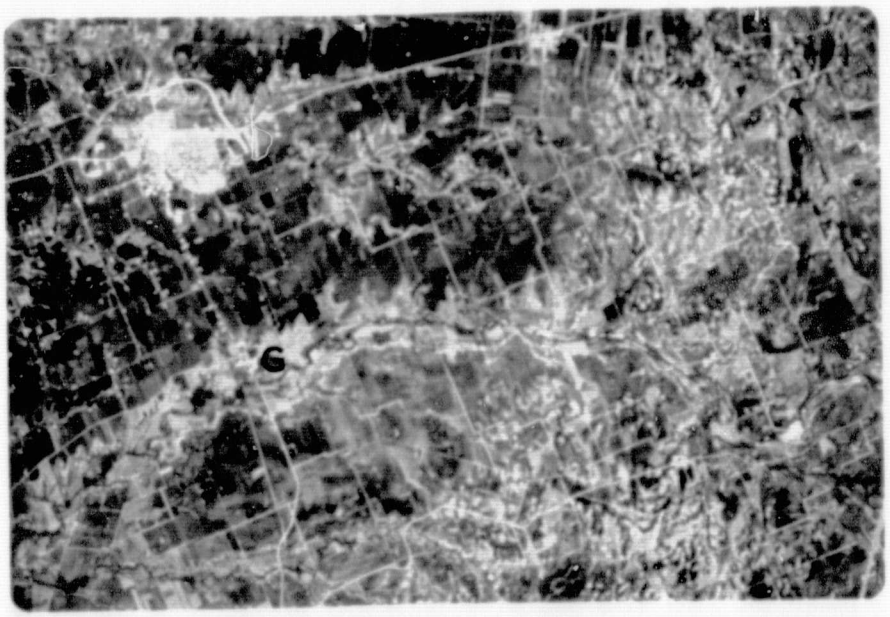

Figure 16. Skylab 4 S-190B imagery of the Inner Coastal Plain northeast of Austin. Galleria forest areas are indicated by the letter "G." Frame depicts a scene approximately 20 by 12 miles (32 x 19 km). (Roll 94, Frame 123, 29/1/74, hi-resolution SO-242 color film.)

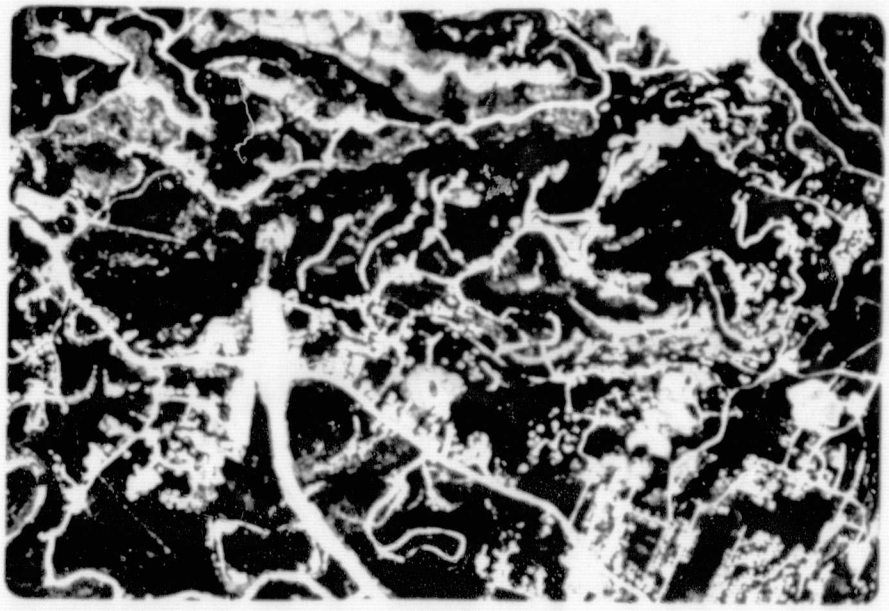

Figure 17. Color aerial IR type 2443 imagery illustrating the high reflectivity of freshly exposed unweathered rock for construction of loop route 290 west of Austin, Texas. Compare resolution of the Bee Creek basin to orbital imagery (Figures 13, 14, and 15). Frame depicts a scene approximately 5 by 3 km.

4) Shadow - Shadow is more important for stream channel recognition on panchromatic than on color or color IR photography, although it is useful on both imagery formats. The black, white, and gray values on panchromatic or black and white infrared photographs lend themselves more to shadow and tone interpretation.

Streams on the Inner Coastal Plain, the area near the Edwards Plateau, do not have deeply entrenched or steep-sided channels. Here, on rolling to flat agriculture land, subtle changes in vegetation, and very slight shadows along stream courses, are important tools in recognizing channels. On this more level land with less relief into the channel bottoms, a lower sun angle would greatly aid interpretation by providing a stronger, more well defined shadow from the little relief available. In the "Hill Country" shadow is also important in interpreting drainage. But on the plateau the increased height and steepness of some slopes create such a strong shadow that it frequently hides drainage lines, especially the lower order channels developing on hill slopes. This is particularly true of steep northwest facing slopes. In the "Hill Country" the shadow cast by dense, brushy vegetation helped to mask stream networks, especially the lower order streams. On the Coastal Plain subtle changes of vegetation and its attendant shadow help to emphasize the change of land use along stream channels, especially where there is little relief. An area of future investigation should be an attempt to determine how much of the recognition of stream channels is due to vegetation alone and how much is the result of its underlying shadow. Because of cost and time constraints we were not able to follow this line of investigation in our study.

5) Linearity - The linearity of stream channels is closely related to land

use and is frequently emphasized by vegetaion. This is especially true in drainage basins on the Coastal Plain, such as Wilbarger Creek, where channels with their attendant land use change extend at angles across the more regular tones, textures and patterns of the cultivated land. The angular trend of these linears frequently allows an interpreter to trace a stream channel to a bifurcation point which might go unnoticed, especially among lower stream orders. Linearity is even important in the basins on the Edwards Plateau, such as Bee Creek. In these hill country basins dendritic patterns of linear erosion are incising into the stair-step topography of steep-sided hills. The incisions clearly reveal even the lower order channels, although thick brushy vegetation or strong hill slope shadow might more readily mask the linear nature of the channel. The absence of an ordered land use pattern in these basins means there is less opportunity for angular trending streams to stand out as the result of abrupt land use change along the stream course.

6) Erosion and minor soil change - In Coastal Plain basins both sheet and gully erosion reveal lighter colored soil horizons exposed by surface removal of over-laying darker soil horizons. These exposed lighter soil horizons have a higher albedo and a strong reflective response on both panchromatic, color and color IR photographs. These areas of light soil serve as a measure of the down slope movement of basin soils.

In the "Hill Country," erosion on the steep slopes of basins quickly removes the thin layer of soil and the highly reflective bedrock is exposed. Continual erosion over these exposed rock surfaces produces distinctive sub-basins in the sides of interfluves. The sub-basins have steep sides, a steep longitudinal profile, and this lends to easy interpretation of even low order streams on stereo-pairs of air photographs, when they are available.

At the time of aircraft imagery generation there had been no significant rain in over 35 days. The soils were dry in all basins, except for one small area along Wilbarger Creek where the soil had been wetted by agricultural practices. This area could be observed on the photographs and it is undoubtedly a valuable recognition characteristic of land use and stream location, especially in semi-arid to arid regions.

7) Tone and texture - Tone and texture are always cited as major photographic characteristics important for imagery interpretation. These characteristics have long been known to air photograph interpreters as principal recognition characteristics. Tone and texture are actually composites, integrating the signatures of all of the previously discussed factors by which we were able to delineate stream channels. The total effect is itself significant, especially in the basins of the Coastal Plain where drainage lines, because of differing vegetation, stand out dramatically from the smooth, even tones and textures of uniform agricultural fields. In the "Hill Country" basins the irregular nature of the vegetation and lack of uniform tone and texture associated with cultivated land does not lend itself to the contrasts of Coastal Plain basins. Tone, and in some cases, textural contrast is observable in the vegetation patterns of "Hill Country" basins, but it is subtle, and non-geometric. The valley floors are filled with alluvium and have an increased moisture content. The alluvium forms level terraces which support large, broadleaf trees and a mixture of species in a dense vegetation cover. Upward, on valley sides, thinner soils, increased runoff, droughty edaphic conditions produce varying ecological niches. Generally, this results in fewer species and smaller trees, more coniferous, and less broadleaf vegetation. In this case the lower order streams are in areas of less vegetation cover and this

makes their identification somewhat easier.

8) Pattern - The ordered pattern of agricultural land stands out in sharp contrast to the irregular, dendritic paths of stream channels in the Coastal Plain basins. These sinuous ribbons of land use change and break or interrupt the regular pattern of land use which makes it easier to identify stream channels. Such patterned features as meander scars and the dendritic fingers of first order erosion channels etched into an agricultural field make pattern an important element in channel recognition. On the Edwards Plateau, where land use is more irregular and areas of pattern are small or difficult to observe, this recognition characteristic is less important.

9) Scale - Scale, or really size of ground objects resolved, is the most difficult of all imagery recognition characteristics with which to deal. There is no doubt that as imagery scale increased or got larger, we were able to resolve more lower order stream channels. But very high altitude aircraft imagery still provides an effective means of measuring stream networks.

We had less luck with space imagery but even from spacecraft altitudes we feel that with increased spatial resolution it would be possible to do detailed stream network analysis. It is our belief that scale is the least important of the recognition characteristics discussed here, providing the sensor producing imagery has sufficient spatial and spectral resolution capabilities to record stream networks from the altitude at which it is operating.

We found 9 x 9 inch transparencies most useful in our study. A careful comparison of this imagery format with 70 mm photographs of the same area indicated that the smaller size contained all information available on the large photographs. However, information was easier to miss by the interpreter

because of its smaller size at this reduced scale.

10) Bedrock exposures - While freshly worked alluvium shows up on the photographs with a bright, strong response, bedrock is not always as apparent, especially if its surface is considerably weathered. Bedrock exposed in main channels may produce a strong signature, but in lower order channels there is seldom a response. Bedrock response is more apparent in basins on the Edwards Plateau than on the Coastal Plains. Reasons for these variations in response seem closely tied to vegetation along channel sides (especially along lower order streams), the degree of weathering of the bedrock, the amount of alluvium in the channel and type and nature of that alluvium. The type of bedrock itself is undoubtedly important as a recognition characteristic. A light colored limestone has a higher reflectivity than a dark colored granite.

Recommendations

The total effect of all these recognition characteristics, acting in concert, makes possible the identification of a nearly complete drainage network. Rarely is one of these characteristics solely responsible for the recognition of a stream channel. Rather it is the sum total of their presence or absence and integration over space that allows identification.

Some recommendations come to mind here if this study is replicated in other areas of the world. First, for areas with considerable local relief (hill or mountain terrain) it is mandatory to have considerable stereo coverage of the drainage basins under study. Subtle changes in relief are important in detailing drainage networks and, because of the high longitudinal gradient, even first order streams show up well in stereo coverage. This relief displacement is particularly important where lack of other recognition

characteristics (pattern, tone, texture, land use change) may be available. Generally, hill or mountain basins are covered with a more natural, less patterned, vegetation cover which might be quite dense and uniform in more humid areas. For such basins stereo coverage is absolutely necessary. We recommend stereo coverage for all drainage basin studies of steeply sloping terrain.

Stereo coverage is less important in flat and especially agricultural areas. Here longitudinal stream gradient is not great, relief is not so apparent and other recognition characteristics become more important. We recommend that single frame coverage is sufficient to do adequately detail studies of drainage basins in flat terrain, especially where there is intensive cultivation.

Light conditions are also important and vary with terrain. In steeply sloping areas shadows frequently mask complete hillsides making it impossible to determine lower order streams developing in these darkened areas. In areas of steep slopes we recommend that photographs be generated with the sun at its highest possible zenithal position for that latitude. The result would be to reduce the size and intensity of shadows on hill slopes to a minimum. In flat areas, where shadows are not large or intense, sun angle is less important. In fact we would follow the lead of other workers (Clark, 1971; Lyon and others, 1970) and suggest that photographs of plains areas should be generated with a relatively low sun angle, which would intensify shadow and aid in locating lower order stream channels.

MORPHOMETRIC PROPERTIES OF DRAINAGE BASINS AND STREAM NETWORKS

The quantitative geomorphic study of drainage basins developed largely from the work of R. E. Horton (1945). Horton resurrected the idea of Grevelius (1914) of classifying streams on the basis of bifurcation, or "order." Horton's ordering scheme has been modified to reduce the number of subjective decisions involved (Strahler, 1952), but the fundamental element on which the scheme is based, the first-order stream, remains the same. A first-order stream is an unbranched tributary - that length of channel furthest upstream which receives water only from overland flow. Second-order streams are defined at their upstream end by the intersection of two first-order streams, and at their downstream end by intersection with another second-order stream and so on for higher orders. In mathematical terms, ordering follows the rule that

$$0*0 = 0+1$$

where 0 is the order of any channel segment, * is the operation joining two segments, and segments without tributaries are assigned an order of 1.

Horton-Strahler ordering ignores contribution of lower order tributaries. This is an important hydrologic concern because increased discharge can arise by numerous junctions of a stream segment with lower order tributaries. Scheidegger (1966) calls this the problem of "lost stream segments." Shreve (1967) has developed an ordering scheme that may have much greater hydrologic significance. In his method of segment ordering, each outer link, i.e., first-order segment, is given a magnitude of 1. Each subsequent link is then given a magnitude equal to all its tributary first-order segments.

Although Lewin (1970) has criticized the Shreve system for ignoring inner links in the system, we will employ the method as hydrologic tool in the flood-response studies later in this report.

Based on the Horton/Strahler ordering scheme, many quantitative geomorphologists have investigated the geometric properties of drainage networks and formulated several empirical laws (Horton, 1945; Strahler, 1952, 1957, 1964; Schumm, 1956; Maxwell, 1960; Melton, 1957, 1959; Morisawa, 1959). The "laws" are well illustrated in the literature (Chorley, 1957). We will employ certain of these relationships as a descriptive tool for comparing the resolution of various types of imagery formats. The most fundamental relationship is the "law of stream numbers," which states that the number of stream segments of different orders in a specific basin tend to approximate an inverse geometric series in which the first term is unity:

$$N_o = R_b^{(s-o)}$$

where,

N_o = the number of stream segments of a given order, o

R_b = the bifurcation ratio, a constant for a specific basin, equal to N_o/N_{o+1}

s = the order of the highest order segment in a specific basin.

The result of the development and discussion of these empirical "laws" and others that have been postulated is that geomorphologists generally agree that drainage basins can be seen as orderly systems which tend to obey certain "laws" in their development, rather than as haphazard, random, or abstract patterns. Recently Shreve (1966, 1967, 1969), Scheidegger (1965, 1966), and Smart (1972) have approached drainage network analysis from purely mathematical point of view. They have suggested changes in the

ordering scheme to make it more mathematically consistent and have demonstrated by random simulation of branching networks that the most probable networks to develop are those which follow the various empirical relationships outlined above. Most of these studies emphasize network topology rather than network geometry.

NETWORK AND CHANNEL RESOLUTION

Leopold and Langbein (1963) noted that in geomorphic systems the ability to measure may always exceed any ability to forecast. Only a portion of a drainage network's form can be attributed to deterministic factors of geology and hydrology. The rest must be accounted for by topological randomness (Smart, 1969). In this study we are concerned with aspects of the network geometry that have adjusted to climatic and geologic factors. In the previous section we presented a qualitative assessment of various imagery formats for channel recognition. We will now present quantitative comparisons of network and channel resolution.

Previous Quantitative Studies of Drainage Network Definition

Detailed interpretation of drainage network geometry is the initial step in quantitative drainage basin studies, and is greatly influenced by the cartographic or photographic source on which the interpretation is based. The most precise data, of course, come from field determinations. Because these methods are slow and often costly, standard topographic maps have become a favorite source of data (see Slaymaker, 1966). But these have many problems associated with resolution. Morisawa (1959), for example, showed that 1:62,500 U.S.G.S. maps were unreliable for measuring nearly all morphometric properties except drainage basin area.

From their study of high density drainage basins in semi-arid New Mexico, Leopold and Miller (1956, p. 16) concluded that the definition of a first-order stream depends on the scale of map used in establishing the drainage hierarchy. They added that corrections could be made for less

accurate maps by utilizing a constant correction factor. Stall and Yang (1970) concurred with this result showing that data obtained from variously scaled maps are proportional. It is still not settled, however, as to whether a proportionality exists between small scale maps and the actual drainage net (Coffman and others, 1971, p. 4-11.).

Coffman (1970) suggested that the most consistent network definition results were obtained with 1:20,000 scale black and white aerial photographs. His most important result was that proportionalities between different mapping sources were quite variable. Properties were found to vary with different physiographic provinces. He concluded that topographic maps are incapable of showing a drainage system which is proportional to the real network.

The generally arduous nature of quantitative drainage network analysis has resulted in relatively few studies that compare network resolution on a variety of map and remote sensing imagery formats (Table 2). One of the purposes of the present investigation is to use streamlined computer procedures to generate network data more efficiently for this purpose than had been possible by manual techniques.

Gregory and Walling (1973, p. 47-48) note that the method used to obtain the drainage network definition (or drainage density) depends on the purpose of the analysis. A concern with topographic dissection would require the most accurate possible depiction. This might be contour crenulation identification from topographic maps. However, a concern for streamflow would emphasize functioning elements of the channel system, as opposed to functioning elements of the hillslope-interfluve system. The distinction is difficult to make, but it is critical to properly assessing the optimum data format for network analysis.

Table 2. Some studies of drainage network definition

Study	Results
Morisawa (1957)	Horton's (1945) "blue line method" does not incorporate all streams represented on a topographic map. For areas in the eastern U.S. there is no significant difference between the contour crenulation method and networks defined by field survey. The blue lines on topographic maps should not be used to give networks for basins smaller than 7 km^2 in area.
Giusti and Schneider (1962)	Demonstrated that the number of first-order streams per square kilometer in the Piedmont province varied from 0.14 to 3.2 on map scales ranging from 1:250,000 to 1:24,000 respectively.
Eyles (1966)	Comparison of 1:62,500 scale maps with aerial photographs in Malaysia revealed that the topographic maps gave highest drainage density values on granite outcrops while aerial photographs showed that densities on these rocks were the lowest in the study region.

Table 2 (cont'd)

Study	Results
Selby (1968)	Drainage densities of 5.4 measured from aerial photographs compared with densities of 2.8 from 1:15,840 topographic maps in New Zealand.
McCoy (1969, 1971)	Compared with 1:24,000 scale topographic maps, reliable estimates of stream lengths and drainage density can be obtained from edge-enhanced radar imagery.
Coffman (1970)	Using 1:20,000 scale aerial photographs as a standard, he found the "blue-line stream" method identified very few first- and second-order streams, 1/3 of the third-order streams, and almost all of the fourth-order streams in Indiana watersheds. The "method of V's" identified 1/4 of the first-order streams, 1/2 of the second-order streams, and nearly all third- and fourth-order streams.

In central Texas we assume an overland flow model for run-off. In contrast to many humid regions of thick soils, dense vegetation, and prolonged precipitation, the Hill Country of central Texas does not follow the throughflow model of dynamic drainage density adjustment to storm input (cf. Gregory and Walling, 1973). Thus, it appears that the resolution problem must be studied functionally, in relation to predicting streamflow. Moreover, it must be studied economically in terms of a resolution/cost ratio that might be defined as follows:

$$\frac{\text{total number of stream segments identified in an area}}{\text{cost in time and money of completing the survey.}}$$

Stream Network Definition Studies in Central Texas

In order to quantitatively compare the resolution capabilities of various imagery formats and to later evaluate flood response, we selected specific study basins which met as fully as possible the following criteria: (1) a workable number of morphometric data points within the basin, which is a function of drainage density and drainage area; (2) homogeneous rock type within the basin; (3) no large-scale alteration of the natural drainage network by urbanization, agricultural practices, or surface water control structures; (4) availability of remote sensing imagery covering the basin; and (5) availability of flood peak data. Approximately 30 basins were investigated (Table 3), although many basins could only be examined on a single type of imagery. Information contained in the basin drainage maps was used (1) as a measure of resolution for a given type of imagery, and (2) as a basis for flood-response investigations. Special attention was

Table 3. Summary of morphometric data compiled from central Texas drainage basins.

Basin Name	Drainage Area Km^2	Drainage Density Km/Km^2	Magnitude Ms	Relief m	Relief Ratio	Geology	Source -Compiler
Bee Creek	8.2	7.8	316		.03	Glen Rose Ls.	Stereo Pairs-MP
Wilbarger Creek	14.3	2.1	24		.01	Austin Chalk	7.5' Topo-SH
Upshaw Creek	13.4	3.85	105		.017	Schist	7.5' Topo-PP
Rinard Creek	20.1	4.4	186	72.5	.011	Pecan Gap-Taylor	7.5' Topo-ML
Pier Branch	13.6	3.8	123	73.2	.015	Glen Rose Ls.	7.5' Topo-ML
Nancy Creek	9.6	7.2	221	171.0	.031	Edwards Plat.	7.5' Topo-CT
Satan Creek	4.9	4.3	135	57.0	.011	Edwards Plat.	7.5' Topo-CT
Milam Branch	10.7	3.6	103	18.0	.003	Coastal Plain	7.5' Topo-CT
Hasting Creek	9.3	5.0		35.4	.011	West	7.5' Topo-SS
Johnson Branch	7.0	4.7		39.6	.013	Coastal Plain	7.5' Topo-SS
#1 South Cow Bayou	9.3	3.3	109	82.3	.012	Austin	7.5' Topo-SB
#2 South Cow Bayou	9.7	1.3	38	45.7	.003	Taylor	7.5' Topo-SB
Ripstein Creek	18.4	3.3	110	73.2	.015	Edwards Plat.	7.5' Topo-SD
Can and Dry Can Creeks	17.9	4.7	192	146.4	.030	Edwards Plat.	7.5' Topo-SD
Sycamore Canyon	44.0	4.2	280	152.4	.020	Edwards Plat.	7.5' Topo-SD
Walnut Tributary	1.9	9.3	72	30.5	.030	Gullied Taylor	7.5' Topo-Class
Dry Creek (Austin)	5.5	5.1	68	91.4	.050	Glen Rose Ls.	7.5' Topo-Class
Bergstrom AFB	8.9	2.8	38	33.5	.012	Coarse Gravel	7.5' Topo-Class
Pin Oak Creek	34.6	3.4	215		.002	Wilcox	7.5' Topo-Class
Dry Creek Buescher Lake	8.6	7.4	82		.015	Coastal Plain	7.5' Topo-SH
Dry Prong Deep Creek	22.0	2.4	90		.021	Permian	7.5' Topo-PP
Deep Creek No. 8	14.2	2.1	48		.014	Permian	7.5' Topo-PP
Clear Creek	27.5	6.98		220.0	.022	Igneous-Mmic	7.5' Topo-CW
a. Gneiss/Granite	1.0	7.56		91.4	.037	Gneiss	7.5' Topo-CW
b. Schist	1.0	6.53		61.0	.030	Schist	7.5' Topo-CW
Upper Bee Creek	2.93	6.17	82		.03	Glen Rose Ls.	7.5' Topo-CW
Schweiner Creek	17.0	4.5	131	146.4	.028	Sandstone & clay	7.5' Topo-KG
Antelope Creek	38.8	4.7	299		.027	Limestone	7.5' Topo-KG
Lang Creek	31.9	5.6	249		.039	Granite/gneiss	7.5' Topo-KG
Bear Creek	61.1	3.9	370		.033	Limestone	7.5' Topo-KG
Onion Creek	57.7	4.9	430		.053	Limestone	7.5' Topo-KG

given to the resolution capabilities of small-scale, orbital imagery formats in comparison to suborbital imagery, conventional aerial photographs, and topographic maps. The drainage map information was then transformed to numerical data and analyzed by the W.A.T.E.R. program, a system of computer programs for watershed analysis developed at Purdue University and the University of Toronto (Coffman and others, 1971). Geomorphic parameters calculated by the W.A.T.E.R. program were later correlated with flood peak estimates.

In the following sections we will discuss the definition of drainage networks in detail for selected study basins.

Bee Creek Study Area.--As a baseline for evaluating the resolution capabilities of various scales and types of drainage network data sources, a number of detailed studies were completed on Bee Creek, a small tributary of the Colorado River near Austin, Texas. The most detailed imagery analysis utilized low altitude black and white aerial photographs at 1:13,000 scale. Photographic mapping on stereo pairs was used to interpret the most subtle changes in shadow that could be interpretated as a stream channel. Besides the continuous channel network, the small discontinuous gullies which develop on the slopes of Bee Creek were easily interpreted from the stereo pairs. The resulting drainage map (Figure 18) resolved 316 unbranched tributaries (first-order segments or 1st magnitude links) in the continuous network exclusive of the hillslope gully system. The total number of first-order collectors, discontinuous gullies plus first-order segments, was approximately 1000.

The topographic map used as one mapping source was the Austin West Quadrangle, with a 1:24,000 scale and 20 foot contour interval (Figure 19).

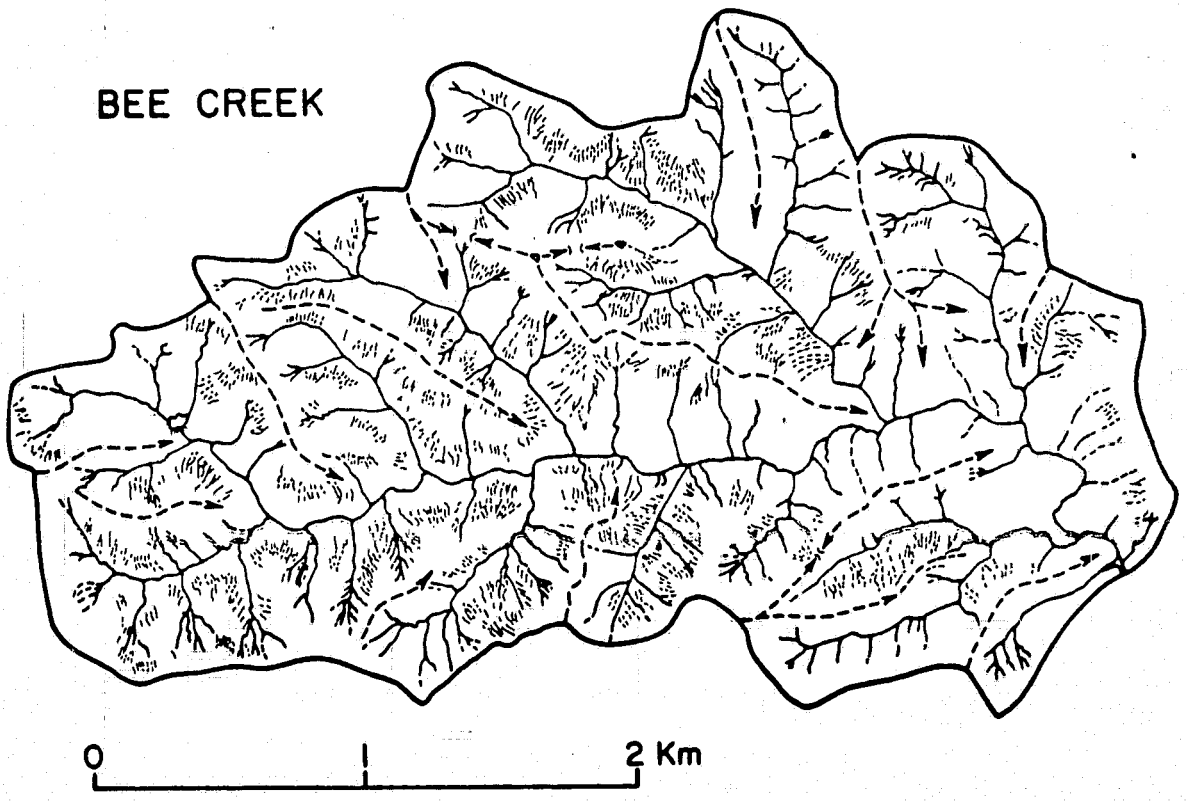

Figure 18. Drainage map of Bee Creek constructed by detailed stereoscopic interpretation of a pair of low altitude black and white aerial photographs at 1:13,000 scale.

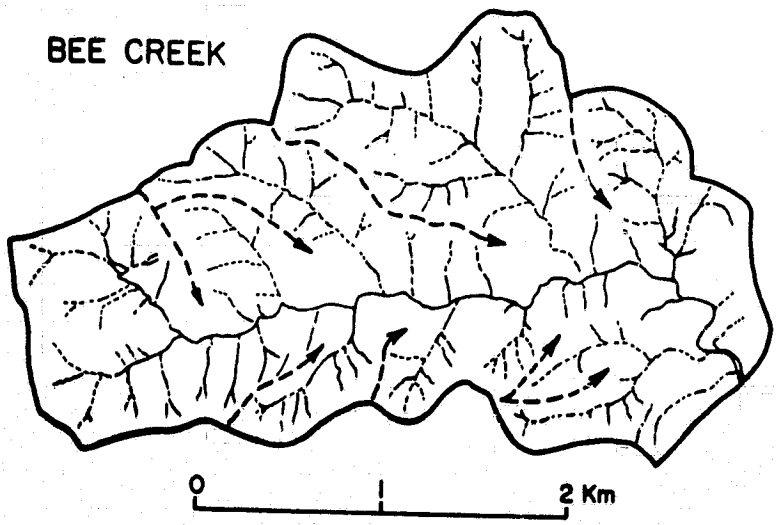

Figure 19. Drainage map of Bee Creek constructed by the "method of V's" using the Austin West 7.5' topographic quadrangle map (1:24,000).

The more detailed drainage network interpreted from the stereo pairs was due to several factors, all of which stem from limitations inherent in any cartographic mapping base. Subtle changes in shadow on the black and white photos allowed interpretation of low-order channels which do not fall more than 20 feet, and thus do not produce contour line crenulations on topographic maps using a 20 foot contour interval. The vegetation in Bee Creek Basin is uniformly brushy except where ledges of flat-lying limestone crop out. These ledges can be used almost as contour lines as an aid in interpreting channels. Where particularly heavy vegetation obscured slopes and channels, higher order reaches could be integrated into the drainage network as a whole, but first-order channels could not be distinguished. Besides the continuous channel network, the small discontinuous gullies which develop on the slopes of Bee Creek could be interpreted from the stereo pairs.

A variety of N.A.S.A.-generated remote sensing imagery was also examined for Bee Creek. Suborbital imagery (Figure 20) revealed the greatest number of first-order streams with the RC-8 camera, using film in the reflective infrared (Baker and others, 1974). However, the network maps reveal that the lengths of the first-order streams recognized by monoscopic viewing of infrared transparencies at 1:48,000 scale are 50% or less of the first-order stream lengths recognized at the larger scale on the topographic map. The tips of the first order streams were apparently obscured by dense vegetation on the infrared imagery.

Orbital imagery (Figure 21) revealed the considerable resolution capabilities of the S-190B camera over the S-190A. Over 44 first-order streams were identified on the S-190B frame, compared to 14 on the S-190A, 109 on the topographic map, and 316 on the detailed low altitude stereo pairs

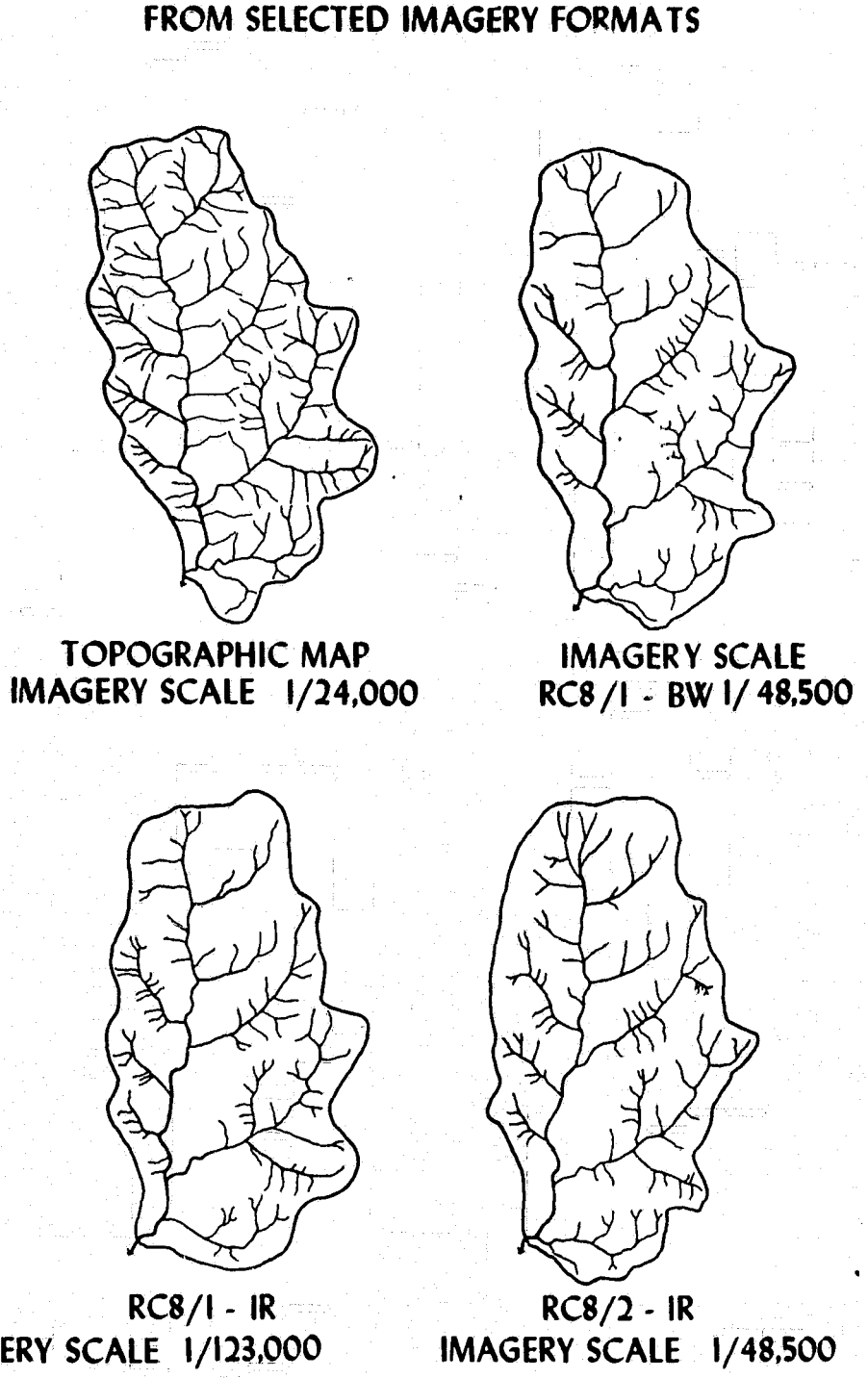

Figure 20. Drainage maps of upper Bee Creek derived from sub-orbital imagery sources. The maps show a drainage area of 6.9 miles^2 compared to the total basin area of 8.8 miles^2 (Figures 18 and 19).

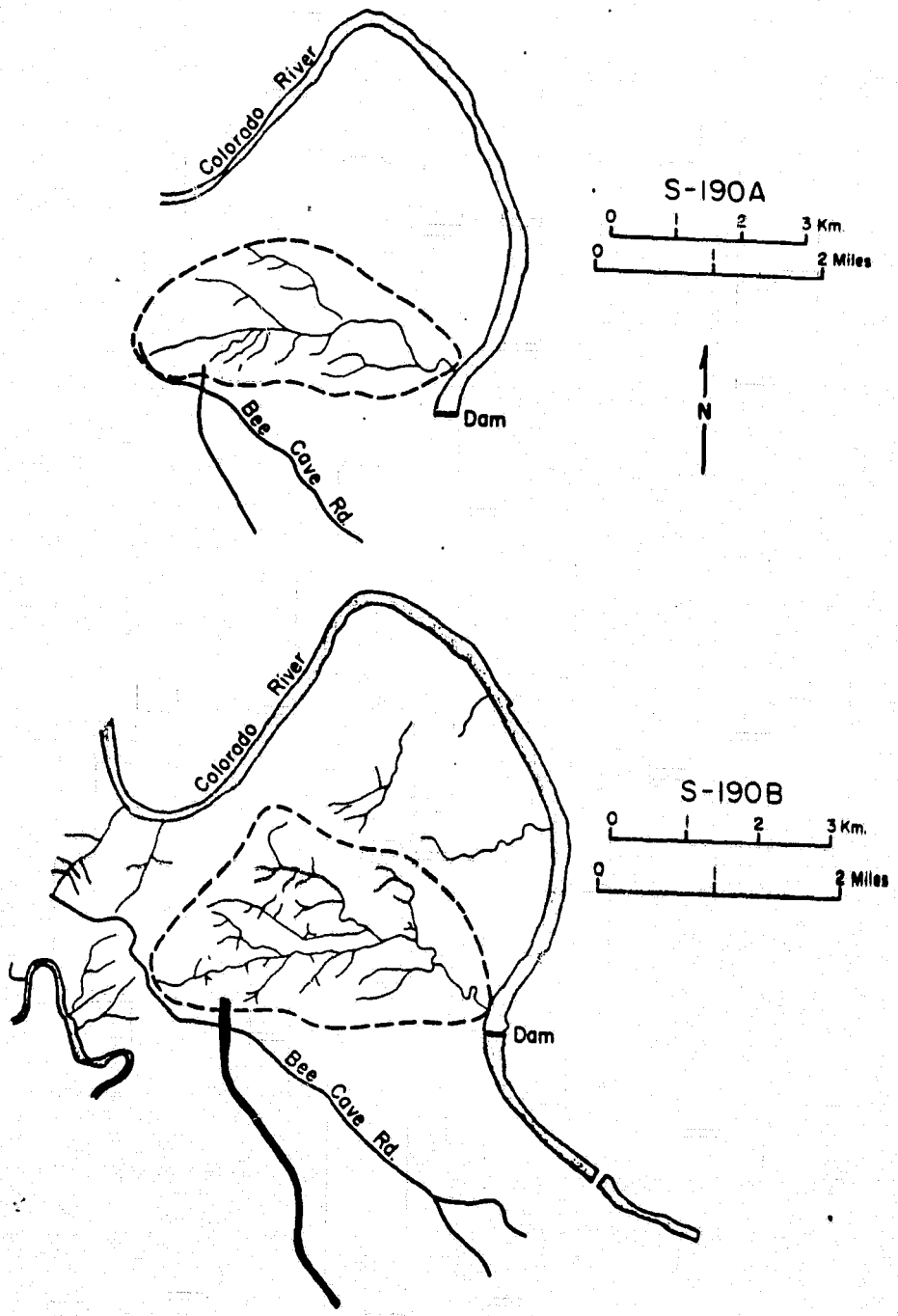

Figure 21. Drainage maps of the Bee Creek basin: (A) Skylab S-190A, high resolution color film SO-356 with FF filter, enlarged from 9"x9" format to scale 1:56,000, (B) Skylab S-190B, roll 94, frame 123; the original 9"x9" transparency was enlarged to 1:48,480 scale.

of panchromatic photographs. Resolution over the whole range of orders is illustrated in Figure 22.

Dry Creek at Buescher Lake.--This basin was analyzed by topographic map at 1:62,500 scale, and by orbital imagery (Figure 23). Resolution over various stream orders is illustrated in Figure 24.

Upshaw Creek.--This basin was analyzed by topographic map at 1:24,000 scale (Figure 25), Skylab S-190A (Figure 26), and suborbital infrared imagery. Resolution over various stream orders is illustrated in Figure 27.

Dry Prong Deep Creek.--This basin was analyzed by topographic map at 1:62,500 scale (Figure 28), suborbital N.A.S.A. color imagery (Figure 29), Skylab S-190A (Figure 30A), and Skylab S-190B (Figure 30B). Resolution over various stream orders is illustrated by Figure 31.

Wilbarger Creek.--This basin was analyzed on Skylab S-190B imagery (Figure 32) and by 1:24,000 scale topographic map. Apparently because of low relief in this area, the resolution of orbital imagery compared quite favorably with that of the large scale topographic map (Figure 33).

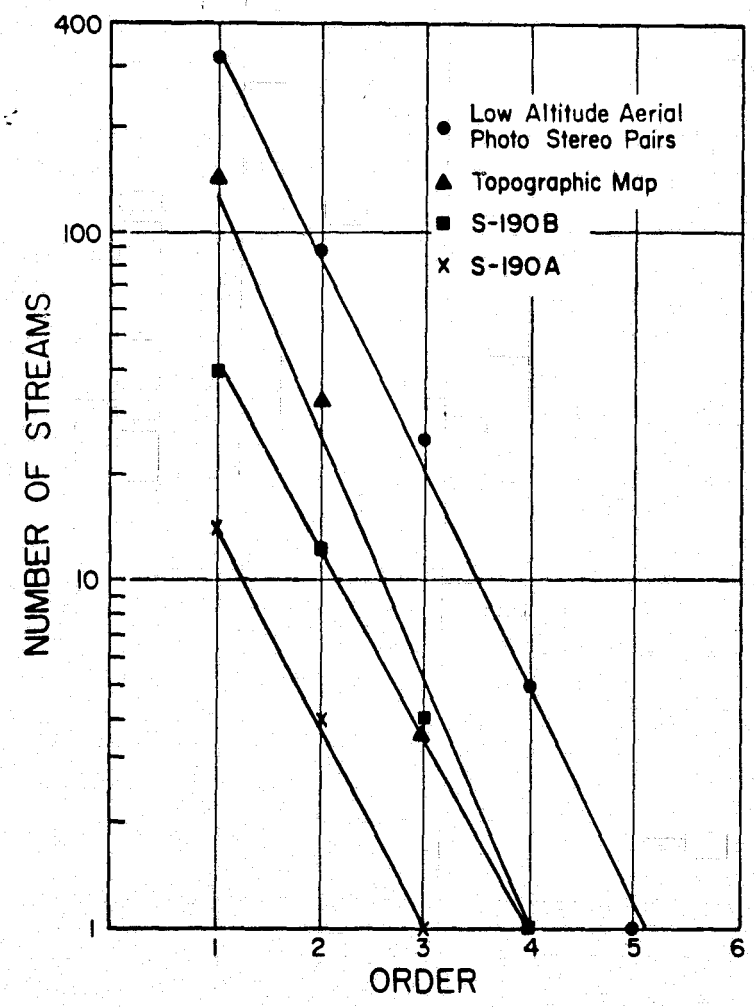

Figure 22. Horton's law of stream numbers for Bee Creek networks mapped from various imagery sources.

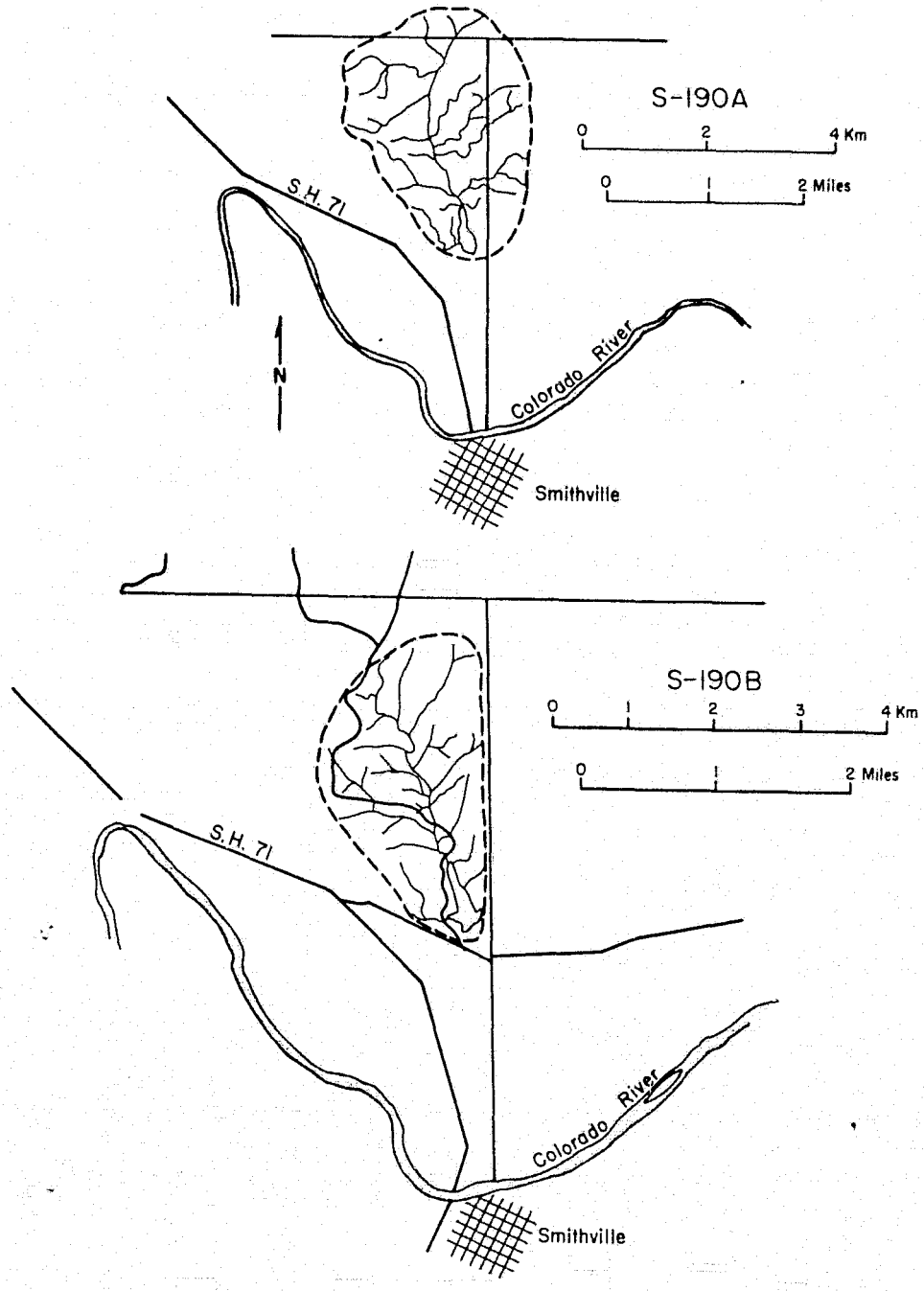

Figure 23. Drainage maps of the Dry Creek basin: (A) Skylab S-190A, high resolution color film SO-356 with FF filter, scale 1:77,600, (B) Skylab S-190B, roll 94, frame 125, 9"x9" transparency analyzed at 1:40,625 scale.

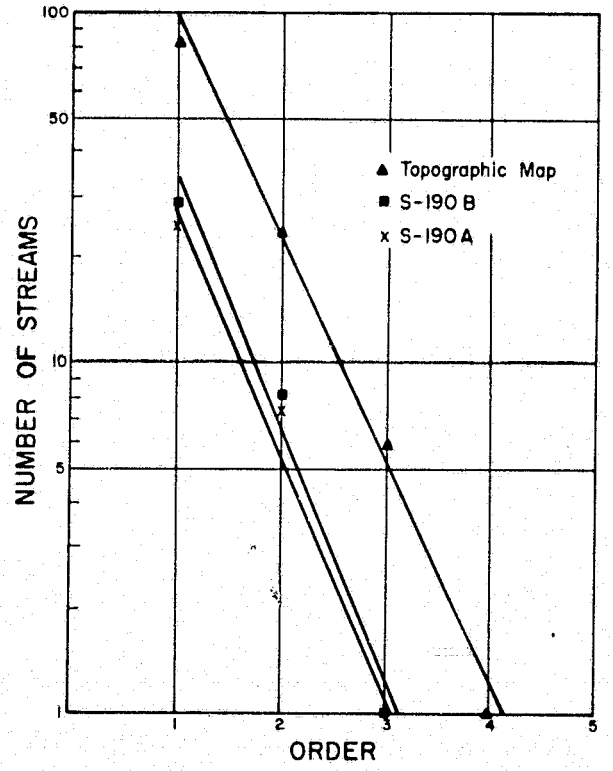

Figure 24. Horton's law of stream numbers for Dry Creek networks mapped from various imagery sources.

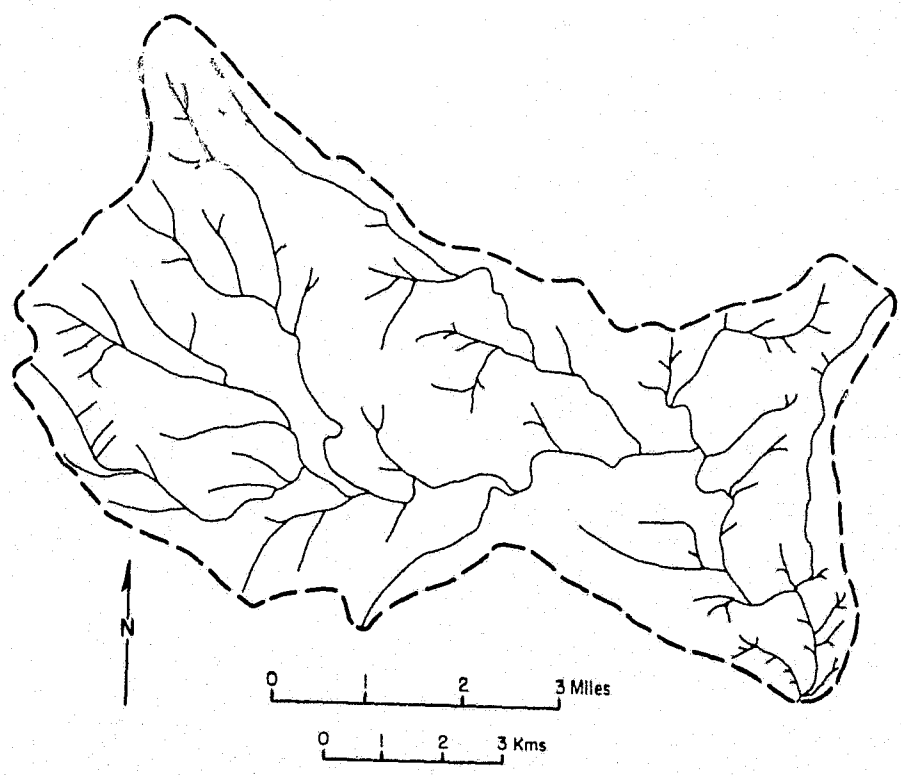

Figure 25. Drainage map of Upshaw Creek constructed by the "method of V's" using the Click, Dunman Mountain 7.5' topographic quadrangle map.

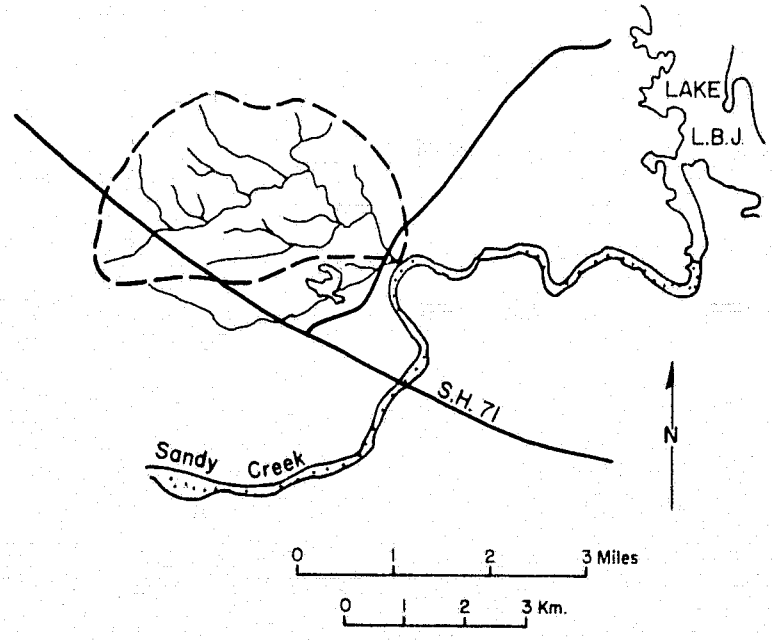

Figure 26. Drainage map of the Upshaw Creek basin constructed by analysis of Skylab S-190A imagery (high resolution color film SO-356 with FF filter) at 1:58,378 scale. Original 9"x9" formats were enlarged by procedures described in text.

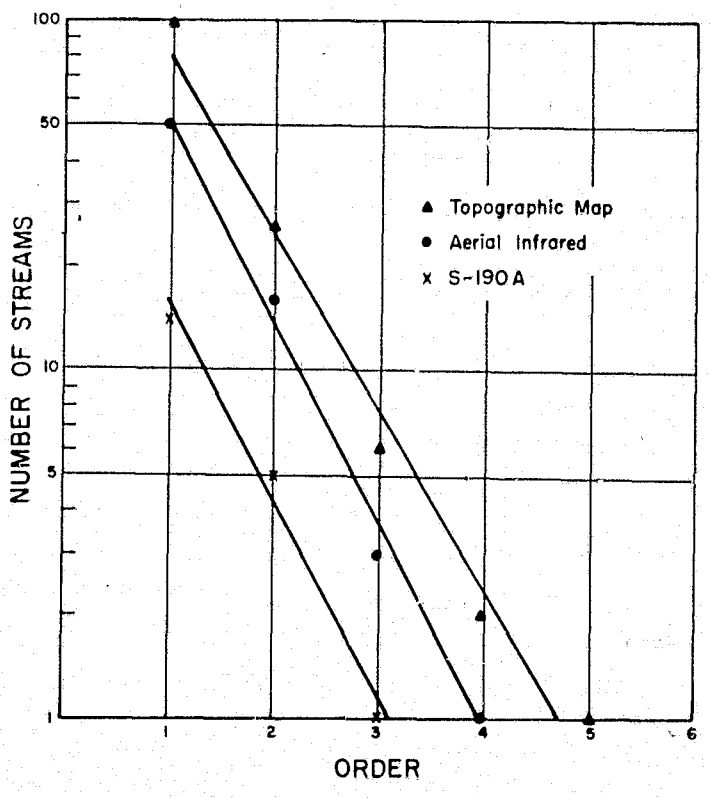

Figure 27. Horton's law of stream numbers for Upshaw Creek networks mapped from various imagery sources.

Figure 28. Drainage map of Dry Prong Deep Creek constructed by the "method of V's" using a 1:62,500 scale topographic map.

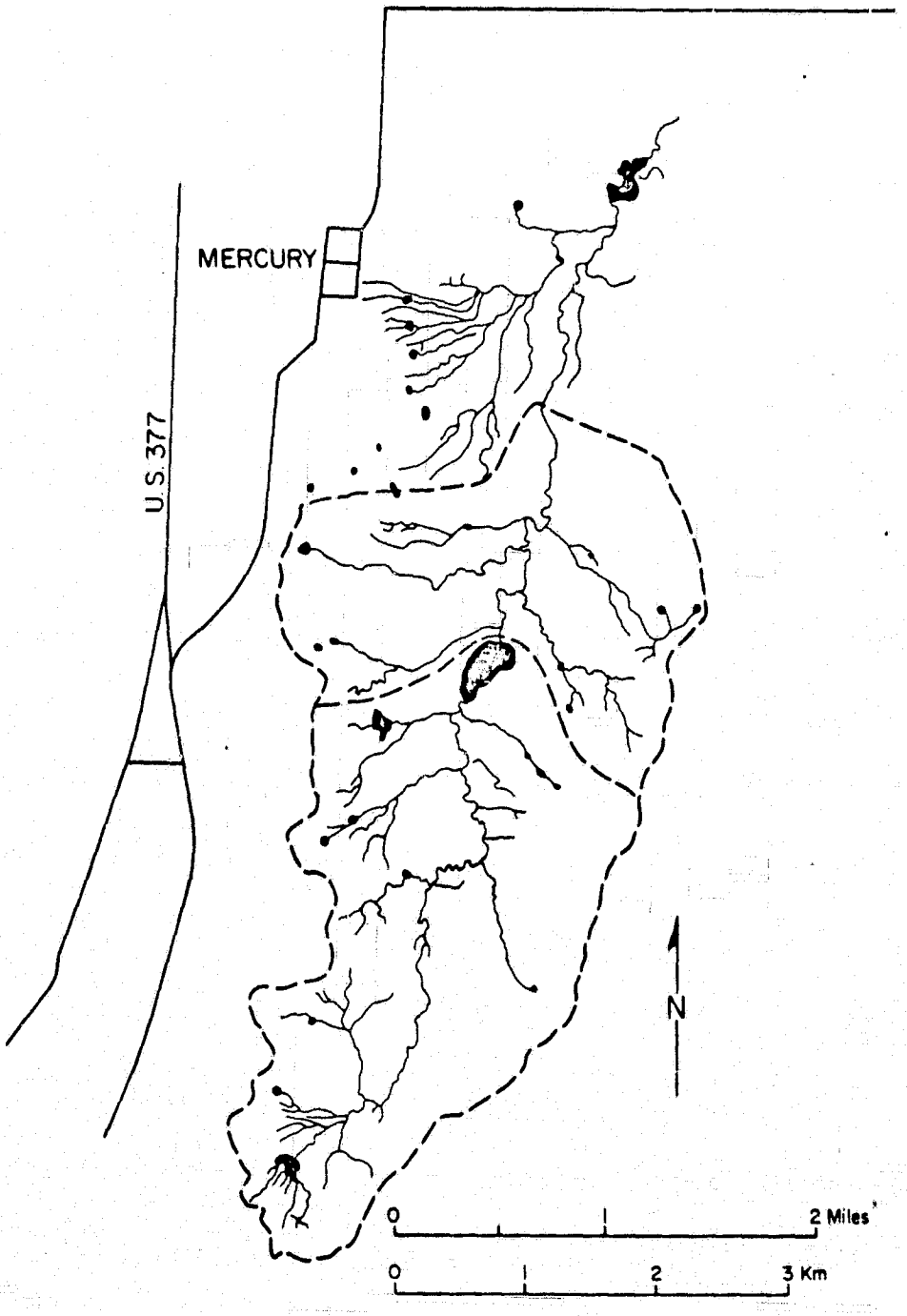

Figure 29. Drainage map of Dry Prong Deep Creek constructed from a N.A.S.A. color infrared image in 9"x9" format at 1:24,768 scale (Aircraft mission 261, image RL13-D017, RC8 camera).

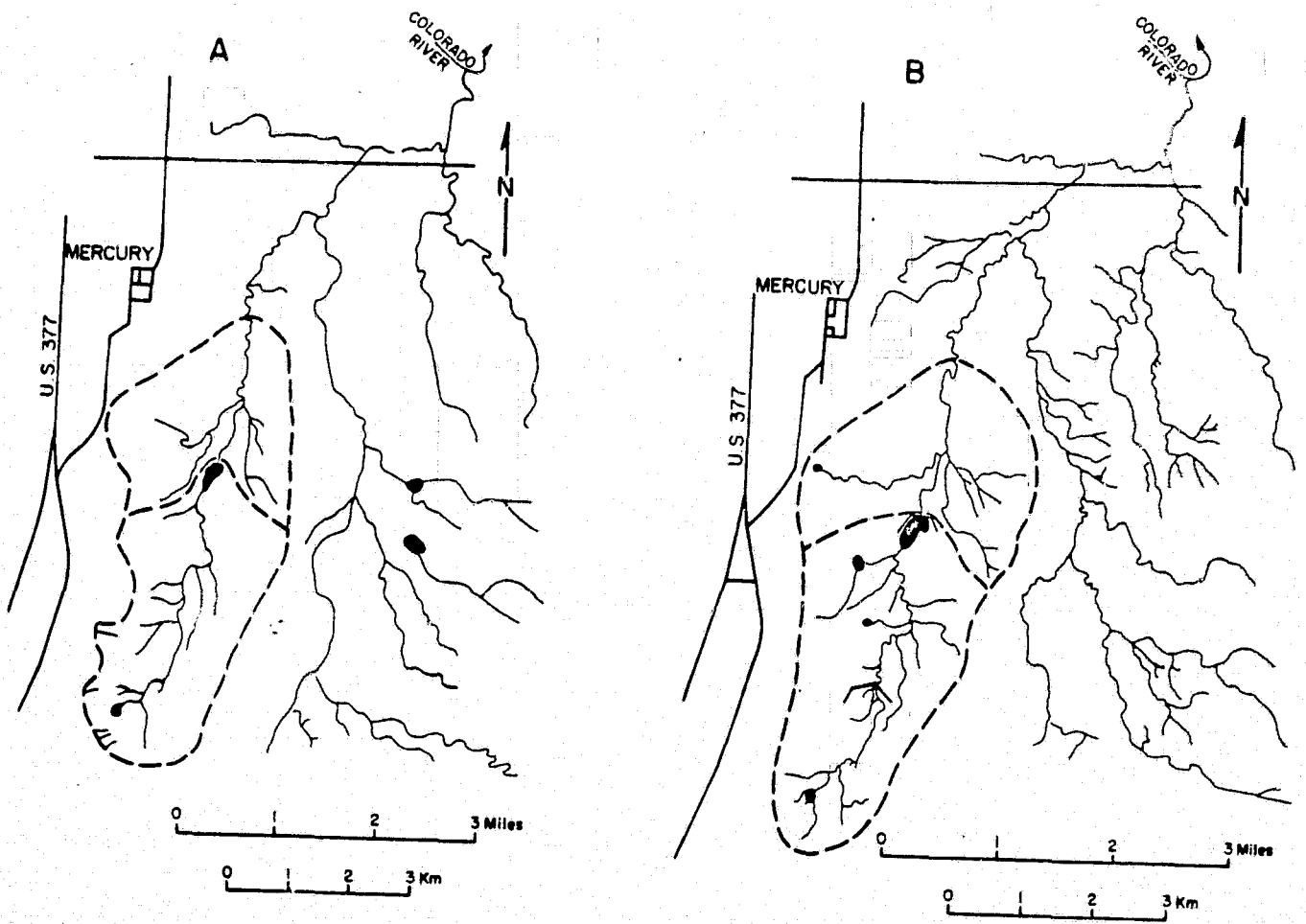

Figure 30. Drainage maps of the Dry Prong Deep Creek basin constructed from the following imagery formats: (A) Skylab SL-4 S-190A enlarged to 1:53,879 scale from 9"x9" format (high resolution color film SO-356 with FF filter), (B) Skylab SL-4 S-190B, roll 94, frame 123; the original 9"x9" transparency was enlarged to 1:45,625 scale.

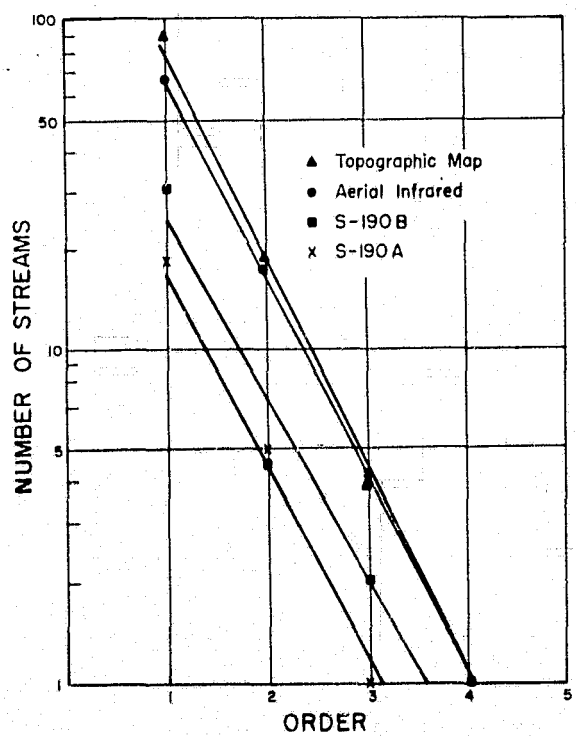

Figure 31. Horton's law of stream numbers for Dry Prong Deep Creek networks mapped from various imagery sources.

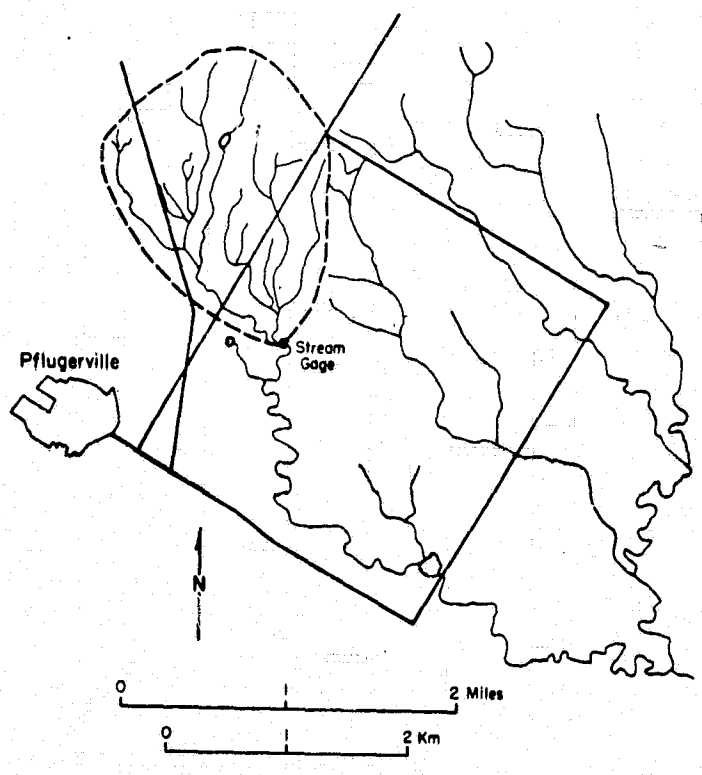

Figure 32. Drainage map of Wilbarger Creek based on analysis of Skylab S-190B imagery, roll 94, frame 123, 9"x9" transparency enlarged to 1:48,480 scale.

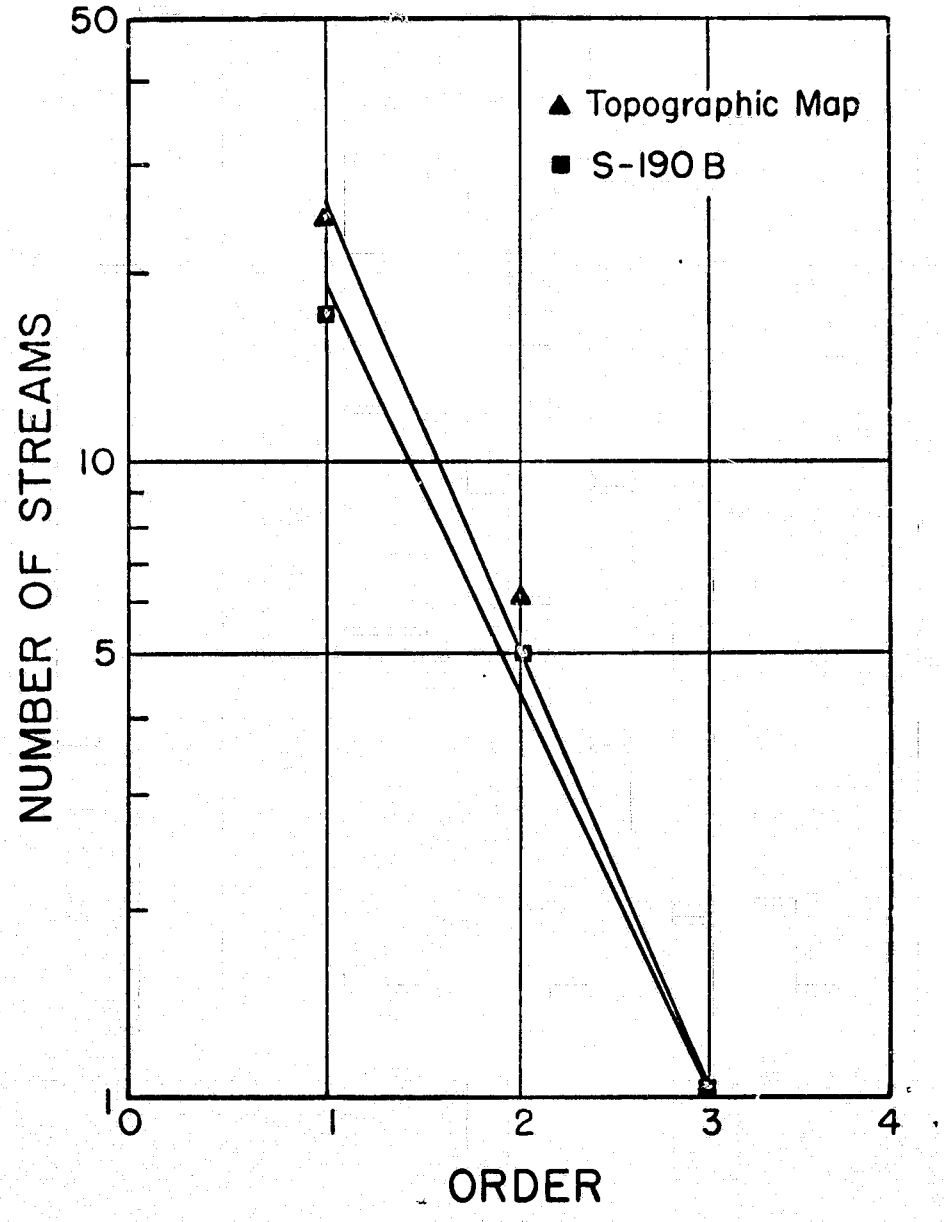

Figure 33. Horton's law of stream numbers for Wilbarger Creek networks mapped from various imagery sources.

Field Surveys of Stream Channels and Drainage Networks

To establish an absolute basis for resolution drainage networks on various scales and types of imagery, we performed several detailed field surveys of selected subbasins. Four areas were chosen from the Bee Creek basin for field mapping (Figure 34). The features which acted as first-order stream segments in the field were found to be precisely those segments mapped as discontinuous gullies in the detailed stereoscopic interpretation of low altitude black and white aerial photographs (Figure 18). The gullies were found to average 30 meters in length and were characterized by broad shallow valleys cut in rock (Figure 35).

Stream frequency is equal to the summation of stream segments per unit area. For Bee Creek the topographic map analysis yielded a first-order channel frequency of 31 per square mile, whereas the detailed mapping by tape and compass survey in the field indicated a first-order gully frequency of 290 per square mile. The mapping on stereo pairs of low-altitude panchromatic imagery (Figure 18) had indicated a first-order gully frequency of 310 per square mile.

Two additional high density, gullied basins were examined in the field. Rinard Creek (Figure 36) is located on the Pecan Gap Member of the Taylor Formation. This unit has a low permeability and is locally gullied, possibly as a result of land-use practices which remove native vegetation for agricultural purposes. A detailed map of a gullied subbasin (Figure 37) shows numerous first-order gully segments which average 70 meters in length. The gullies have discontinuous gradients and small headcuts which appear to be actively extending the network. The frequency of gullies in the field

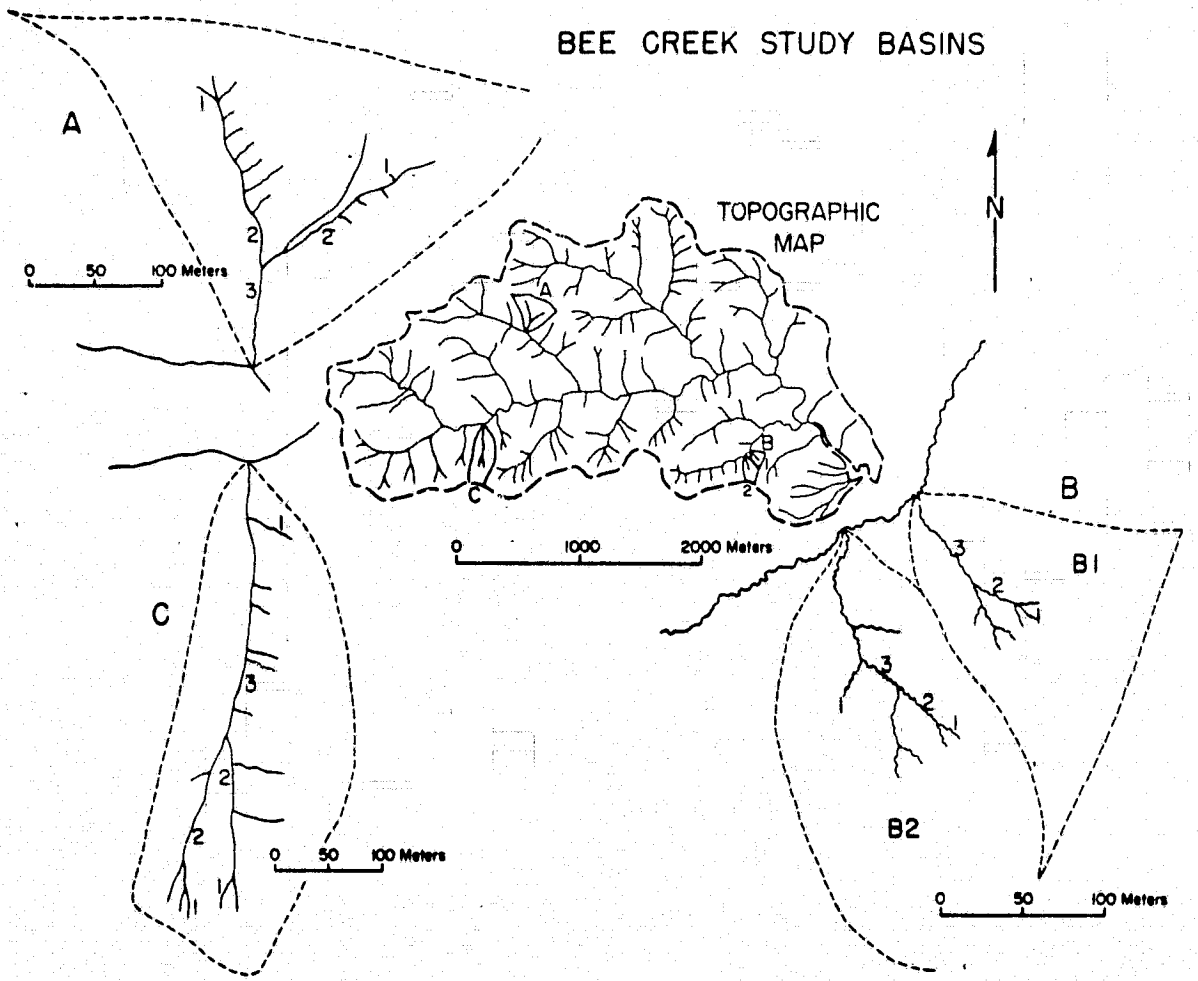

Figure 34. Subbasins of Bee Creek analyzed by detailed field survey. Stream lengths were measured mostly by pacing and compass technique. Heavy vegetation made mapping by tape survey extremely tedious.

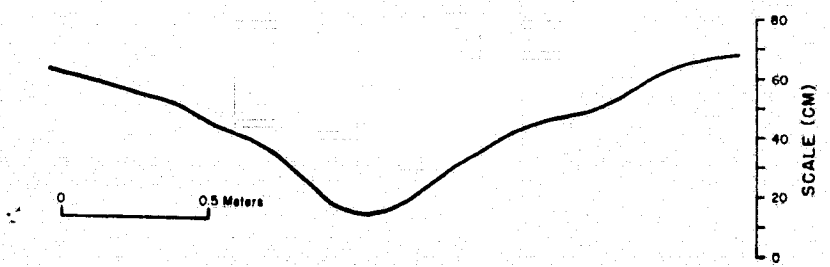

Figure 35. Measured cross section of a first-order gully in the Bee Creek drainage basin.

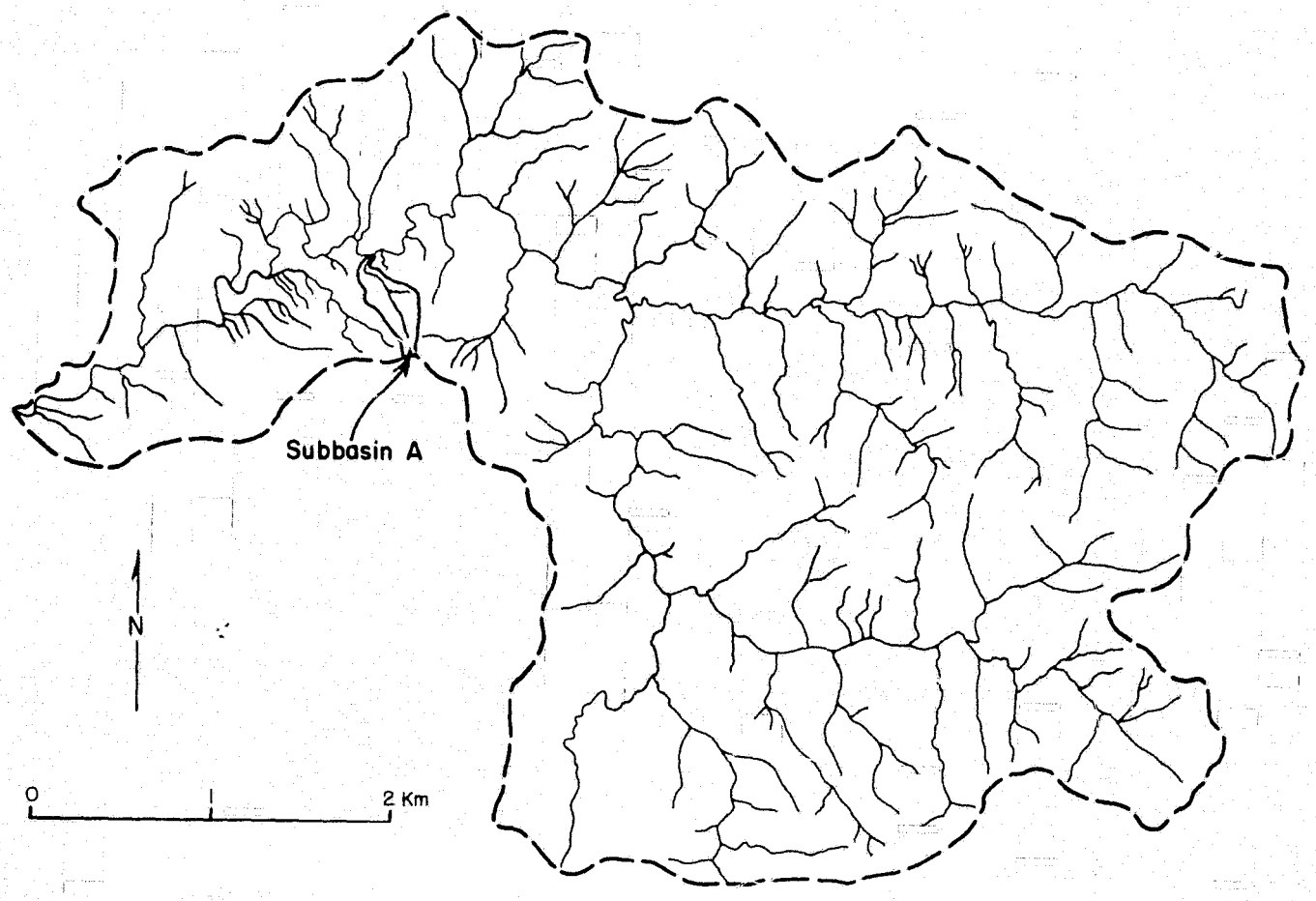

Figure 36. Drainage map of Rinard Creek constructed by the "method of V's" using the Oak Hill and Buda 7.5' topographic quadrangle maps. The location of Figure 37 is designated "Subbasin A."

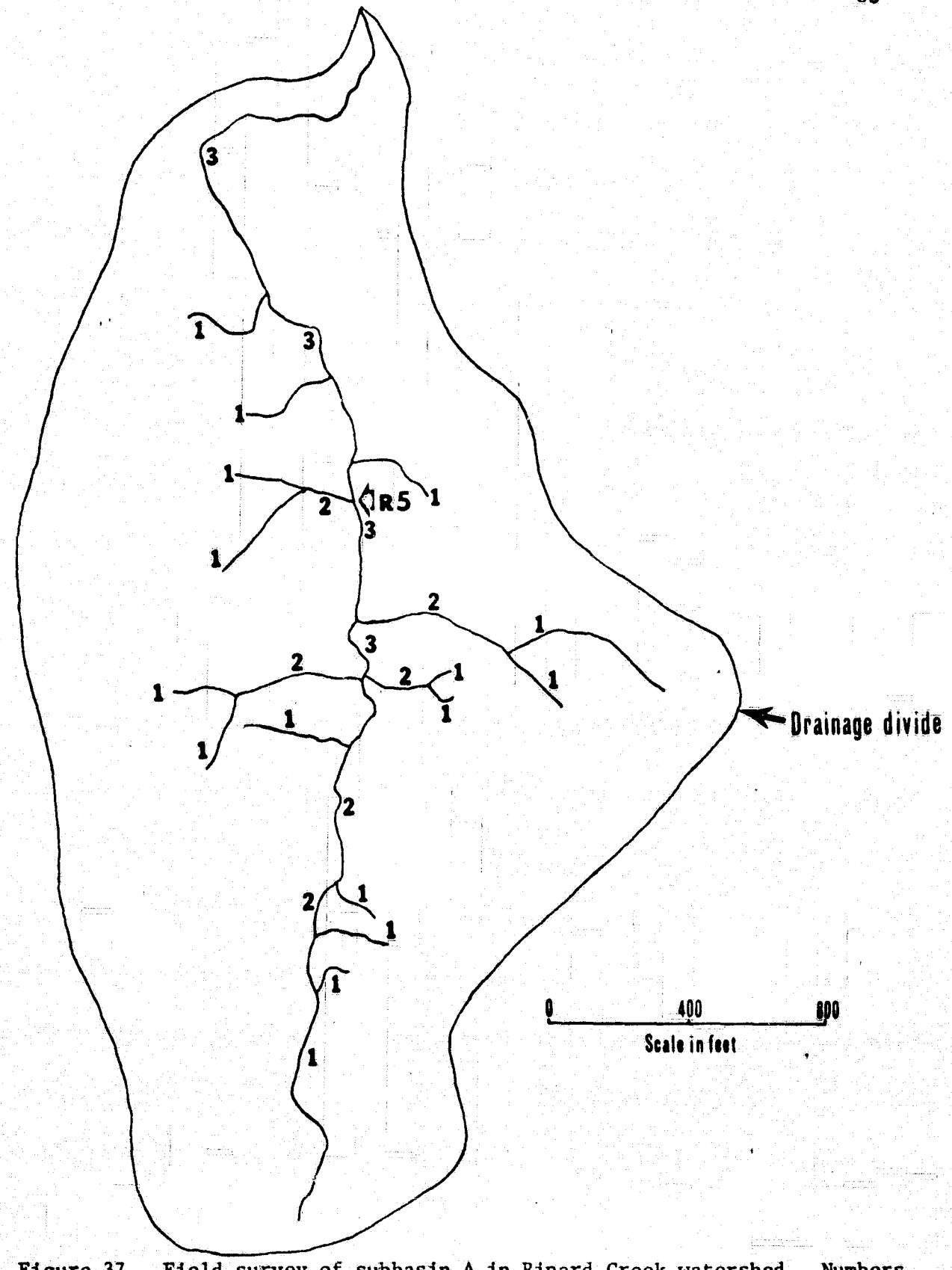

Figure 37. Field survey of subbasin A in Rinard Creek watershed. Numbers show Strahler ordering of stream segments.

subbasin area was 130 per square mile compared to a first-order stream frequency of 23 per square mile measured from the topographic map. Linear extrapolation of the subbasin data to the entire 7.77 square mile basin would indicate a total number of gullies equal to 1003. The result is strikingly similar to the number of small gullies observed in the Bee Creek basin (Figure 18).

Pier Branch is located on the Glen Rose Formation, an alternating sequence of thin to medium bedded hard limestone interbedded with marl and marly limestone. The topographic map analysis (Figure 38) identified 123 first-order streams in a drainage area of 5.32 square miles for a first-order channel frequency of 23 per square mile. Detailed field mapping of a subbasin (Figure 39) indicated a first-order gully frequency of 265 per square mile. Average gully length was found to be 100 meters. The gradients of individual gullies are highly irregular, and are often broken by rock ledges and dams of coarse debris blocking the channels. Many gullies are so choked with vegetation that they would be extremely inefficient in conveying surface runoff into the network stream channels.

The field studies show that all forms of imagery for drainage network mapping fail to adequately depict the high density gully system that characterizes the high relief study basins. These gullies generally range from 30 to 100 meters in length and were only mapped in detail by stereo observation of very low altitude photography (Figure 18). Most of the gullies studied in the field would result in an order of magnitude increase in first-order stream frequency for a given basin. However, the hydrologic significance of the gullies is certainly much less than that of the continuous channel network. The gullies probably constitute a channel flow component

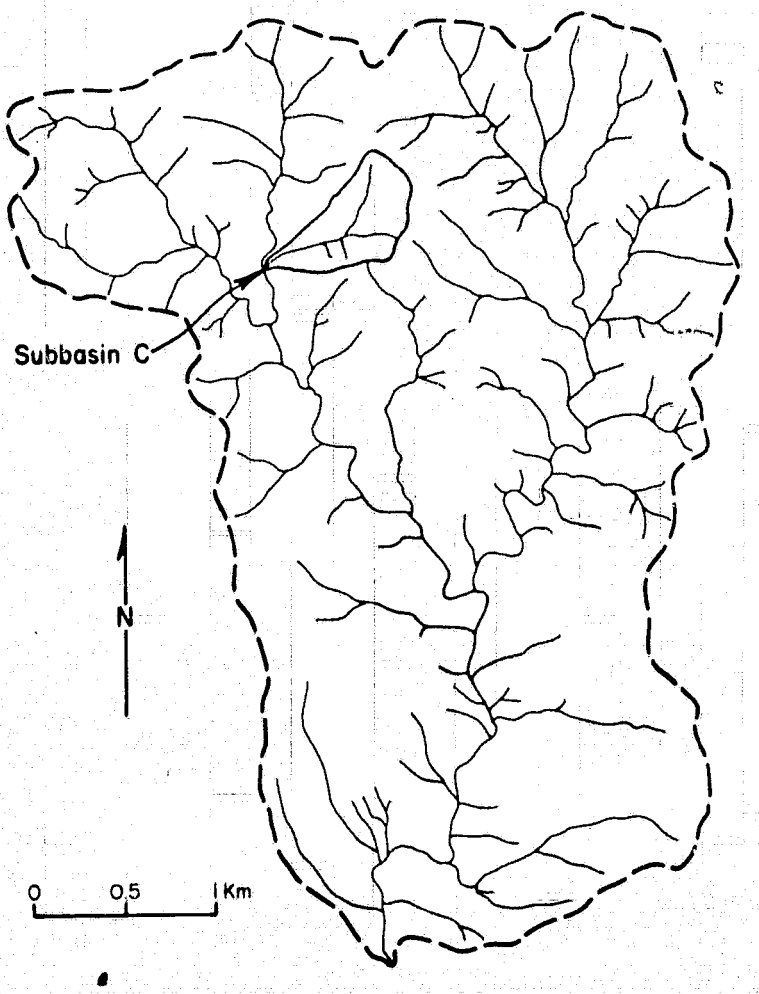

Figure 38. Drainage map of Pier Branch constructed by the "method of V's" using the Dripping Springs 7.5' topographic quadrangle map. The location of Figure 39 is designated "Subbasin C."

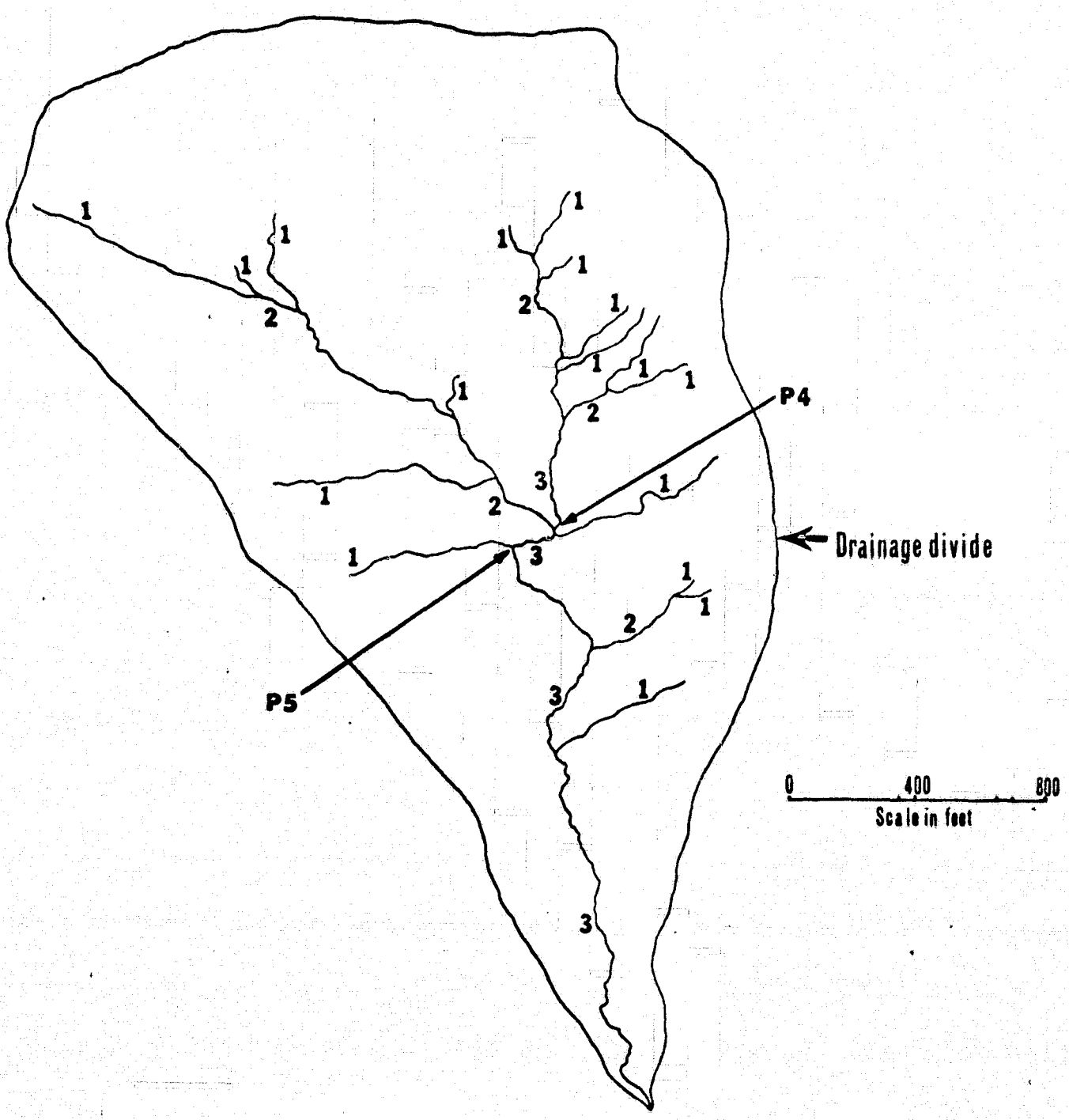

Figure 39. Field survey of subbasin C. in Pier Branch watershed. Numbers show Strahler ordering of stream network segments.

of local hillslope hydrologic systems. Their high channel roughness and irregular gradients clearly distinguish them from the more efficient stream channel system that is accurately displayed on the small scale imagery.

Drainage Network Resolution from Orbital Imagery

We selected seven drainage basins for study using Skylab imagery. Basins were selected that had also been mapped from suborbital imagery and also from topographic maps. Basins studied from orbital imagery included (1) Bee Creek near Austin, (2) Wilbarger Creek near Pflugerville, (3) Dry Creek at Buescher Lake near Smithville, (4) Dry Prong Deep Creek near Mercury, (5) Deep Creek subwatershed no. 8 near Mercury, (6) Mukewater Creek near Bangs, and (7) Upshaw Creek near Lake L.B.J. Drainage maps for most of these basins have already been presented.

We experimented with several techniques in order to gain the maximum resolution from the S-190A camera. Using mostly the ektachrome images in 9"x9" format, mapping was attempted using (1) a light table with a magnifying lens, (2) a Bausch and Lomb zoom transfer scope, (3) photographic enlargements of both ektachrome and color infrared images, and (4) an overhead projector. The overhead projector provided the best results. Transparencies were taped on the projector and projected approximately 25 feet onto large sheets of white paper from which tracings of the drainage networks were made. The scale of the resulting enlargement ranged from 1:47,600 to 1:58,380.

Of the seven basins chosen for study, two (Mukewater and Wilbarger) could not be easily identified on the S-190A transparencies. With more sophisticated enlargement procedures these basins could probably be identified. For each of the remaining five basins, the following variables were

measured: (1) drainage area, (2) Strahler order, (3) Shreve magnitude (number of first-order streams), (4) numbers of streams of a given order, (5) total stream length, (6) basin length, (7) main stream length, and (8) number of segments of all orders. These eight parameters were chosen because of their demonstrated significance in previous studies and because they are easily amenable to computer-assisted measurement techniques. Horizontal scale was determined by mapping in known geographic locations, such as road intersections, and then measuring distances between these locations. Scale was then determined by comparison with the topographic map base. Because the transparencies deal only in planimetric qualities, relief as measured from the topographic map was considered a constant and incorporated in several calculations for comparison.

The S-190B imagery was analyzed in the same way as the S-190A imagery. Of the seven basins, only Mukewater could not be adequately located, although the image (SL2) containing the Upshaw Creek basin was obscured by cloud cover and was therefore excluded. The scale of the enlargements ranged from 1:38,640 to 1:48,480. Again relief was treated as a constant and employed in several calculations.

Resolution of drainage networks varied for several reasons. Important considerations were total relief, natural vegetation, land use, and sun angle. In locating the study basins on orbital imagery, uniqueness of the geographic location was also important. For example Bee Creek, located in a high relief area on a prominent bend of the Colorado River near Austin, was easily distinguished, whereas Mukewater Creek, located in a region of subdued topography with no distinguishing landmarks was much more difficult to isolate.

Increasing relief tended to enhance the resolution of major drainageways, as at Bee Creek and Dry Creek, because the physiography of the valleys was enhanced. However, many of the small first-order streams present in high-relief areas were obscured by vegetation. Where sun angle was low, valleys in high relief areas were marked by prominent shadows. In lower relief areas, drainageways were often marked by the strong contrast between the cultivated fields and stands of trees along the channels. However, in some instances, small channels were completely obscured by continuous cultivation across them. However, these channels were identifiable as crenulations on the topographic map or as dark responses from the high altitude color infrared aircraft imagery.

Several comparisons of morphometric parameters demonstrate the relative resolution of the Skylab imagery with topographic maps and aircraft imagery. Because there is no absolute scale when dealing with photographs, relief was chosen as an independent variable upon which comparisons could be based.

Because the number of first-order streams (Shreve Magnitude[4]) correlates directly with relief ratio (total basin relief/basin length) (see Figure 52), we decided to use this relationship to quantify the above qualitative observations on orbital imagery resolution. When morphometric data from various mapping sources are plotted on the same graph (Figure 40), the plot illustrates the relative resolution of the drainage network by different imagery formats. The base topographic map has the highest resolution of

---

[4] The term "Shreve Magnitude" will be employed from here on in the report because of its implied correlation to discharge or flood response in the channel.

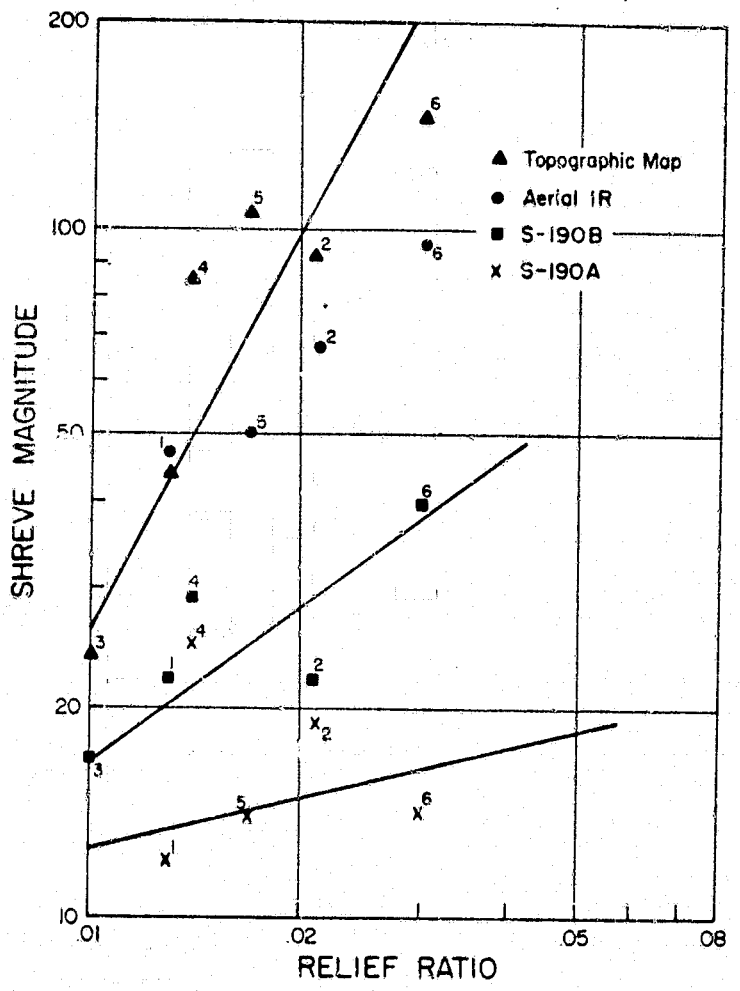

Figure 40. Shreve magnitude (i.e., total number of first-order streams) versus relief ration for similar-sized drainage basins with morphometric data supplied from differing imagery formats. Basins are indicated by number as follows: (1) Deep Creek no. 8, (2) Dry Prong Deep Creek, (3) Wilbarger Creek, (4) Dry Creek at Buescher Lake, (5) Upshaw Creek, (6) Bee Creek. Basin areas vary from 8 to 20 km^2. The three lines represent general trends for S-190A (A), S-190B (B), and topographic map data (C).

first-order streams, while the S-190A imagery has the lowest. Furthermore, with increasing relief ratio the number of first-order streams "lost" in this sequence increases, as the decreasing slope of the individual lines demonstrates. This is probably because many of the first-order streams in regions of high relief ratio are small gullies which are easily masked by vegetation and not enhanced by shadow effects.

Total channel length measured in a basin can also be used as a quantitative guide to resolution. A plot of this parameter against relief ratio (Figure 41), reveals greater losses in total channel length between topographic map and Skylab measurements for basins of high relief ratio than for basins of low relief ratio.

Other interrelated variables were plotted for all the available data. For example Melton (1957) demonstrated a strong direct correlation between drainage density and the frequency of first-order streams. When this relationship is plotted for the topographic map and Skylab data (Figure 42), the slope of the relationship is preserved, although the data plots closer to the origin as resolution decreases. The fact that the slope of the line is preserved indicates that the decrease in drainage density on the Skylab imagery is a result of the loss of first-order stream lengths, and not a result of the loss of higher order stream lengths.

These relationships demonstrate that the drainage network results obtained from Skylab imagery, in spite of the various external controls on resolution, conform proportionately to the topographic map base data. The results are encouraging, for it should be possible, because of this proportionality, to generate additional relationships similar to the drainage density, channel frequency Shreve magnitude-relief ratio relationship and thereby

C-2

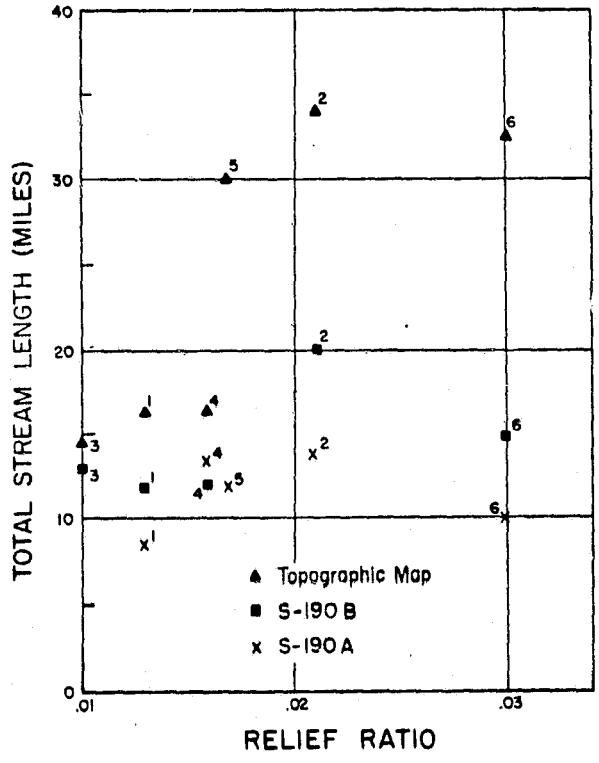

Figure 41. Total stream length versus relief ratio for drainage basins interpreted from different imagery formats. Basins are indicated by number as in Figure 40.

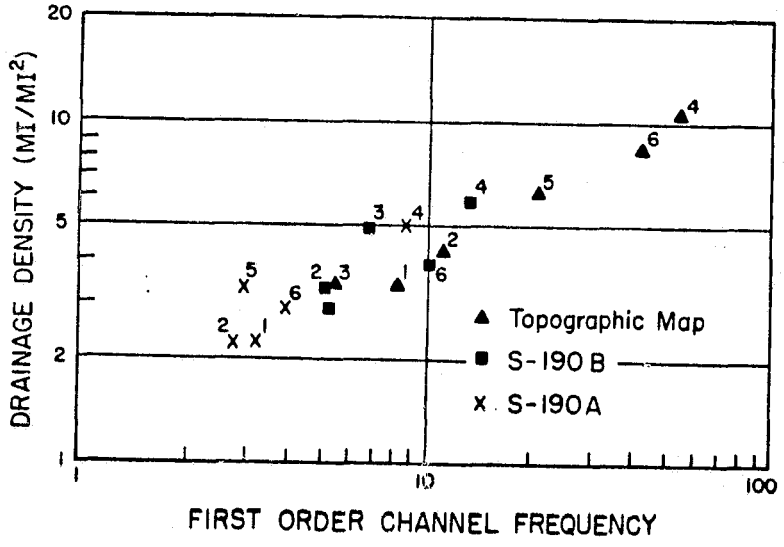

Figure 42. First-order channel frequency versus drainage density for topographic map and Skylab data. Channel frequency is the total number of streams of a given order per unit drainage area (in this case 1 mi^2).

more accurately portray drainage basin characteristics from Skylab data.

QUANTITATIVE STUDIES OF DRAINAGE BASINS

Once a network pattern has been interpreted from a data source, the various stream junctions, lengths, and sources need to be reduced to morphometric parameters. To avoid the tedious nature of manual morphometric analysis from photographic or cartographic data sources, we have incorporated machine-assisted digitization of drainage networks and computer reduction of data into a systematic analytical procedure. We report here on preliminary testing of this procedure, as a first step in relating morphometric measurements from various remote sensing imagery to flood hydrology.

Digital Computer Techniques

The W.A.T.E.R. System, a computer program for watershed analysis developed at Purdue University and the University of Toronto (Coffman and others, 1971), was used to calculate quantitative geomorphic parameters from digital input data. The transformation of spatial data (drainage maps) to digital data can be accomplished by selecting points within the drainage network which describe the branching pattern of the network (network topology) and assigning cartesian coordinates to these points to resolve their spatial position (Figure 43). Network topology can be described by a sequence of numbers which define the function of selected data points (Table 4).

Data point selection for the W.A.T.E.R. System follows that of other workers (Coffman and others, 1971; Scheidegger, 1967; Shreve, 1967) as follows:

1. Start at the mouth of the basin, and assign it code 5.
2. Move upstream recording "junctions" (code 3) until a "source"

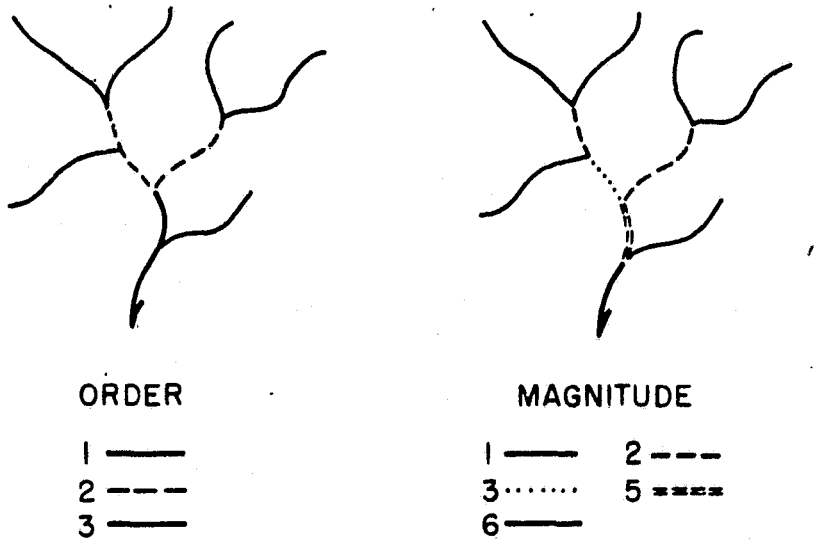

Figure 43. Assignment of Strahler orders and Shreve magnitudes.

Table 4. Numeric function codes used by the W.A.T.E.R. System

Code Number	Function of Point
1	Source point (tip of unbranched tributary)
2	Mid-point (defines Reaches)
3	Junction
4	Basin boundary point
5	Mouth of stream network
6	Dummy point indicating end of data
7	Contour line crosses stream

(After Coffman and others, 1971)

(code 1) is recorded. It is important to be certain that each junction has a Y-shape of intersecting tributaries; two upstream segments of the network must join to form a single downstream segment. Multiple junctions, having more than two upstream segments, must be arbitrarily rearranged as closely spaced Y-shaped junctions. It is also necessary to decide which upstream segment to follow when a junction is encountered. In this study, a "left-hand rule" has been used consistently, but a similar "right-hand rule" could have been adopted.

3. After a code 1 source is recorded, return to the last recorded junction with an untraversed right-hand upstream segment, and continue upstream recording junctions until another source is attained. Repetition of the procedure will lead to complete coverage of the network in an orderly sequence; no point should be recorded twice or missed.

4. After the drainage network is defined, the perimeter of the basin is recorded as a series of "basin boundary points" (code 4) by sweeping in a clock-wise (or counter-clockwise) curve around the basin; it is not necessary to re-record the basin's mouth to close this curve.

5. To indicate the "end of data," add a code 6 dummy point.

Besides recording data point function codes sequentially, it is necessary to record the spatial positions (cartesian coordinates) of the points in the same sequence. (X and Y coordinates of the end of data dummy point are ignored.) These positions were automatically digitized with an accuracy of ± .005 inches (.013 cm) using a d-mac pencil follower (Figure 44).

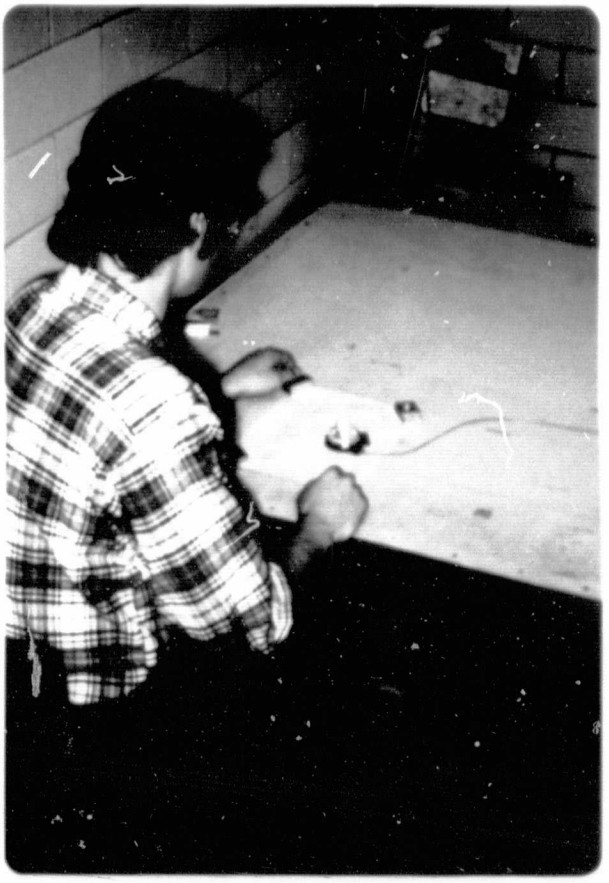

Figure 44. Digitizing equipment used at The University of Texas at Austin. The pencil follower is manufactured by d-mac Ltd., Glasgow, Scotland. Output is recorded on 7-track magnetic tapes.

Output from the pencil follower was recorded on 7-track magnetic tape. Input data to the W.A.T.E.R. System were the three sequential arrays of X and Y coordinates and associated function codes of the data points, and the scale of the digitized drainage network.

It is obvious that the method outlined above creates a schematic digital model of a drainage network. A more detailed model can be defined by inserting "midpoints" which break up curving segments of the network into several short straight segments rather than one long straight segment (Figure 45). Also, the W.A.T.E.R. System can perform three-dimensional analysis if the elevation is included as a Z coordinate in defining the spatial position of data points. Computer storage requirements are high with this system, so a CDC 6600 computer was employed in the analysis.

After the recording of coordinates for each data point on magnetic tape, a series of operations ensues to determine accuracy in the data array, to edit, and finally to interface the data with the W.A.T.E.R. System (Figure 46). The RCUHELP program was used to transfer data to punch cards or permanent file (disk). The KAREDIT program was used to properly align data words as stored in the permanent file. The MIXER program was used to read work storage to transform data back to a graphical output for error detection. Errors were located on CALCOMP plots of network data at the same scale as the original spatial input (Figure 47). By overlaying the two spatial formats, data errors were quickly recognized.

Errors were frequently encountered in the digitizing operation. We attribute this to the extremely monotonous and inflexible way in which the data must be collected. Minor errors are easily corrected, but major errors often resulted in discarding the original data and starting again at

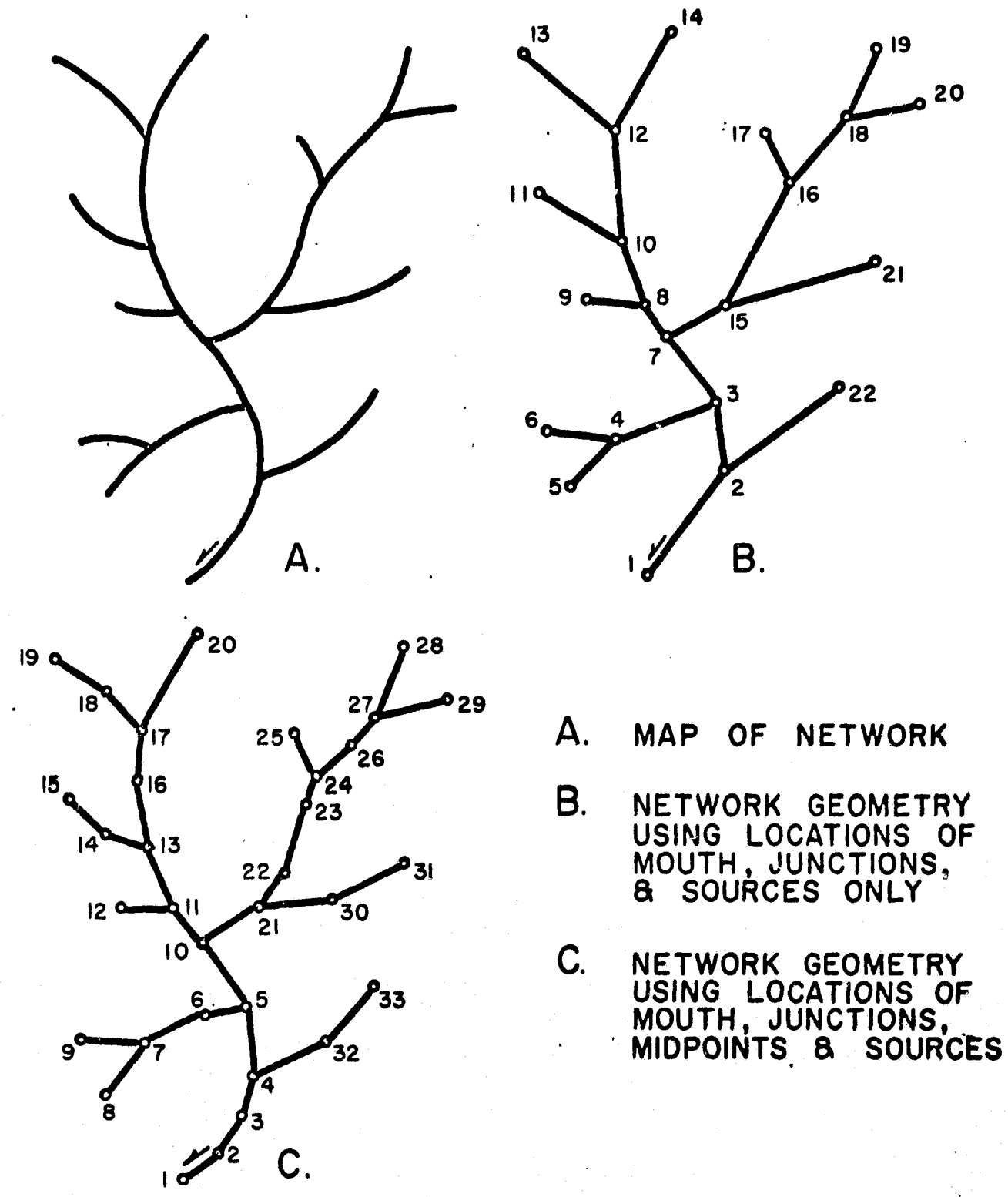

Figure 45. Method of inserting "midpoints" to provide more detailed digital information on drainage network geometry (from Coffman and others, 1971).

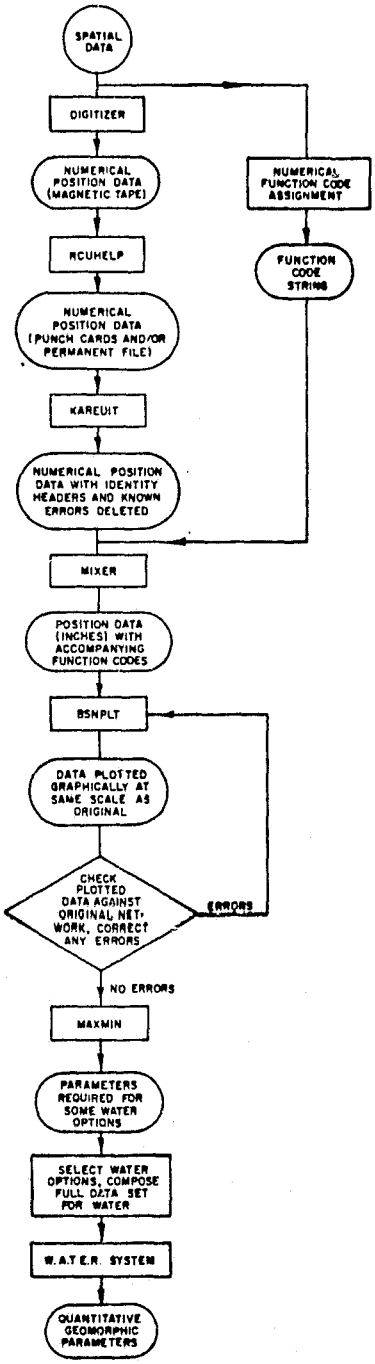

Figure 46. Flow chart of operations to transform spatial drainage network data to quantitative geomorphic parameters using the W.A.T.E.R. System.

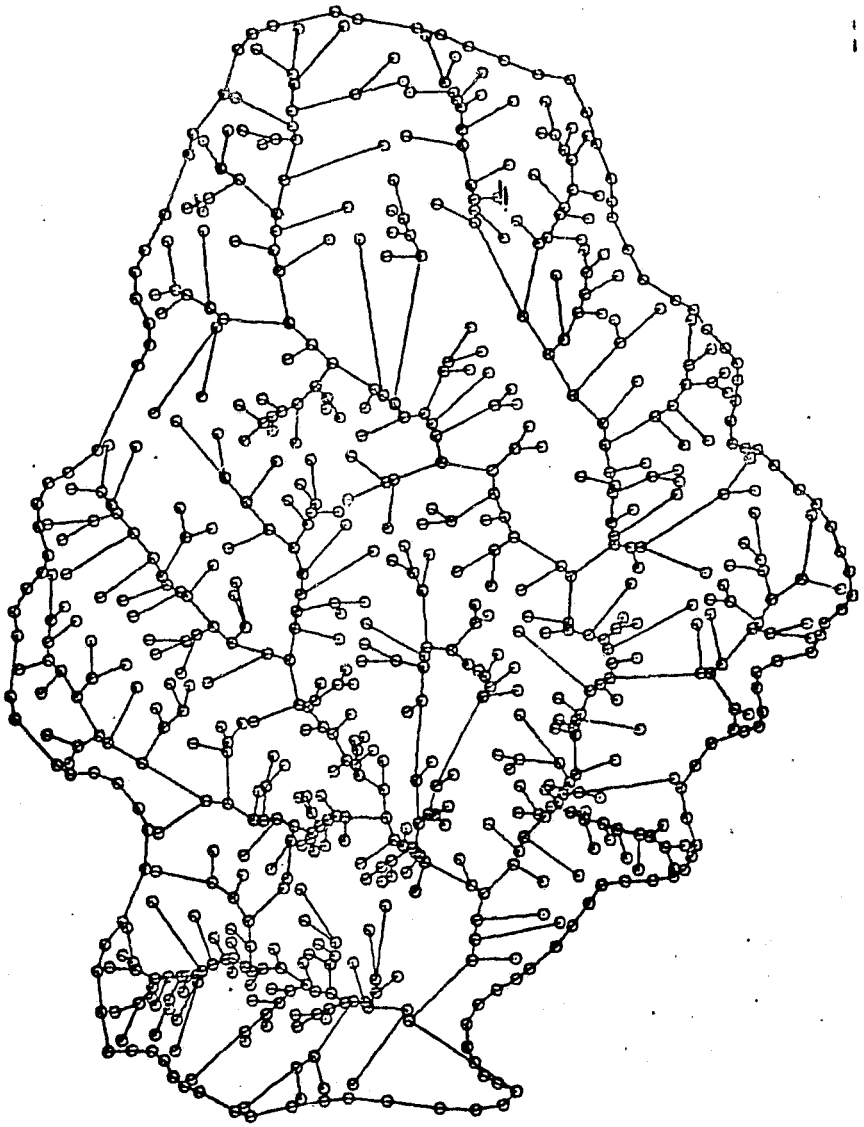

Figure 47. CALCOMP plot of drainage network data used for detecting machine or operator errors encountered in the digitizing operation. Map was derived from N.A.S.A. aerial infrared imagery of the Miller Creek basin near Johnson City, Texas.

the digitizing step. This concern with error is extremely important. Aberrant data points, incorrect X or Y coordinates, incorrect function codes, or mis-matching of position and function data will inevitably lead to errors in parameter calculation by the W.A.T.E.R. System. The involved editing routine (Figure 46) was developed to overcome these difficulties.

From the edited numeric data, the W.A.T.E.R. System assigns the Strahler orders to all segments of the drainage network, determines segment lengths, basin perimeter and area, and calculates basin statistics. Shreve magnitudes, link lengths, and basin statistics are likewise calculated. The various options for data input and analysis are listed in Table 5. The output of the W.A.T.E.R. System characterizes a drainage network geometry as interpreted from a specific imagery source.

Examples of Computer Output

The following example compares two W.A.T.E.R. System analyses of Bee Creek, as follows: (1) the topographic map interpretation (Figure 19), and (2) the mapping from low altitude black and white aerial stereo pairs (Figure 18). Data relevant to comparison of the two mapping sources are shown in Table 6, with composite parameters defined in Table 7 as they were calculated by the W.A.T.E.R. System.

The data show quantitatively what can be recognized qualitatively by looking at the two Bee Creek drainage maps. The number and length of unbranched tributaries (1st order segments or 1st magnitude links) recognized are the most important indicators of drainage network resolution. From the topographic map network, 145 unbranched tributaries, with a mean length of .164 km, were recognized. Three-hundred sixteen (316) unbranched tributaries

Table 5. The W.A.T.E.R. System options

Name	Purpose
*IDSW	Identifies data as point data or order-magnitude data
*SCALE	Allows maps to be produced at set scale
*WATER	Begin new basin, initialize all counters
*DATA	Start of co-ordinate data set
*END	End of all options and data for a basin
*ENDALL	End of all sets of options and data
*HYPSOMETRY	Elevation data being supplied
*STRAHLER	Classify network into Strahler's orders
*MAGNITUDE	Classify network into Shreve's magnitudes
*ANGLES	Compute junction angle statistics
*JUNCTION	Addition of orders and magnitudes for independently analyzed sub-basin
*CONNECT	Simultaneous analysis of multiple interconnected basins
*NETWORKS	Make printer-maps of orders and/or magnitudes. Requires *STRAHLER and/or *MAGNITUDE options.
*PROFILES	Display longitudinal profiles (max = 11) of main stream and from selected points. Requires *HYPSOMETRY option.
*AZIMUTHS	List azimuths of ordered segments. Requires *STRAHLER option.
*LENGTHS	List lengths of segments by order and/or links by magnitude. Requires *STRAHLER and/or *MAGNITUDE options.
*FALLS	List falls of segments and/or links. Requires *HYPSOMETRY and *STRAHLER and/or *MAGNITUDE options.

Table 5 (conti'd)

Name	Purpose
*GRADIENTS	List gradients of segments and/or links. Requires *HYPSOMETRY and *STRAHLER and/or *MAGNITUDE options.
*HISTOGRAM	Display histograms of azimuths, lengths, falls, and gradients of segments and/or links. Requires combinations of *HYPSOMETRY, *STRAHLER, *MAGNITUDE, and *AZIMUTHS, *LENGTHS, *FALLS, and *GRADIENTS options.
*PUNCH	Causes lists produced by *AZIMUTHS, *LENGTHS, *FALLS, and/or *GRADIENTS options to be punched onto cards identified by header cards.

(After Coffman and others, 1971)

Table 6. Basin statistics for Bee Creek from topographic map and aerial photo sources

Parameters	Data from topographic map	Data from stereo pairs
Basin Strahler Order:	4	5
Total Number of Segments:	186	434
Number of Segments, by Strahler Order:		
1st	145	316
2nd	34	87
3rd	6	25
4th	1	5
5th		1
*Bifurcation Ratios:	Dimensionless	Dimensionless
1/2	4.265	3.632
2/3	5.667	3.480
3/4	6.000	5.000
4/5		5.000
Mean Segment Lengths, by Strahler Order:	km (mi)	km (mi)
1st	.164 (.102)	.098 (.061)
2nd	.328 (.204)	.175 (.109)
3rd	.953 (.592)	.370 (.230)
4th	4.148 (2.578)	1.105 (.687)
5th		2.706 (1.682)
Basin Shreve Magnitude:	145	316
Total Number of Links:	289	631

Table 6 (cont'd)

Parameters	Data from topographic map		Data from stereo pairs	
Number of Links, by Shreve Magnitude (up to mag. 5):				
1st	145		316	
2nd	34		87	
3rd	12		45	
4th	14		20	
5th	11		18	
Mean Link Lengths, by Shreve Magnitude (up to mag. 5):	km	(mi)	km	(mi)
1st	.164	(.102)	.089	(.061)
2nd	.166	(.103)	.077	(.048)
3rd	.140	(.087)	.122	(.076)
4th	.150	(.093)	.137	(.085)
5th	.088	(.055)	.116	(.072)
Total Length of all Channels:	44.720	(27.800)	63.65	(39.560)
*Main Stream Length:	5.380	(3.344)	6.504	(4.042)
*Basin Length:	4.645	(2.887)	4.393	(2.730)
Basin Perimeter:	13.660	(8.489)	13.490	(8.386)
Basin Area:	sq. km	(sq. mi)	sq. km	(sq. mi)
	8.891	(3.433)	8.218	(3.173)
*Drainage Density:	km/km^2	(mi/mi^2)	km/km^2	(mi/mi^2)
	5.030	(8.096)	7.746	(12.470)

Table 6 (cont'd)

Parameters	Data from topographic map	Data from stereo pairs
*Elongation Ratio:	Dimensionless .724	Dimensionless .736
*Watershed Shape Factor:	1.600	2.011

* Indicates composite parameters which are defined in Table 7.

Table 7. Definition of composite parameters

Bifurcation Ratio (R_b)	= ratio of the number of segments of one order to the number of segments of the next higher order (Horton, 1945)
Main Stream Length (L_{ms})	= path of maximum length from the basin mouth to the farthest stream tip in the basin (Coffman and others, 1971)
Basin Length (L_b)	= maximum straight line distance between a point on the basin perimeter and the basin mouth (Coffman and others, 1971)
Drainage Density (D_d)	= ratio of the total length of all channels to the basin area (Horton, 1945)
Elongation Ratio (R_e)	= ratio of the diameter of a circle having the same area as the basin to the basin length (Schumm, 1956)
Watershed Shape Factor (F_{ws})	= ratio of the mainstream length to the diameter of a circle having the same area as the basin (Wu, 1964)

were interpreted from the stereo pairs, and they had a mean length of .098 km. The effect that better unbranched tributary resolution has on other parameters is easily seen in Table 6. The number of segments of all orders and the number of links of all magnitudes are greater in the drainage networks interpreted from stereo pairs, and mean segment and link lengths are shorter. The cumulative effect is greater total length for all of the channels interpreted from stereo pairs.

The main stream length as measured on the two networks is significantly different. The major reason for this is that the greater number of data points defined along the main stream from the photographic source resolve the meandering nature, while the fewer data points defined by the cartographic source result in a straighter, shorter main stream.

The difference in basin area resolved from the two sources is about 7.6 percent. The authors are unsure of the reason for, or significance of, this difference. The smaller differences in basin perimeter (2%) and basin length (6%) are related to basin area resolution.

The large difference in drainage density is due to the great disparity in the total length of all channels resolved from the two different sources, although the different basin areas enhance this disparity by a small amount.

The two measures of basin shape shown reflect differences in parameters already discussed. Both compare a length property of the basin to the diameter of a circle having the same area as the basin (see Table 7). This diameter will be approximately the same for the two sources. The two basin lengths are about equal, so elongation ratios are about equal. Main stream length differs between the two sources, and the watershed shape factor

reflects this difference.

Although the examples cited here were for topographic map and sub-orbital photography, the computer methodology developed in this phase of the project is directly applicable to the analysis of orbital imagery. The only problems to be encountered in orbital data analysis are those of scale and resolution discussed earlier.

DRAINAGE BASIN RESPONSE STUDIES

A major potential use of morphometric data is the prediction of runoff events of varying magnitude and frequency. A basic philosophy for this approach has been presented by Baker and others (1974). We assume that the shape and dimensions of a flood hydrograph, a graph of storm runoff as a function of time, are controlled by many interrelated factors. These factors can be separated into two main categories: transient and permanent (Rodda, 1969). Transient controls mainly represent climatic factors, and permanent controls are associated with characteristics of the drainage basin. Because virtually all of the controls are dependent in some way on one another, identifying and quantifying individual factors provide a major difficulty in establishing meaningful statistical relationships between various controls. The usual solution to this problem is selection of variables which are as physically independent as possible, e.g., some specific discharge and drainage area. The importance of quantitative geomorphology is obvious because the most easily obtained data is that which can be quantified from maps and aerial photographs.

Hydrologic Aspects of Flood Response

Flood Hydrographs.--The shape of a hydrograph produced by a small drainage basin is influenced by (1) temporal and spatial distribution of the rainstorm input and (2) by the physical characteristics of the basin itself. Our major concern will be the flood peak, i.e., the point arrived at when the quantity of water draining to the measurement point has reached its maximum. Other important hydrograph properties include (1) lag time, the inter-

val between the center of mass for the storm runoff and the center of mass for the rainfall input, and (2) the base flow separation line which separates storm runoff from the base flow, a property that is attributed to ground-water discharge.

Because of the highly variable shapes of flood hydrographs, the unit hydrograph procedure was established to standardize the control exerted by causative rainfall. This form is arbitrarily generated by applying a unit depth of rainfall, e.g., 1 inch, uniformly in space and time over a watershed. Unit hydrographs for Texas (Figure 48) reveal the variation in response to climatic and physiographic controls. In east Texas, a region of low relief, heavy vegetation cover, higher baseflow, and a more uniform temporal distribution of precipitation inputs, the hydrographs have greater internal width, increased lag times, and lower flood peaks. In central Texas, peak discharge increases while lag time decreases. This seems to be associated with more sporadic rainfall, higher relief and drainage density, sparser vegetation, and increased importance of overland flow. These qualitative controls follow the reasoning of other investigators (Heerdegen, 1974). The importance of these controls for Texas, however, is substantiated by the flood-response model derived later in this report.

Magnitude and Frequency Analysis.--Evaluation of a flood hazard requires a measure of the frequency in which an event of a specific magnitude is likely to occur. This frequency is calculated as the recurrence interval:

$$\text{Recurrence Interval} = \frac{n+1}{m} ,$$

where

n = number of years of discharge records ,

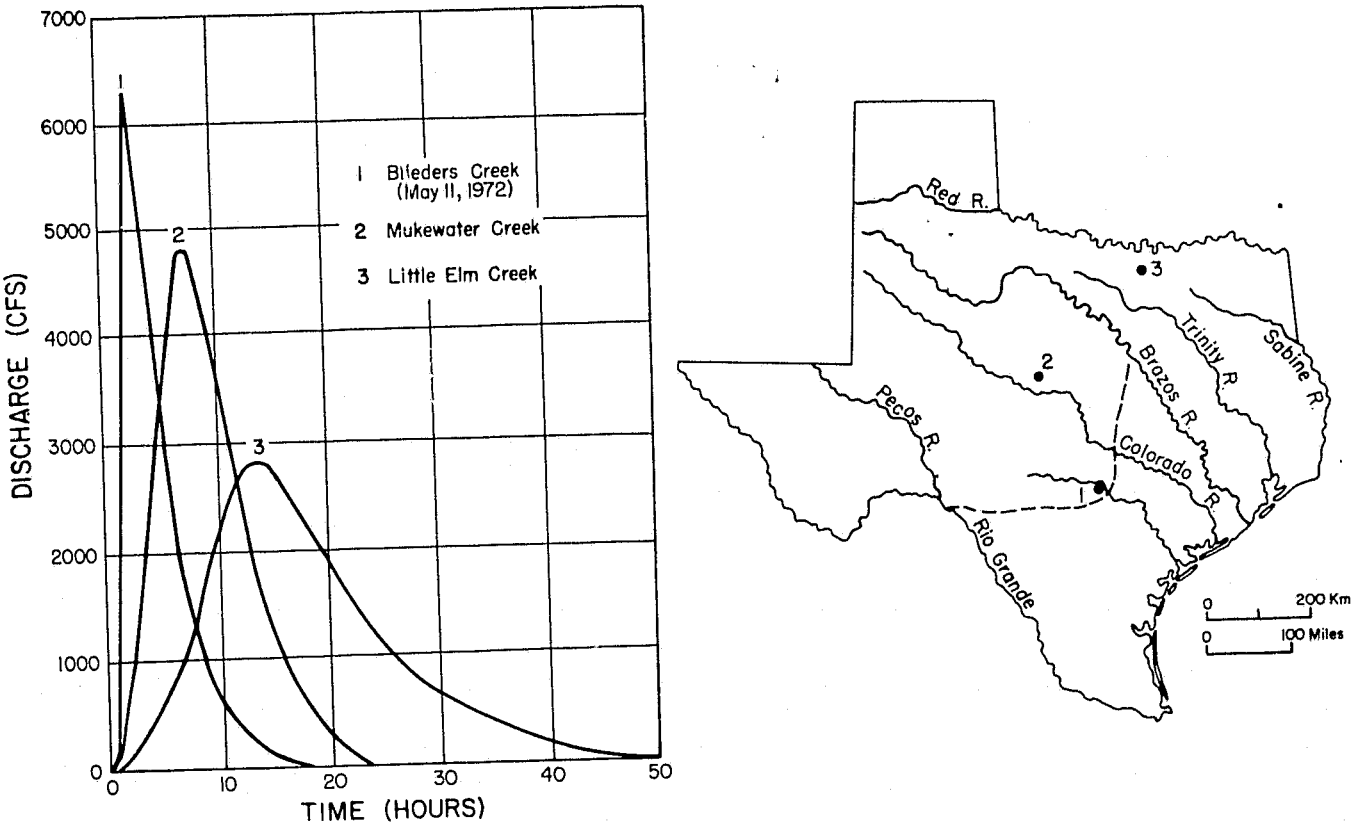

Figure 48. Two-hour unit hydrographs for three Texas watersheds. The Mukewater and Little Elm Creek hydrographs are average values determined by Meier (1964). The Blieders Creek hydrograph was calculated from runoff data presented by Colwick and others (1973). Dashed line indicates Balcones Fault Zone.

m = rank of a specific magnitude of flood, i.e., for largest recorded discharge, m = 1.

This simple statistic is the basis of a host of probability analyses. The major problem encountered in frequency analysis is that accurate historical flood data is required. Long data records are necessary to put confidence in frequency analyses. In central Texas there are few gaging station records as long as even 30 years, and those that do exist are likely to be on large rivers, whose natural regimes have been considerably disturbed by engineering projects.

Flood-response Models.--Models of flood phenomena are derived in an attempt to accurately predict the behavior of the prototype phenomenon, i.e., the flood. The model system is composed of elements that have specifically defined analogies to the important features of the prototype. Input data (e.g., rainfall) is transformed into an output (e.g., a flood hydrograph). Models can be continuously refined by comparison to their prototypes.

Parametric models of flood response are the most amenable to geomorphic data. These involve the identification and analysis of relationships between drainage basin characteristics, meterological inputs, and flood hydrograph response. The most commonly employed models identify variables that are known to be significant in the processes that transform drainage basin input (high intensity rainfall) to output (flood response). Functional relationships between various process controls and selected measures of flood response are usually established by multiple regression analysis. A standard logarithmic expression would take a form as follows:

$$Q_t = aX_1^{b} X_2^{c} X_3^{d} \ldots\ldots,$$

where

Q_t = the peak discharge with return period t (or some other flood hydrograph property such as lag time),

a, b, c ... = regression coefficients, and

X_1, X_2 ... = factors controlling the flood response.

In practice this approach has resulted in many "flood formulas," nearly all of which include basin area as one of the variables. Problems with the parametric approach include (1) interpreting the interdependence of variables, and (2) explaining the physical reality of the variables included in the analysis. The investigator frequently finds that unless many variables are held constant, no single variable will account for a large percentage of the variability in flood response.

To overcome these difficulties our study attempted to assess the influence of a large number of hydrogeomorphic parameters on flood response (Figure 49). Computer generation of morphometric measures eased the data acquisition problem and allowed the comparison of data generated from various types of imagery.

The Hydrogeomorphic Approach to Flood Response

Hydrogeomorphology (Coates, 1971) can be thought of as that part of geomorphology that directly concerns hydrological problems. The discipline involves practical applications of a basic science, in much the same way as hydrometeorology is an application of meteorology to flood prediction and other water resources problems. Such applications were probably first recognized by Horton (1945) and Langbein (1947), who pointed out that drainage

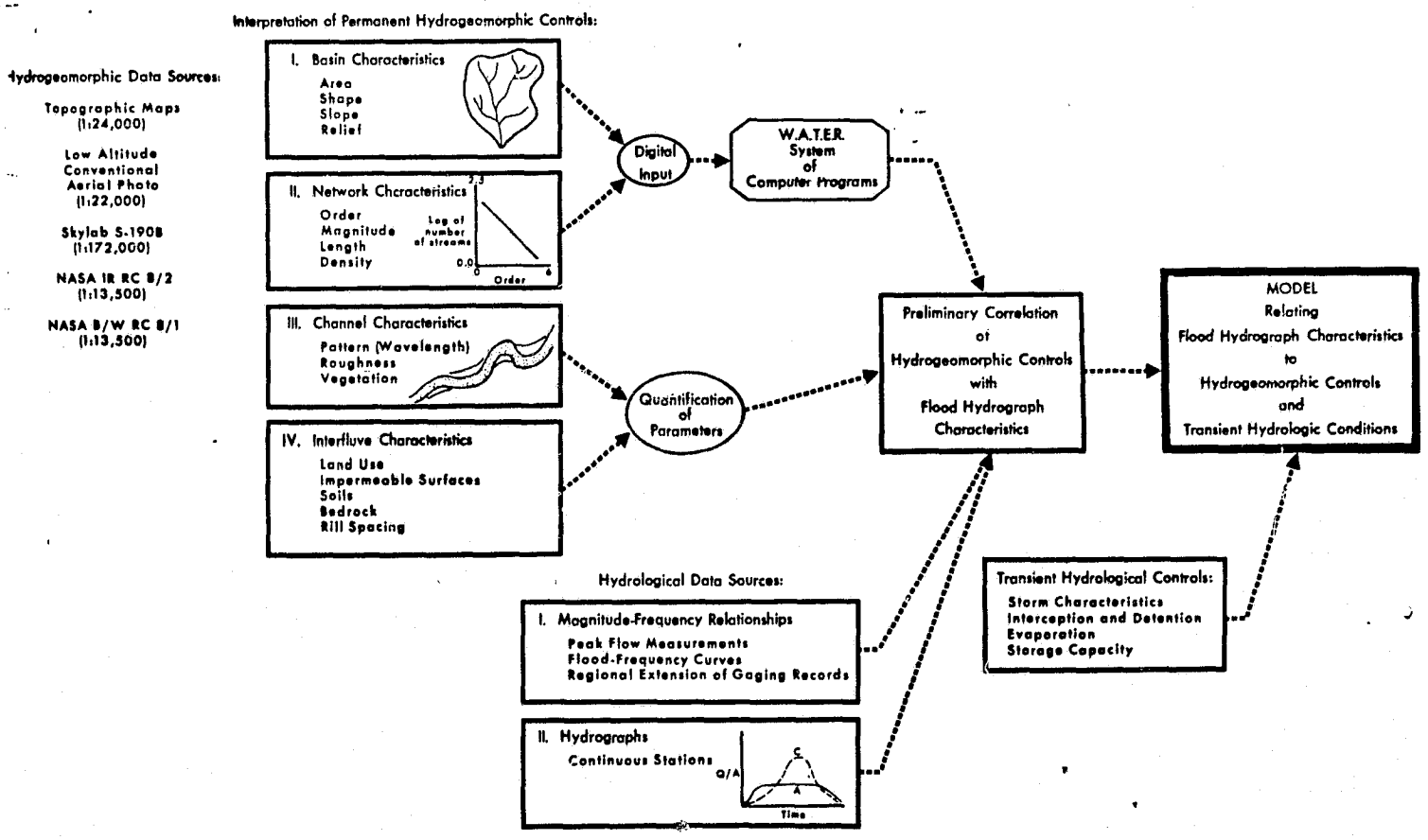

Figure 49. Flow chart of operations used to estimate flood response from the hydrogeomorphic parameters derived from analysis of remote sensing imagery (from Baker and others, 1974).

basin morphology could be quantified for hydrological use. Horton's morphometric work has been extended by many investigators, but relatively little research has aimed at relating flood hydrograph properties to permanent hydrogeomorphic controls. Chorley and Morgan (1962) suggested that the stream network of a given region is adjusted to maximum rather than mean runoff. Their work supported the application of morphometric parameters to studies involving the understanding of extreme runoff events. Many physical characteristics of channel form and drainage network geometry have been related to differing magnitudes of runoff (Table 8).

Drainage area has been the most often employed correlation with discharge (Langbein, 1947). Its ease of measurement and obvious physical significance allows meaningful correlation with runoff in both humid (Benson, 1962) and arid (Burkham, 1966) regions. Drainage area is correlated with varying magnitude and frequency of runoff (Benson, 1962; Patton and Baker, 1975). These formulas are generally of the form:

$$Q = kA^b ,$$

where Q is discharge, A is drainage area, and k and b are constants.

An adaptation of this form is the rational equation in which the average rainfall intensity is included with a coefficient related to storage, time of concentration and overland flow (Linsley, Kohler, and Paulhus, 1958).

Horton (1932, 1945) suggested that, in addition to area, stream slope and drainage density should be highly correlated with maximum flood discharge. Drainage density, the length of channel per unit of drainage area, reflects numerous variables including relief, rainfall, infiltration

Table 8. Some hydrogeomorphic controls on flood hydrograph characteristics.

Control	Morphometric Parameters Used in This Study	Reference	Hydrologic Influence
Drainage Basin Characteristics			
Area	Drainage Area Stream Area Ratio	Schumm (1956)	Size of basin is dominant control on precipitation interception.
Shape	Circularity Ratio Elongation Ratio	Miller (1954) Schumm (1956)	Elongate basins may produce more subdued flood peaks than oval basins.
Relief	Relief Ratio	Schumm (1956)	Proportional to sediment loss (Schumm, 1956).
Gradient	Stream Slope Ratio	Horton (1945)	Correlated to flood peaks (Thomas and Benson, 1970).
Drainage Network Characteristics			
Stream Order	Bifurcation Ratio	Horton (1945)	Distortion of maximum flood hydrograph (Strahler, 1964).
Stream Magnitude	Shreve Magnitude	Shreve (1967)	Probably reflective of channel capacity.
Stream Length	Stream Length Ratio	Horton (1945)	May effect lag time (Strahler, 1964).
Drainage Density	Total Channel Length/Basin Area	Horton (1945)	Proportional to mean annual flood peak (Carlston, 1963; Rodda, 1967).
Channel Patterns	Meander Wavelength	Dury (1965)	Proportional to bankfull discharge (Dury, 1965) and mean annual discharge (Carlston, 1965).

capacity of the terrain, and the resistance of the land to erosion (Horton, 1945). Strahler (1958) employed dimensional analysis to demonstrate that drainage density is a function of runoff intensity, relief, Horton's erosion proportionality factor, density and viscosity of the fluid medium, and the acceleration of gravity. Measures of relief (relief ratio) have been correlated with drainage density (Schumm, 1958; Hadley and Schumm, 1961). Correlation of drainage density with Thornthwaite's precipitation effectiveness index (Melton, 1957) and with intensity of precipitation (Chorley, 1957) has been accomplished. Although it is difficult to quantify resistance to erosion, qualitative comparison has been achieved, indicating an inverse relationship between drainage density and resistance to erosion (Schumm, 1956; Miller, 1954).

There are numerous examples of the relationship of drainage density to stream runoff. Drainage density has been correlated with base flow (Carlston, 1963; Trainer, 1969) and the mean annual flood (Carlston, 1963; Hadley and Schumm, 1961). Drainage density has been used in multiple regression models for estimating peak discharge (Maxwell, 1960). In addition, drainage density is one variable related to peak discharge for small streams in central Texas (Patton and Baker, 1975). Other studies have demonstrated, however, that drainage density by itself is not sufficient to define the runoff characteristics of a basin (Morisawa, 1962). Nevertheless, because of the interactions between process and form variables summarized by the drainage density measure (Horton, 1945; Strahler, 1958; Melton, 1958) and because of the wide range of naturally occurring values of drainage density (Schumm, 1956) it should be considered in any analysis of stream runoff.

Drainage density has been theoretically related to runoff intensity,

an erosion proportionality factor, relief, density and viscosity of the fluid medium, and the acceleration of gravity (Chorley and Morgan, 1962). In simpler terms, drainage density measures basin efficiency in removing precipitation inputs. If stream channels all possessed uniform properties and if drainage basins were uniform in soils, geology, vegetation, relief, precipitation input, etc., then streamflow would be proportional to the total contributive stream length in a basin's network. The situation would be comparable to sewers draining a city of uniform hydrologic properties. Unfortunately, the natural case is more complex, with local variation induced by soils, rock, type, and land use among other factors.

Stream order has been directly correlated with discharge by numerous workers (Blyth and Rodda, 1973; Rodda, 1969; Stall and Fok, 1967). Stall and Fok (1967) noted an increasing goodness of fit with decreasing frequency of the runoff event, suggesting that higher magnitude events are most important in establishing the drainage network. Leopold and Miller (1956) used hydraulic geometry studies of different order streams to establish empirical correlations of channel width to discharge and channel width to stream order. The two curves could then be combined to develop a relationship between channel-forming discharge and stream order. Such a relationship would, of course, be of local significance for the controlling factors that characterize the region in which the relationship was established.

Shreve's (1967) method of ordering has been advocated by a number of investigators as being more descriptive of network form in relation to streamflow. Lewin (1970) noted that Shreve's system neglects inner links that also gather water from the drainage basin. Nevertheless, the frequency of first-order streams (Shreve magnitude) has been correlated with peak

discharge of Appalachian streams (Morisawa, 1962) and central Texas streams (Patton and Baker, 1975). In addition, Blyth and Rodda (1972) noted that the number of flowing first-order streams increased with total rainfall and rainfall intensity. They noted that during dry periods flowing first-order streams constituted less than 20 percent of the total flowing length of the network. At the maximum extent of the network, the total length of first-order stream constituted over 50 percent of the total basin stream length.

The bifurcation ration of a basin could theoretically affect the shape of the flood hydrograph (Strahler, 1964). However, in natural systems, wide variation in bifurcation ratio is not observed and therefore only under unusual conditions would this measure be of importance.

Some investigators (Sherman, 1932; Strahler, 1958; DeWiest, 1965) have realized the importance of drainage basin form on the time distribution of runoff. Numerous shape factors have been derived. The simplest, a ratio of basin width to basin length, was employed in a runoff model for western Washington (Bodhaine and Robinson, 1952). Morisawa (1962) used basin circularity, the ratio of the area of the basin to the area of a circle with the same perimeter as the basin, in a multiple regression model of peak discharge. Chorley (1957) has suggested that the most accurate mathematical description of drainage basin form is one loop of a lemniscate having the equation:

$$Q = 1 \cos k\theta$$

shere k is a measure of the relationship between maximum basin length and maximum width, and 1 is the longest dimension of the loop.

Considerable controversy still exists in the literature concerning

the precise significance of relief, area, and shape factors on flood response. Gregory and Walling (1973) suggested that this may result from the fact that drainage basins exhibit a complex dynamic response to spatially varied inputs. High magnitude inputs in humid climates seem to involve a greater percentage of the channel network than is used to convey more frequent, low magnitude inputs.

A Parametric Model for Peak Discharge in Central Texas

Data Base.--The model was formulated from morphometric data collected from topographic maps of various study basins (Table 3). All but three of the basins selected for analysis were covered by 1:24,000 scale topographic maps with contour intervals not exceeding 20 feet. The remaining three basins were measured from 1:62,500 scale topographic maps which also had contour intervals less than 20 feet. The drainage networks for these basins were quantified by performing a Horton analysis (Horton, 1945) so that quantitative comparison between basins and remote sensing imagery could also be accomplished. Stream lengths were determined by the crenulation method (Horton, 1945; Morisawa, 1957) and streams were ordered both by the Strahler (1957) and Shreve (1966) method. The following variables were recorded for each basin: drainage area; Strahler order; Shreve magnitude or number of first-order streams, number of streams of a given order, total stream length, basin length, relief, main stream length, and number of segments of all orders. From these variables additional measures of the drainage basin were calculated, as follows: drainage density, relief ratio, ruggedness number,[5] and first-

[5] Ruggedness number is the product of relief and drainage density where both parameters are expressed in the same units.

order channel frequency. Linear measurements were made with a map wheel. Areal measurements were made with a polar planimeter.

The hydrologic response component of the model was generated from a data base collected from 25 stream gaging stations in central Texas. These data and the drainage area for each station were entered into a correlation analysis (Table 9). It should be noted that correlation analysis demonstrates the mutual relationship between two independent variables (Snedecor and Cochran, 1972), and therefore no cause and effect is implied. As the correlation matrix demonstrates, the maximum discharge of record is better correlated with drainage area than either bankfull discharge or the mean annual flood discharge. This result differs from observations in more humid climates by many other investigators. See, for example, Hack (1957) for the Potomac River where he demonstrated that drainage area was highly correlated with average annual runoff, and by Morisawa (1962) for the northern Appalachian Plateau where drainage area is more highly correlated with the mean annual flood than with maximum discharge.

The Model.--Runoff data was available for eight of the study basins that formed the data base. To extend this data, maximum discharge was estimated from the least squares relationship between drainage area and peak discharge derived from 52 sites in central Texas (Figure 50). Although there is considerable deviation from the best fit line, this relationship was considered more applicable than regional frequency equations because the frequency of the maximum runoff events for streams in central Texas varies considerably.

The morphometric and runoff data were entered into a correlation analysis and morphometric variables highly correlated with area (total stream length, basin length, and main stream length) and area were eliminated from

Table 9. Correlation matrix of stream runoff data and contributing drainage area. Sources of data were Benson (1964), Patterson (1963), and Schroeder (1973).

	$Q_{1.2}$ [1]	$Q_{2.33}$ [2]	Q_{max}	Drainage Area
$Q_{1.2}$	1.000			
$Q_{2.33}$	.759	1.000		
Q_{max}	.537	.868	1.000	
Drainage Area	.525	.902	.942	1.000

1 Assumed to be approximately equivalent to bankfull discharge

2 Mean annual flood discharge

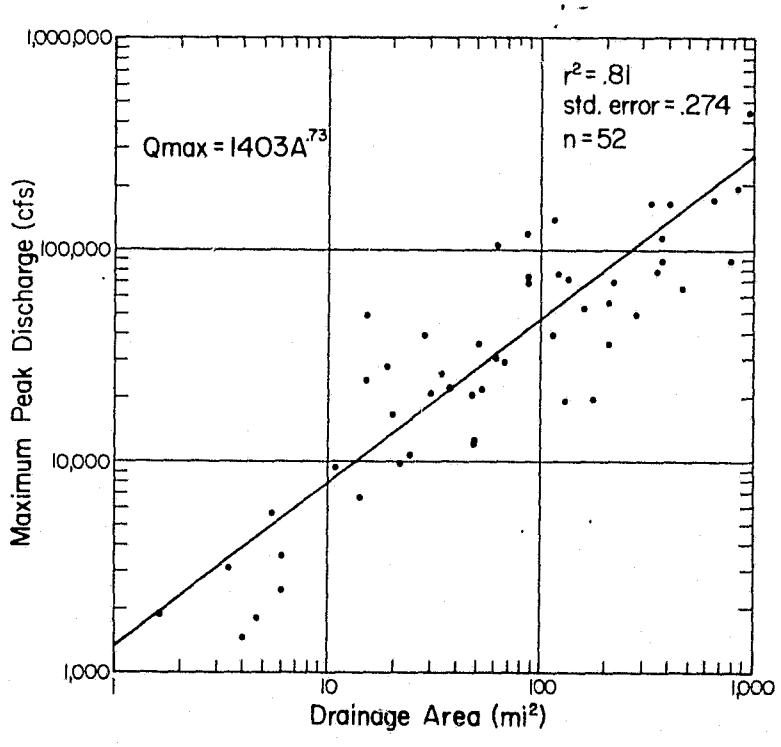

Figure 50. Maximum peak discharge versus drainage area for locations in central Texas.

further analysis to avoid spurious results (Table 10). The eliminated variables may be important estimators of runoff magnitude, but because the runoff data was generated from an equation employing area, the resulting high coefficient of determination (R^2) for a regression equation employing these variables would directly reflect the high correlation coefficients with area. Morphometric variables related to discharge, Shreve magnitude, drainage density, ruggedness number (relief times and drainage density) and total relief were entered into a stepwise multiple regression analysis. The multiple regression technique allows for the selection of that variable which initially explains the most variability in the dependent variable, in this case, maximum peak discharge.

In descending order of importance, the additional variables are included in the regression until there is no significant increase in the variability explained. The resulting relationship was:

$$Q_{max} = 5930.3 + 20.7\ M_s - 616.1\ Dd,$$

where

Q_{max} = maximum flood discharge of record (cubic feet/second),

M_s = Shreve magnitude of the basin, and

$\overline{Dd}$ = drainage density (miles/miles^2).

In statistical terms, Shreve magnitude and drainage density explained 86 percent of the variability in maximum discharge. Comparison of the model to the input data is facilitated by comparing observed and computed maximum discharge for the study basins (Figure 51).

The importance of Shreve magnitude in the relationship is also illustrated by its direct relationship to ruggedness number (Figure 52), a measure

Table 10. Correlation matrix of morphometric data and runoff data for

	Drainage Area	Strahler Order	Shreve Magnitude	Total Stream Length	Drainage Density	Basin Length	Relief	Relief Ratio	Total Number Stream Segments
Drainage Agea[1]	1.000								
Strahler Order	.499	1.000							
Shreve Magnitude	.470	.842	1.000						
Total Stream[1] Length	.715	.872	.905	1.000					
Drainage[1] Density	-.390	.517	.570	.360	1.000				
Basin Length[1]	.896	.396	.323	.639	-.368	1.000			
Relief	.455	.737	.795	.808	.434	.385	1.000		
Relief Ratio	-.156	.423	.526	.333	.632	-.307	.737	1.000	
Total Number Stream Segments	.327	.875	.920	.882	.727	.295	.763	.523	1.000
Main Stream[1] Length	.911	.387	.371	.654	-.367	.941	.454	-.158	.318
Ruggedness Number	.177	.695	.847	.712	.686	.093	.918	.845	.813
Maximum Peak[1] Discharge	.999	.500	.470	.714	-.389	.895	.453	-.157	.327

Log 10

FOLDOUT FRAME

lation matrix of morphometric data and runoff data for central Texas

Drainage Density	Basin Length	Relief	Relief Ratio	Total Number Stream Segments	Main Stream Length	Rugged-ness Number	Maximum Peak Discharge
1.000							
-.368	1.000						
.434	.385	1.000					
.632	-.307	.737	1.000				
.727	.295	.763	.523	1.000			
-.367	.941	.454	-.158	.318	1.000		
.686	.093	.918	.845	.813	.170	1.000	
-.389	.895	.453	-.157	.327	.910	.175	1.000

FOLDOUT FRAME 2

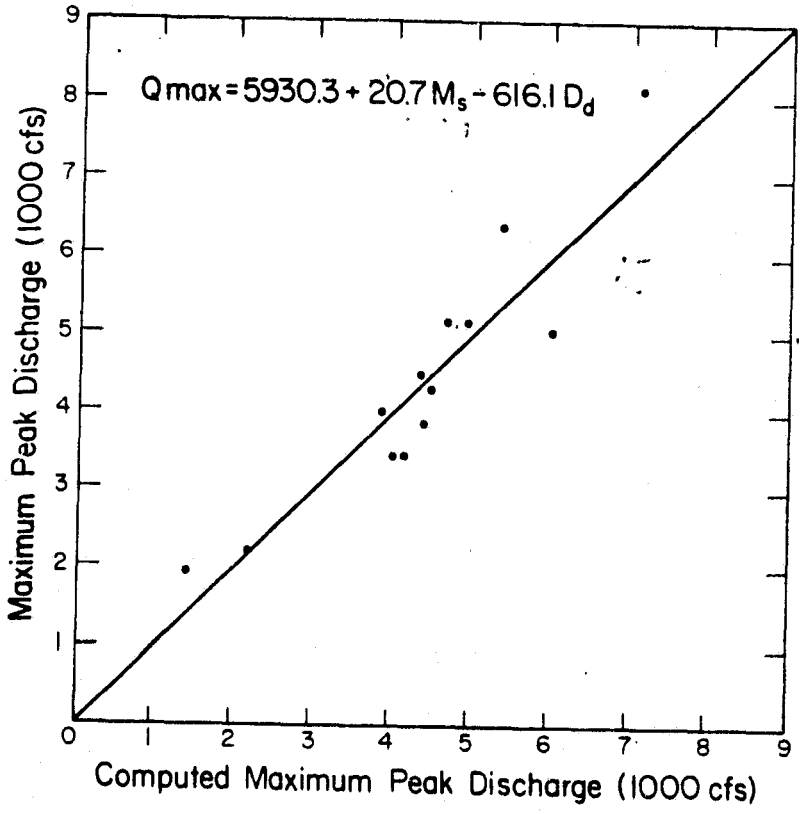

Figure 51. Comparison of measured maximum peak discharge values versus maximum discharge computed from the equation Q_{max} = 5930.3 + 20.7 M_s - 616.1 Dd. The 45° line represents perfect agreement.

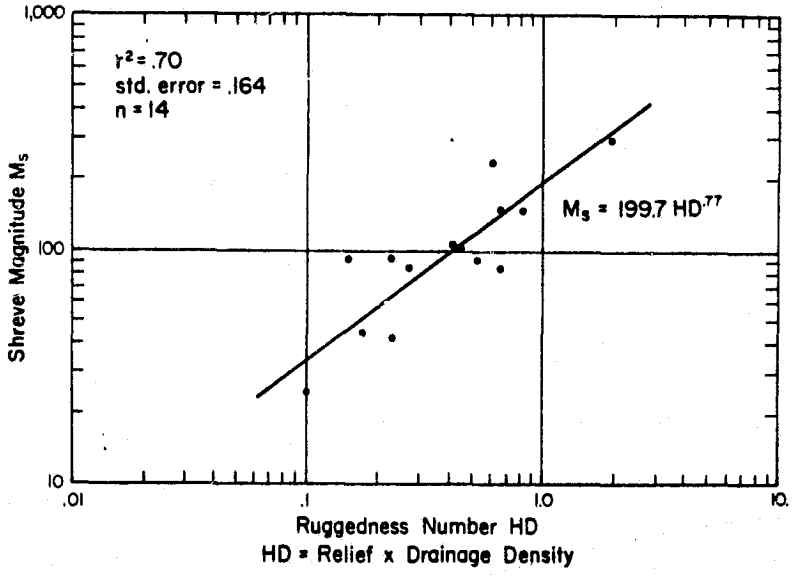

Figure 52. Shreve magnitude versus ruggedness number (drainage density times relief).

of relief and drainage texture. This relationship has considerable value in interpreting relief from planimetric imagery.

Although conventional methods were used to measure the morphometry in this aspect of the study, the observed proportionality relationships between morphometric variables measured on topographic and Skylab data sources (Figure 40) could be used to apply the model to orbital remote sensing imagery.

Other Approaches to Evaluating Flood Response

The correlation model just presented suggests that drainage basin morphology in central Texas is adjusted to processes of low frequency and high magnitude, i.e., the maximum flood discharge of record. Wolman and Miller (1960) recognized that, within a given landscape, different elements of that landscape react and are shaped by events of differing magnitude and frequency. Nonetheless, most investigators (Dury, 1964, 1965; Carlston, 1963, 1965; Hack, 1957; Leopold and Maddock, 1953; Leopold and Miller, 1956) have related stream morphology to events of intermediate frequency such as bankfull discharge (recurrence interval 1.0-1.5 yrs.) and the mean annual flood (recurrence interval 2.33 yrs.). Relatively little emphasis has been given to the importance of extreme events of low frequency. Exceptions include Beatty (1974) and Schick (1974).

A much-cited example of magnitude-frequency, process-response adjustment is the correlation of meander wavelength to bankfull discharge (Figure 53). Dury (1964, 1965) has used this relationship to suggest that, in instances where the present-day stream in underfit, the larger valley meanders were formed during periods of greater discharge of the same frequency. Based on this analysis he has suggested that valley meanders repre-

sent a climate of greater precipitation in the past for many diverse regions.

Recently, Tinkler (1971) suggested that active valley meanders in central Texas are related not to discharge events having the frequency of bankfull discharge as characteristic of alluvial channels, but rather to high magnitude runoff events which completely fill bedrock channels in the Texas hill country. He suggested the term channel full for these runoff events and he interpreted a recurrence interval of 10 to 50 years.

To test this hypothesis meander wavelength data were collected at or near 21 gaging stations in central Texas where long term records are available. A plot of meander wavelength against drainage area reveals that all but three values fall in the valley meander portions of Dury's graph (Figure 54). The wavelength data therefore conform to Dury's criteria for valley meanders and should be considered as present-day active valley meanders as suggested by Tinkler.

For each station bankfull discharge, mean annual flood, and the maximum discharge of record were entered into a correlation analysis with meander wavelength. Meander wavelength was more highly correlated with the maximum discharge of record that with bankfull discharge or mean annual flood. The best fit least squares regression equation was calculated for each relationship. Unlike correlation analysis, regression analysis assumes one variable to be dependent on one or more independent variables and therefore implies causality (Draper and Smith, 1966). In this instance, meander wavelength is assumed to be dependent solely on discharge. The relationship between bankfull discharge and meander wavelength (Figure 55) is extremely poor. The r^2 value of .06 indicates that only 6 percent of the variance in meander wavelength is explained by flows having the recurrence interval of

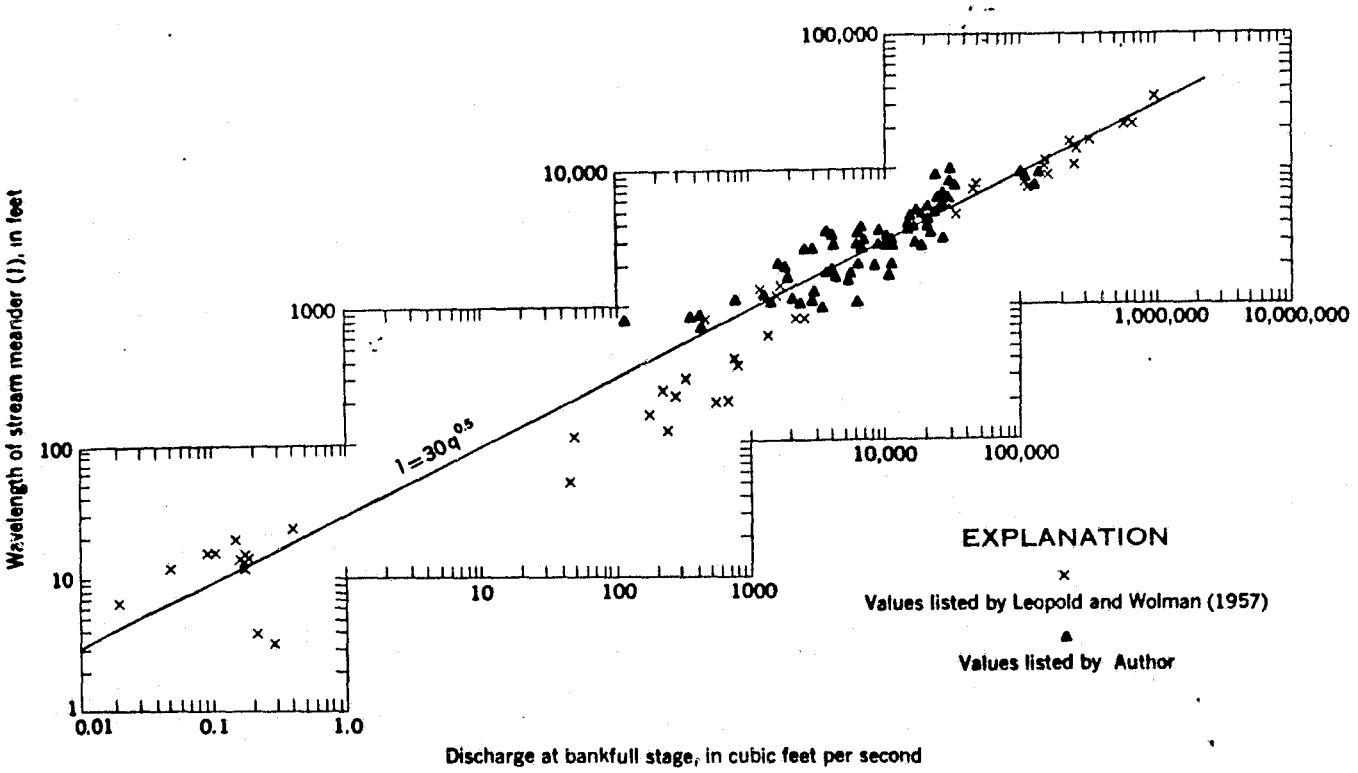

Figure 53. Meander wavelength versus bankfull discharge (Dury, 1965).

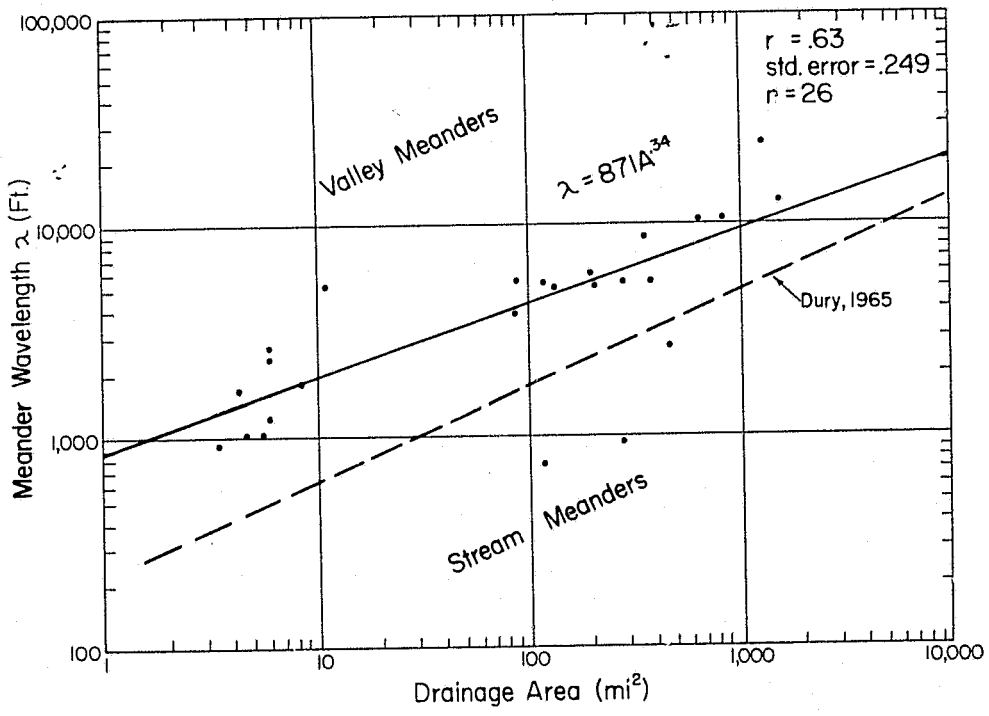

Figure 54. Meander wavelength versus drainage area for central Texas streams. Dashed line from Dury (1965) represents the boundary between valley meanders and stream meanders. Solid line is the best fit least squares regression line for the central Texas data.

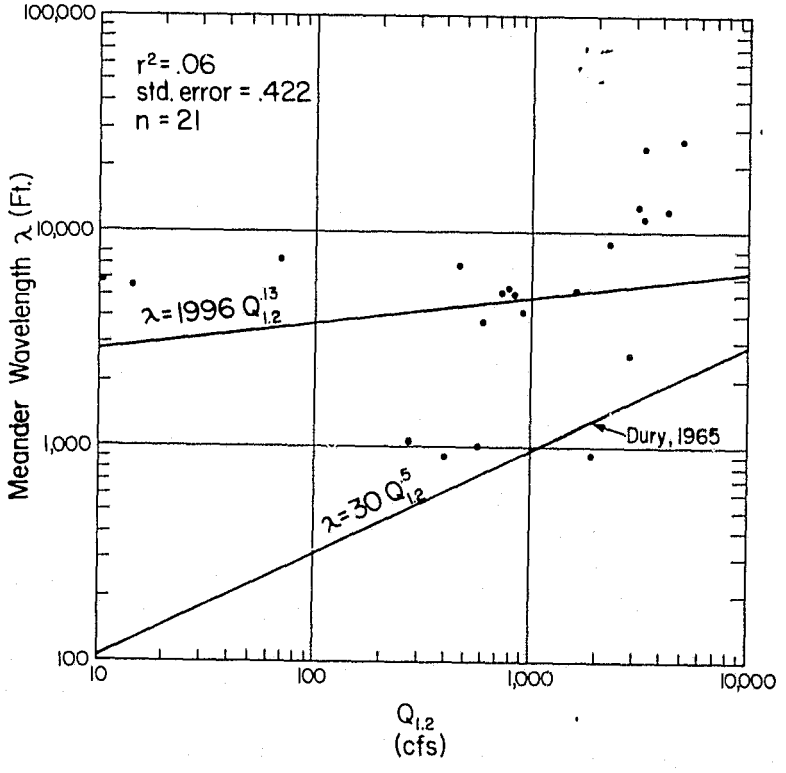

Figure 55. Meander wavelength versus bankfull discharge (assumed equal to $Q_{1.2}$).

bankfull discharge. The null hypothesis, that the slope of the regression is equal to zero, cannot be rejected ($p < .25$). The relationship between mean annual flood discharge and meander wavelength (Figure 56) is somewhat more statistically valid. The slope of the regression line is significant ($p > .01$), however, only 45 percent of the variation in meander wavelength is explained. Statistically the best relationship is between maximum discharge and meander wavelength (Figure 57). The slope of the regression line is significant ($p > .01$) and 78 percent of the variation in meander wavelength is explained. The maximum discharges in this analysis all exceed the expected discharges at the frequency of the 50-year flood and many exceed those at the expected frequency of the 100-year flood.

These examples demonstrate the effect on stream morphology exerted by low frequency high magnitude runoff events. The practical implications of these results suggest that some morphometric variables can be used to predict severe floods in central Texas. In fact, the meander wavelength versus maximum discharge relationship can be considered as one example.

The flood plain mapping studies discussed below (Figure 63 and 67) demonstrate that meander wavelength can be accurately determined from S-190A orbital imagery. If wavelength-discharge correlations can be established as in Figure 57, orbital imagery should prove to be an important hydrologic reconnaissance tool in underdeveloped nations which lack accurate topographic maps.

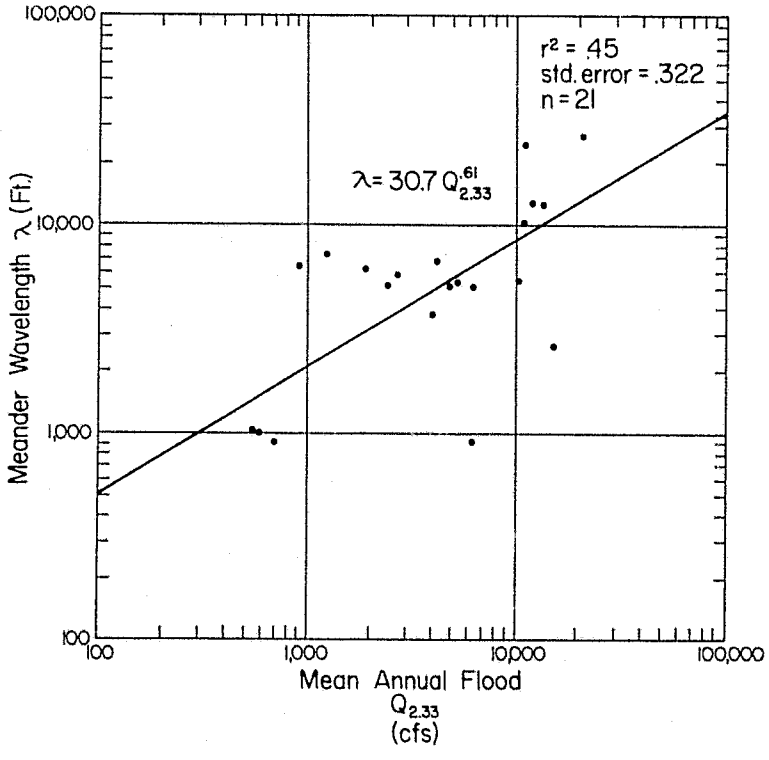

Figure 56. Meander wavelength versus mean annual flood discharge ($Q_{2.33}$).

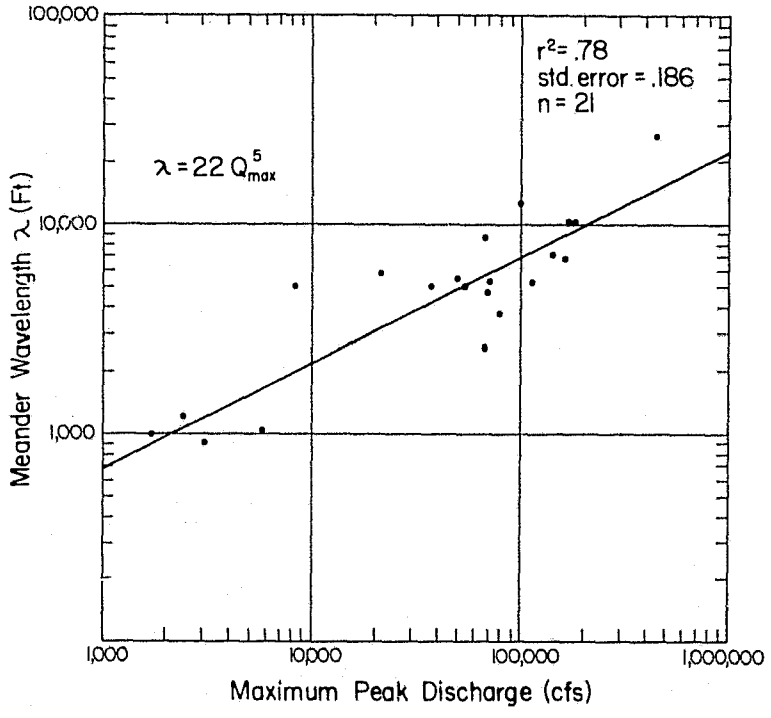

Figure 57. Meander wavelength versus maximum recorded peak flood discharge.

FLOOD PLAIN MAPPING STUDIES

The accelerating demand for flood hazard information makes imperative an evaluation of alternative techniques to standard engineering flood line and regional flood analyses (Wolman, 1971). Different mapping techniques may be appropriate to different localities depending on the local hydrologic regime, the level at which planning is being performed, and the funds available to finance the study. A geomorphic approach to flood hazard mapping can be used effectively at the state-wide or regional scale to provide interim information prior to detailed hydrologic and hydraulic studies on a local basis. If included within an overall program of regional environmental geological mapping, morphological flood plain mapping can provide a relatively inexpensive by-product of a general program of environmental inventory based on the interpretation of remote sensing imagery.

White (1964) has shown that from the theoretically broad range of choice for those with authority over flood plain management, only a few choices are generally considered in decision-making. This makes for far less efficiency than could be achieved by considering the whole range of possible choices. Two main factors seem to limit choice, as follows: (1) the flood manager's perception of the nature and magnitude of the flood problem, and (2) his perception of alternative responses. The preliminary results presented here suggest that remote sensing imagery has an important role to play in this perception process. Careful study of the imagery can delimit the hazard on a regional scale much more rapidly than conventional hydrologic-hydraulic flood plain mapping techniques and at a small fraction of the cost. This is achieved at an accuracy loss that is acceptable for regional planning purposes.

Alternative Approaches to Flood Hazard Mapping

The pressing national need for flood hazard information has led to a re-evaluation of various techniques for flood plain mapping (Wolman, 1971). Techniques in which remote sensing can play a significant role are the occasional flood, botanic, pedologic, and geomorphic approaches. Traditional engineering hydraulic-hydrologic methods are generally considered to be the most desirable for planning and management purposes in urban areas (Wiitala and others, 1961). However, these methods also tend to be the most expensive, costing as much as $1,000 per mile for delineating flood profiles by backwater curve analysis of large scale topographic maps (Wolman, 1971, p. 1384). In contrast, the mapping of topographic features or soil associations that may correlate to flood levels could cost as little as $1-4 per mile of channel (Wolman, 1971).

The Occasional Flood Method. -- This approach involves establishing flood lines on the basis of aerial photographs taken during flood events, historic evidence of floods, and actual local observation of flood heights (Wolman, 1971). Remote sensing offers many advantages for providing wide coverage of inundated areas. Unfortunately, however, poor weather may inhibit aerial surveys of floods. Orbital space platforms for earth resource sensors have an important advantage in this regard. Their multidate photographs allow continuous monitoring of river conditions without necessitating emergency plans for aerial surveys of broad areas.

A striking example of the use of satellite imagery for occasional flood mapping occurred in the spring of 1973, when severe flooding affected the entire alluvial valley of the Mississippi River. Special optical data

processing techniques were used to produce a variety of multispectral composites of ERTS-1 imagery taken before, during, and after overbank flooding (Deutsch and Ruggles, 1974). In a single view, the entire lower Mississippi from St. Louis to the Gulf of Mexico could be depicted. An important discovery was that the effects of flooding on the reflectance characteristics of the flood plain allow the delineation of areas from which flood water has recently receded. This eliminates the need for continuous monitoring of the flood crest (Deutsch and Ruggles, 1974).

The Botanic Approach. -- Regional ecological studies (Blair, 1950; Tharp, 1926) suggest that some zonation of vegetation occurs along the river valleys of the Edwards Plateau. The most distinctive zonal forms are baldcypress (Toxodium distichum) and pecan (Carya illinoensis). Baldcypress is hydrophilic with shallow, abundant roots that require a constant moisture supply, usually by submergence. The species only occupies the low-flow channel banks of streams with a permanent base flow. Lines of dead baldcypress occasionally mark former channels isolated by meander cutoffs. Pecan is a dominant species in the alluvial zones bordering low-flow channels. Pecan is confined to areas of well-drained loamy soils not subject to prolonged flooding, which local residents term "pecan bottoms." At Stonewall, Texas, one such pecan bottom was completely removed from the point bar of a Pedernales River meander by the 1952 flood. Trees and supportive soil were scoured, leaving a flat bedrock surface.

American sycamore (Platanus occidentalis), eastern cottonwood (Populus deltoides), and black willow (Salix nigra) grow in close proximity to stream bottoms, but unlike baldcypress they occur along ephemeral tributaries. The shallow roots of the black willow require a constant moisture supply during

the growing season. Unlike the pecan, American sycamore may extend from flat-lying bottomlands up relatively steep slopes where the water supply is sufficiently abundant. The alluvial soil zones, including wetter terraces and well-drained flats on active flood plains, contain pecan, hackberry (Celtis laevigata), Spanish oak (Q. shumardii), elm (U. americana), black walnut (Juglans nigra), and large live oaks (Q. virginiana). However, not all these species are distinctive. The live oaks extend up nearby limestone ledges, where they mix with Spanish oak, white ash (Fraxinus americana), red mulberry (Morus rubra), and Texas black walnut (Juglans microcarpa). They also occur on the vast limestone interfluves in association with juniper, prickly pear and mesquite. Black walnut tolerates thinner soils and lower moisture than pecan, while Texas black walnut tolerates even drier habitats, such as the limestone ledges adjacent to bedrock streams. Spanish oak, in contrast, remains in the well-drained soils of alluvial terraces and colluvium near active streams.

Preliminary biologic assemblage mapping by The University of Texas Bureau of Economic Geology (Wermund and Waddell, 1974) has shown that the bottomland cypress-pecan assemblage can be easily recognized in the process of environmental geologic mapping from aerial photography. However, the factors which control the zonation of vegetation on Texas river bottom environments are quite complex. Particular combinations of soil conditions and water supply appear to be the dominant controls. Because flooding is not a cause of the zonation, botanical flood studies must be combined with other techniques for flood hazard evaluation.

To test the use of remote sensing imagery for botanic flood hazard zoning in this area, we employed N.A.S.A. - generated aerial infrared type

2443 imagery taken with the RC8 camera. In the Pedernales Falls area (Figure 58) the flood plain botanic association was clearly visible as a light pink response on the imagery. Pools of deep water along the discontinuous river course could also be easily mapped from their distinctive deep blue response. Areas of exposed bedrock in the channel bottom and bars of sand and gravel appeared bright white on the imagery. These frequently flooded zones presented a dramatic contrast to the dull green of adjacent grassy hillslopes and maroon response of local clusters of juniper and live oak in the uplands.

Field investigations near Pedernales Falls revealed that the principal trees giving the pink response were American sycamore, pecan, water hickory, and myrtle oak. The darker, maroon response of vegetation on the hillslopes and interfluves was given by eastern redcedar, juniper, and live oak. A generalized cross section showing the field-botanic associations and past flood levels is given in Figure 59 .

Soils Method. -- Wolman (1971) suggested that locally both soils and topography may correlate with specific flood heights. Distinctive flood plain soils have been studied by Cain and Beatty (1968), Ruhe (1971), and Reckendorf (1973). Reckendorf (1973) found that the soils technique did an adequate job of delineating areas in Oregon flooded by the 100-year return period event when individually mapped soils or groups of soils were compared to hydrologic studies of flood frequency. The principal use of the technique was in extending information from points of known gage data or historical flood elevations to other localities characterized by the same soil-geomorphic associations. Reckendorf concluded, however, that a better extrapolation could be obtained by geomorphic mapping of stair-stepped flood plain surfaces on the basis of "typical flood plain morphologic features."

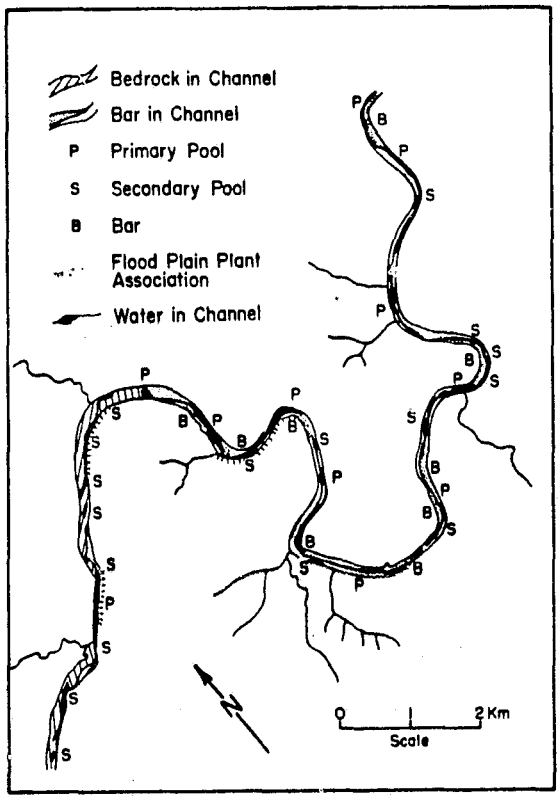

Figure 58. Flood-related features in the Pedernales Falls area mapped from N.A.S.A. aerial infrared type 2443 imagery at 1:48,000 scale.

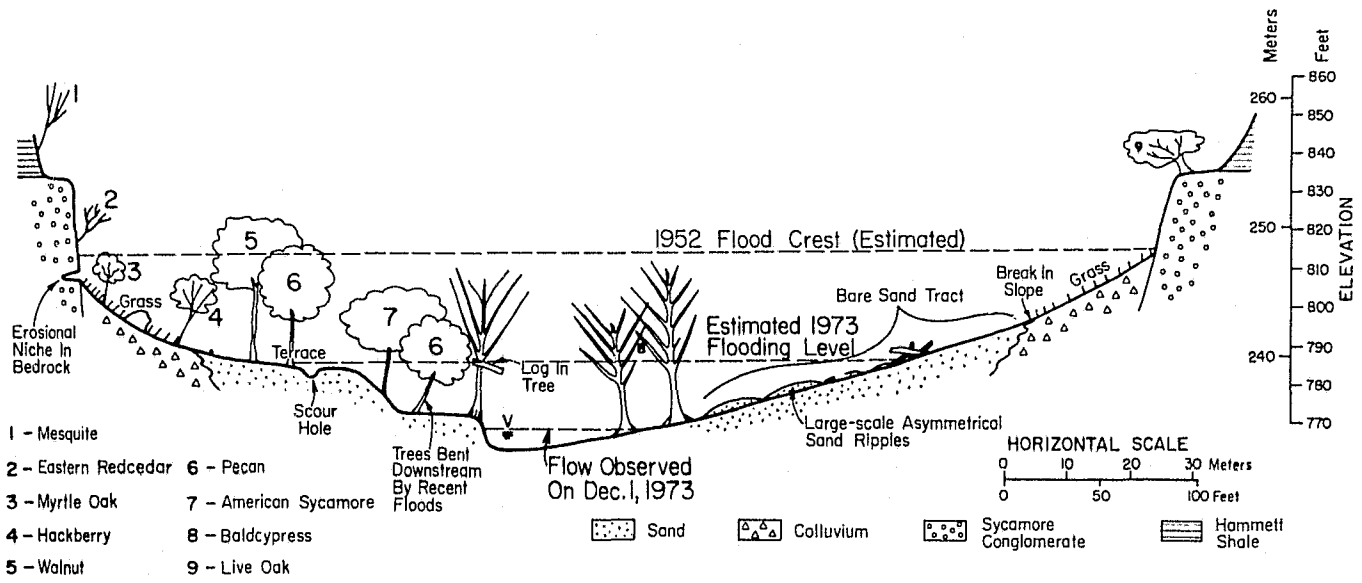

Figure 59. Schematic cross section of Pedernales River valley at Trammel Crossing, Pedernales Falls State Park. Vegetation associations and geomorphic features based on field observations by V. R. Baker, P. C. Patton, and P. A. Smith.

Detailed soil survey maps prepared by the U. S. Soil Conservation Service often provide information on various grades of wetness related to soil permeability or to surface and subsurface drainage conditions. Although the maps do not show actual coverage of water during floods of known frequency and elevation, local correlations can sometimes be drawn. The 100-year flood for the Colorado River near Austin, Texas, for example, shows considerable correlation to certain soil series mapping units (Figure 60). We used this soil mapping information as a guide to interpretations from orbital and suborbital imagery.

Geomorphic Method. -- Geomorphic techniques for flood plain mapping should not be confused with simple physiographic correlation of specific topographic features with flood discharges of known frequency (e.g., Kilpatrick and Barnes, 1964; Woodyer, 1968). They involve the more extensive investigation of morphology, sedimentology, distinctive erosional features (Baker, 1974), time sequences of channel abandonment, and the compilation of existing pedologic, botanic, and hydrologic information. This concept is similar to Reckendorf's (1973) "combination method" for the construction of flood plain maps in Oregon. Reckendorf developed a base map by mapping typical geomorphic flood plain features (see Fisk, 1944; Jahns, 1947; Lueder, 1959) and associated terraces from aerial photography and selected field studies. The available soils, vegetational, historical flood, and hydrologic-hydraulic information can then be superimposed on the geomorphically delineated flood plain. The skilled investigator will use each technique to check and balance the other. Reckendorf found that, in general, there is a strong correlation between geomorphic flood plain surfaces and river stages for floods of particular frequencies, especially the 100-year average recurrence interval event.

Figure 60. Soils of Montopolis Bend area, Colorado River valley near Austin, Texas. Soil associations are compiled and grouped from mapping by Werchan, Lowther, and Ramsey (1974). Soil series are as follows: (1) Lincoln loamy fine sand; (2) Lincoln soils under urban land; (3) Yahola very fine sandy loam; (4) Yahola soils, channeled; (5) Norwood silty clay loam; (6) Norwood soils, channeled; (7) Bergstrom silt loam, 0-1% slopes; (8) Bergstrom silt loam, 1-3% slopes; (9) Bergstrom silty clay loam, 0-1% slopes; (10) Bergstrom silty clay loam, 1-3% slopes; (11) Bergstrom soils and urban land; (12) Frio silty clay loam; (13) Ferris-Heiden complex, 8-20% slopes; (14) Trinity clay; (15) Travis soils and urban land, 1-8% slopes; (16) Houston Black soils; (17) Heiden clay; (18) Dougherty loamy sand; (19) Lewisville silty clay.

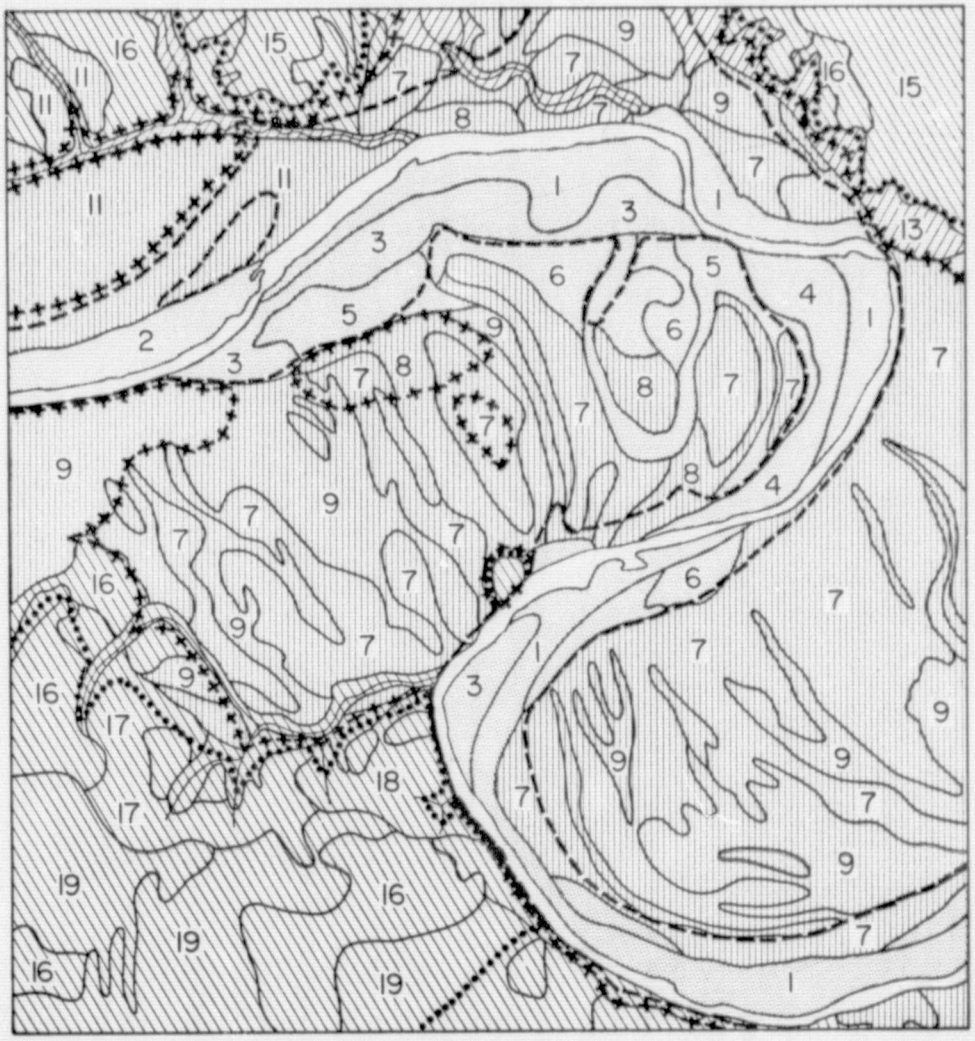

0 1 2 Miles

0 1 2 Kilometers

SCALE

SOIL SERIES

- Lincoln, Yahola, Norwood
- Bergstrom
- Frio, Trinity
- Upland Soils

FLOOD HAZARD ZONE BOUNDARIES

- Intermediate Frequency
- 100 Year Flood
- 1935

The University of Texas Bureau of Economic Geology has mapped flood-prone areas on aerial photographs using geomorphic criteria (Dickerson, 1974) as part of a general program of environmental geological mapping in the Edwards Plateau (Wermund and others, 1974) and adjacent inner coastal plain (Gustavson and Cannon, 1974). Map units were developed by a combination of physiographic, pedological, vegetation, and occasional flood criteria. Flood plains were recognized as relatively high probability flood-prone areas by the occurrence of point bar deposits, scoured channels, and visible evidence of recent flooding. Low terraces were interpreted as low probability flood-prone areas. Generally, such areas have no visible flood evidence but occur at relatively low levels immediately above active flood plains. Higher terrace levels subject only to catastrophic flooding are also mapped. This mapping program has not sought to associate the delineation of flood-prone areas with specific probabilities of occurrence. However, comparisons of Standard Project Flood mapping by the Corps of Engineers and Bureau of Economic Geology mapping of "low-probability flood-prone areas" have shown close agreement along reaches of Salado Creek, San Marcos River, and Blanco River (Morton, 1974). The principal advantage of environmental mapping is that it is relatively rapid and inexpensive. Its benefits are therefore maximized for small communities, subdivisions, resorts, and rural regions that cannot afford the more expensive engineering hydrologic studies used in larger cities (Dickerson, 1974).

A geomorphic approach to flood hazard delineation should include inventories of historical flood marks on the ground surface, aerial photographs of actual flood events, and local interpretations of existing stream gaging data. It should also be a subjective appraisal of all existing

physiographic, botanic, pedologic, occasional flood, and regional hydrologic studies to be done by skilled scientists as a part of a regional environmental inventory. The concept of environmental inventory is especially useful in state-wide planning. The impending development of land-use guidelines by state governments (Brown, 1974) makes it imperative that active flood plain processes be considered with the numerous other inputs that must be brought to the attention of governmental decision makers.

Although the ERTS program achieved considerable success in its mapping of flood inundated areas, relatively little attention was given to preflood hazard studies. The water resources working group of the ERTS investigation team suggested that future studies emphasize mapping of flood plains prior to flooding for zoning purposes (Salomonson, 1973). In this regard, Rango and Salomonson (1974) described the use of ERTS-1 satellite imagery as a tool in mapping flood susceptibility indicators. Many of the geomorphic features used in conventional air photo interpretation of flood hazards (Burgess, 1967) were recognized along the lower Mississippi River flood plain, including the following: upland physiography, watershed characteristics, natural levees, river terraces, backswamp areas, soil and vegetation changes, land-use boundaries, and agricultural development. At a larger scale, the broad range of aerial remote sensing tools (Lee and others, 1972) can be used to supplement initial mapping at 1:250,000 scale on ERTS-1 imagery. Rango and Anderson (1974) tested this approach in the St. Charles County Area, Missouri. An ERTS-1 flood hazard map was constructed from October 2, 1972 imagery and then compared to U. S. G. S. hydraulic-hydrologic maps and to ERTS-1 flood imagery. They found a generally good correlation between ERTS-1 derived maps and products of the U. S. G. S. In the next section,

we will describe the use of orbital imagery for flood hazard mapping in central Texas.

An Illustration of Hydrogeomorphic Flood Hazard Mapping Using Orbital Remote Sensing Imagery

As a test of the hydrogeomorphic method of flood plain mapping, a detailed study was initiated of the Colorado River valley between Austin and La Grange, Texas (Figure 61). The channel forms of the Colorado's valley were mapped from a N. A. S. A. - generated high altitude color aerial infrared (Type S0117) photography (1:116,000 scale). The map (Figure 62) revealed crosscutting relationships for distinct assemblages of channel patterns associated with multiple levels of the Colorado River flood plain. The imagery easily distinguished these channel forms from upland physiography and from modern active channels of the Colorado River.

Resolution of the Skylab S-190B sensor was tested relative to aerial infrared imagery for geomorphic flood hazard mapping (Figure 63). The S-190B map was produced in only 15 minutes. The infrared map, in contrast, required 2 hours for interpretation. The Skylab imagery, although providing less detail, easily distinguished the high and low sinuosity forms recognized by the aircraft imagery as well as the alluvial valley marginal scarps. Man-made features (e.g., Bergstrom A. F. B.) were resolved with nearly equal precision by Skylab and the aerial photography.

Comparison of the mapped channel forms to historic and hydrologic regional flood lines (Figure 64) shows that the low sinuosity channels on the older terraces are flooded by extremely rare, high magnitude events (e.g., the 100-year flood). The distinctive younger bars and channels are flooded

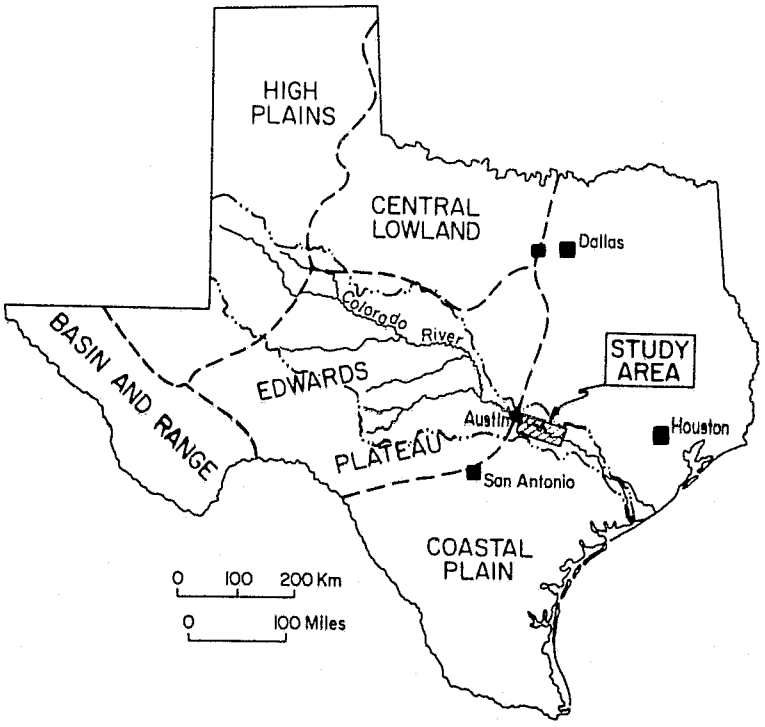

Figure 61. Location of the Colorado River flood hazard mapping project.

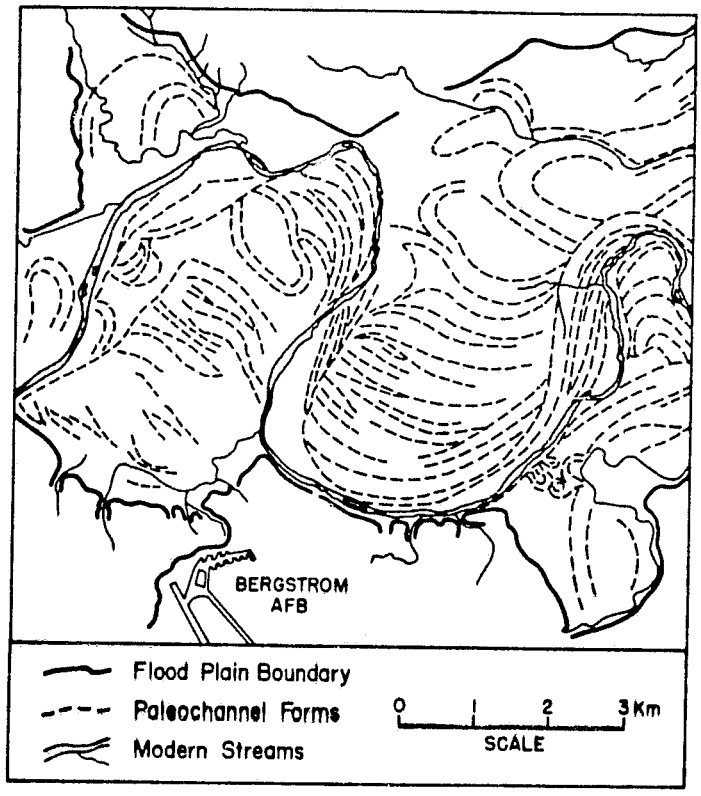

Figure 62. Colorado River flood plain features near Austin, Texas, mapped from high altitude color aerial infrared imagery (Film Type SO-117). Mission was flown by the N. A. S. A. Colorado River-Brazos River Experiment on December 11, 1969, using the RC8/4R sensor.

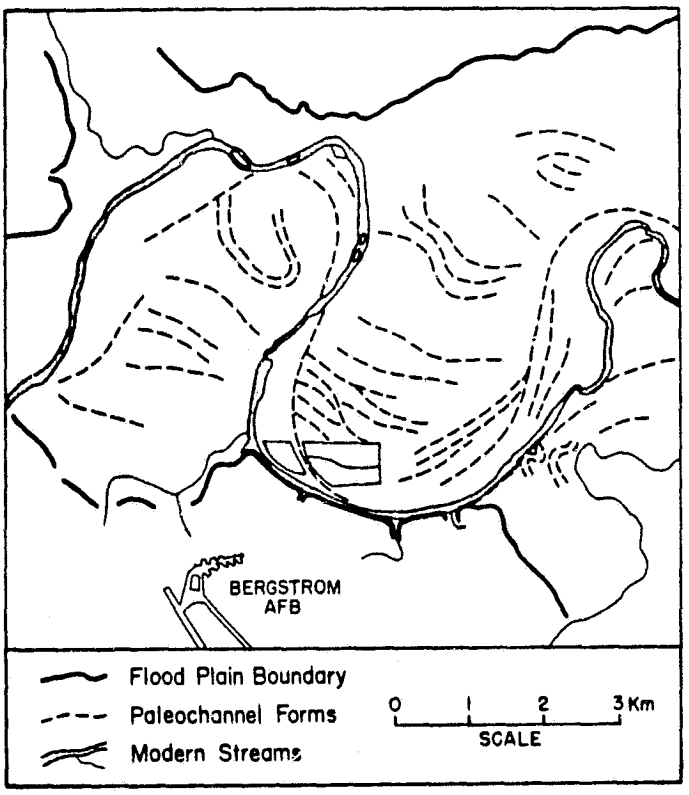

Figure 63, Colorado River flood plain features near Austin, Texas, mapped from Skylab S-190B imagery.

Figure 64. Comparison of geomorphic flood plain features of the Colorado River to regional flood lines from historic and hydrologic surveys (Baker and others, 1973).

with much greater frequency, probably in the 2-15 year recurrence interval range. An upper boundary to flood hazard zone is provided by the scarps bordering the alluvial valley of the Colorado River. Water from the largest historic Colorado River flood reached this margin in 1935.

We conclude that S-190B imagery provides a rapid tool for hydrogeomorphic flood hazard mapping of the type illustrated in Figure 64. The basic flood hazard zones can be distinguished for central Texas rivers, but the precise location of the intermediate frequency hazard zone requires large scale sub-orbital imagery for its interpretation.

In order to establish the precise ground truth for the above analysis, we used stereo pairs of conventional aerial black and white, panchromatic photography at 1:22,000 scale for extremely detailed mapping (Figure 65). Field studies and cross-valley profiles (Figure 66) revealed that the various assemblages are associated with river terrace levels described as "younger non-dissected terraces" in the old descriptive geomorphic literature. Level 6R is a channel cut in bedrock. Levels 6, 6A, and 6B, all occur at the same topographic level, but are composed of alluvium that exhibits at least three distinct channel patterns. Channel 7 includes a complex of highly dissected valley margin surfaces, named the Capitol and Asylum Terraces by the early workers. The valley margin physiography is underlain by deeply weathered stage 7 fluvial gravels. Previous investigators had interpreted these units as ranging in age from mid-Pleistocene to late Tertiary.

Response patterns on the original S-190B image (Figure 67) appear to result from the variation in soil types (Figure 60). Grain size variations were controlled by the changing regimen of the ancient Colorado River (Baker and Penteado, 1975). Figure 68 illustrated the contrast in sediment load

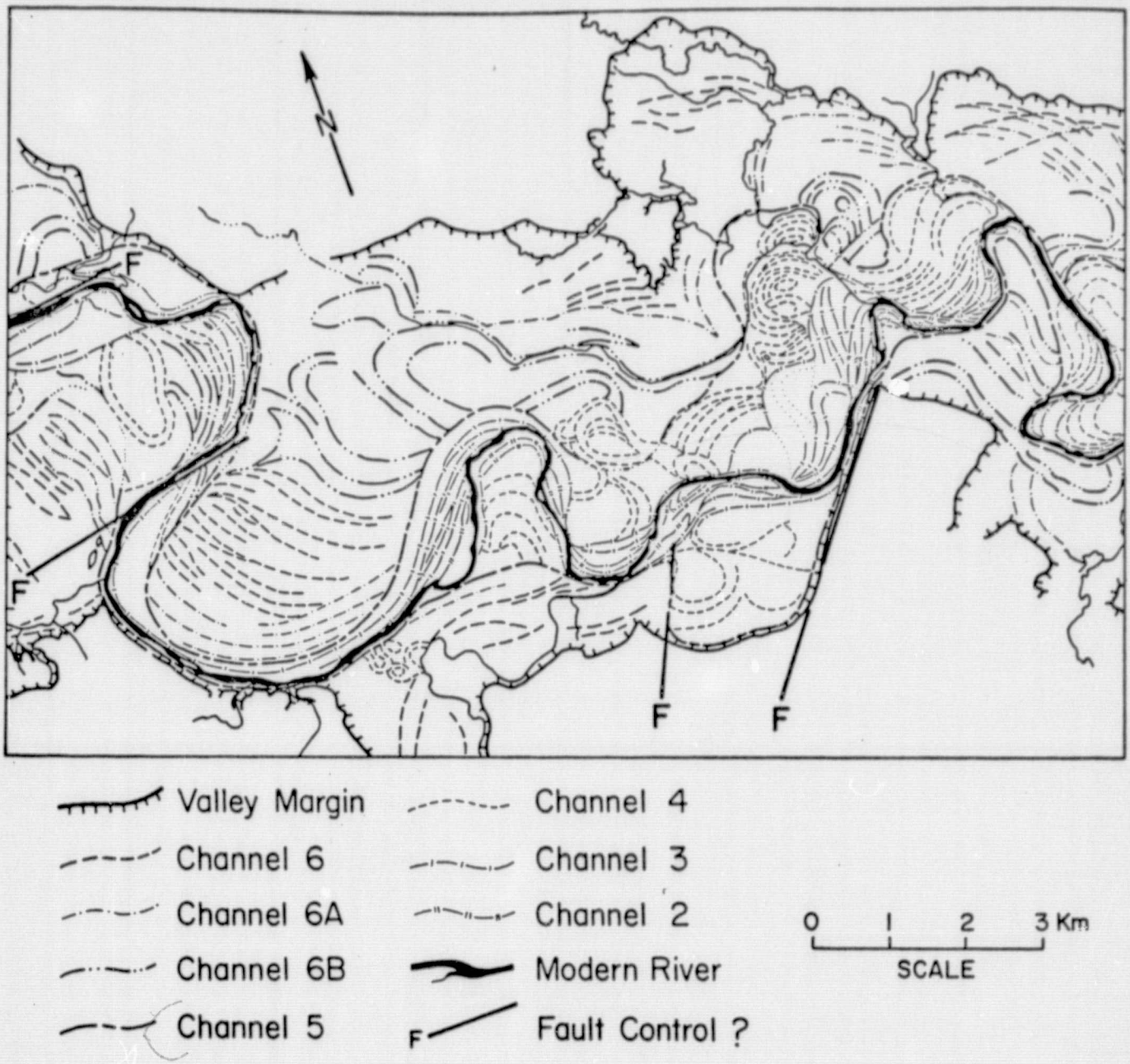

Figure 65. Geomorphic map of Colorado River flood plain and channel morphology between Austin and Bastrop, Texas. Map was constructed by interpretation of stereo pairs of aerial panchromatic, black and white photography flown in April 1969 by the U. S. Air Force. Scale of original photography was approximately 1:22,000. Each channel pattern mapped is associated with specific sediment load characteristics that were established by field sampling.

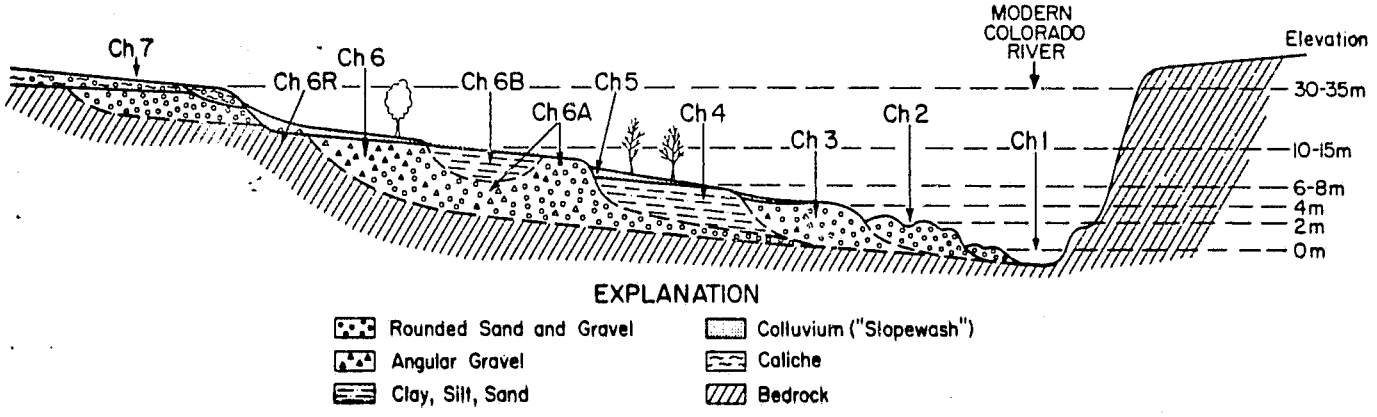

Figure 66. Schematic cross section of the Colorado River near Austin, Texas, showing terrace levels associated with various channel forms.

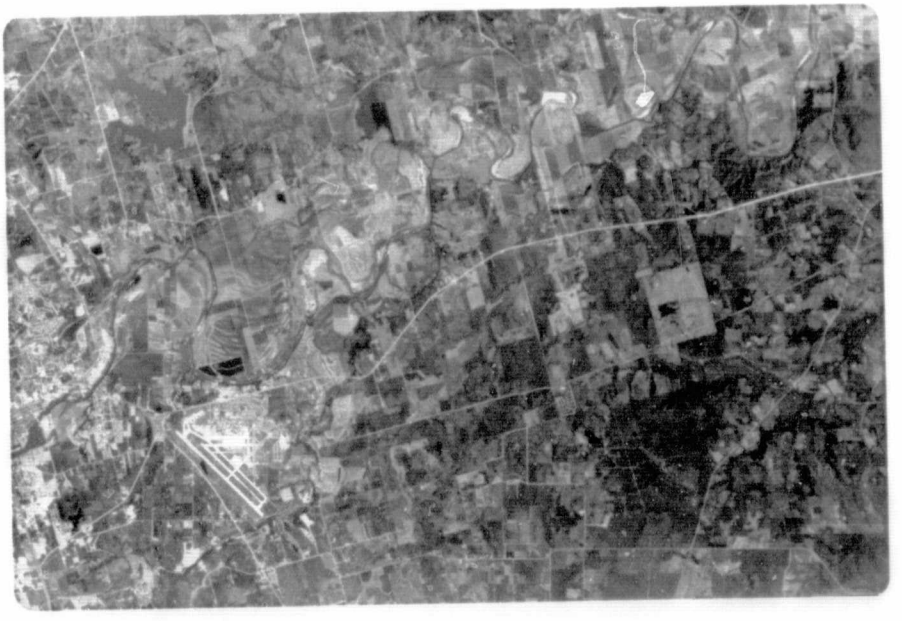

Figure 67. Skylab S-190B image of the Colorado River between Bastrop and Smithville, Texas. Frame covers an area approximately 20 by 12 miles (32 x 19 km).

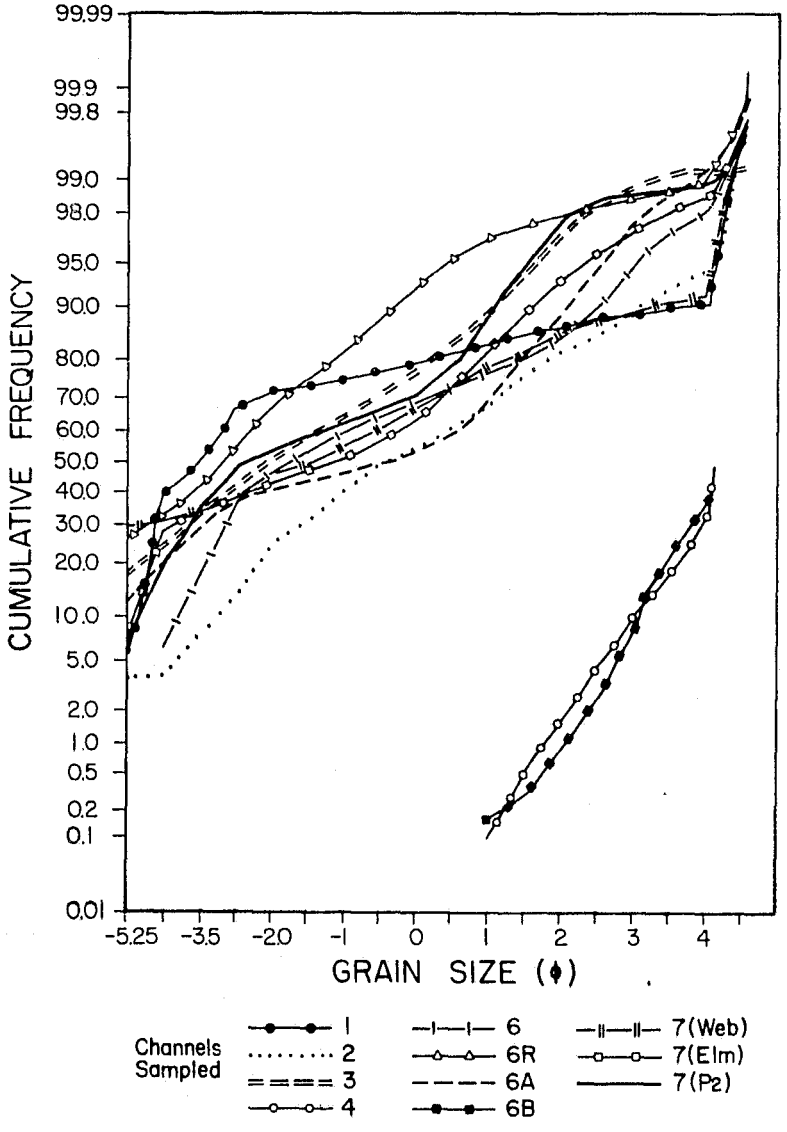

Figure 68. Cumulative frequency curves of grain size for ancient channels of the Colorado River near Austin, Texas (Baker and Penteado, in press). Channel numbers refer to mapping units in Figure 65.

transported by the high sinuosity phases (4 and 6B) and the low sinuosity phases (1, 2, 3, and the channel 6 and 7 complexes). Coarser sediments result in greater permeability, lower soil moisture, and, therefore, a lighter response. Finer sediments result in lower permeability, higher soil moisture retention, and, therefore, a darker response.

Other Hydrogeomorphic Flood Plain Studies Using Remote Sensing Imagery

A striking opportunity for the application of multi-date imagery to a flood event was afforded by the flooding of May 11-12, 1972, near New Braunfels, Texas. Around 8:00 p.m. on May 11, 1972, a series of intense thunderstorms formed southwest of New Braunfels, Texas, and moved northeastward along the Balcones Escarpment. The center of the storm had about 16 inches of rainfall. Reports from local residents indicated that the storm only lasted four hours and spread an average of perhaps eight inches over 300 square miles. Fragmentary evidence of the time distribution of the rainfall indicates that nearly 75 percent fell during the most intense hour, between 8:40 p.m. and 9:40 p.m. on May 11, 1972.

The stream gage on the Comal River recorded much of the storm runoff (Figure 69). Some of the most intense rain fell on the catchment of Blieders Creek, a tributary to the Comal River. Blieders Creek was the closest of the streams contributing runoff from the Balcones Escarpment to the stream gage. The gage recorded the passage of the flood crest from Blieders Creek at 11:45 p.m. on May 11. This represents a lag time of approximately three hours between the centers of mass for the rainfall distribution, and for the flood hydrograph respectively. The crest rose 7.5 feet in 15 minutes,

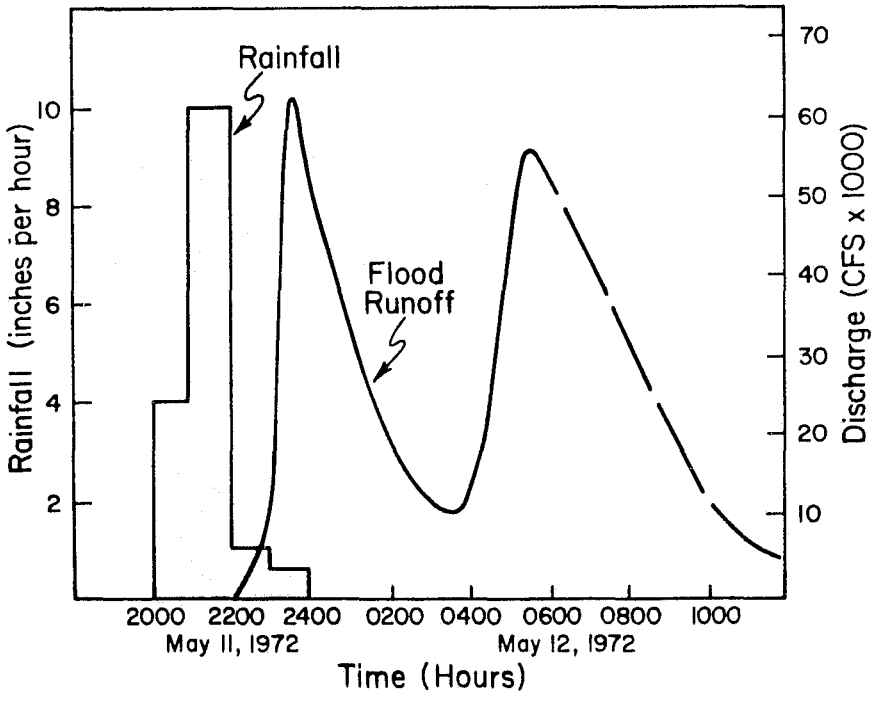

Figure 69. Rainfall and runoff for Comal River at New Braunfels, Texas, flood of May 11-12, 1972. Rainfall distribution assumes that 16 inch recorded maximum was time-distributed according to a unit distribution of storm rainfall recorded at Canyon Dam (Colwick, McGill, and Erichsen, 1973). Runoff was computed by the U. S. Geological Survey from visual observations of water surface elevations at regular time intervals.

and 30 feet in 1 3/4 hours. The second peak on (Figure 69) was caused by runoff that followed the longer flow path along Dry Comal Creek to the stream gage. That crest was delayed until 5:30 a.m. on May 12.

A field study of flood scour and deposition for the 1972 New Braunfels flood has revealed spectacular effects along Blieders Creek. Prior to the thunderstorm cloudburst, the valley floor was mostly covered by an organic soil and turf layer of 6 to 10 inches in thickness that had developed on coarse stream gravels marginal to the low-flow channel. Low brush, scrub oak, and large deciduous trees characterized the channelway (Figure 70A). The estimated peak flood discharge of 48,400 cfs for the 15-square-mile catchment area resulted in widespread devastation to the vegetation and soil cover. The combination of scour, and coarse cobble and boulder deposition, created a bare valley bottom exposing white limestone bedrock and fresh alluvium (Figure 70B). Preflood and postflood channel cross sections show that scour occurred in the deeper portions of the channel, probably at mean flow velocities of 6 - 10 fps. Deposition of gravel berms, similar to those observed by Scott and Gravlee (1968) occurred along the channel margin. Pebble counts revealed that the mean intermediate diameter of the deposited bedload was 1 to 2 inches. Boulders as large as 4 x 4 x 3 feet were transported for short distances by the flood flows.

The Blieders Creek erosion has not been modified by subsequent lower discharges as has been described for the effects of Hurricane Agnes flooding in the humid northeastern United States (Costa, 1974). The morphology of the rock channel of Blieders Creek appears to be adjusted to relatively infrequent, high magnitude controlling discharges. Tinkler (1971) suggested that the morphology of central Texas streams, especially their meander wavelength,

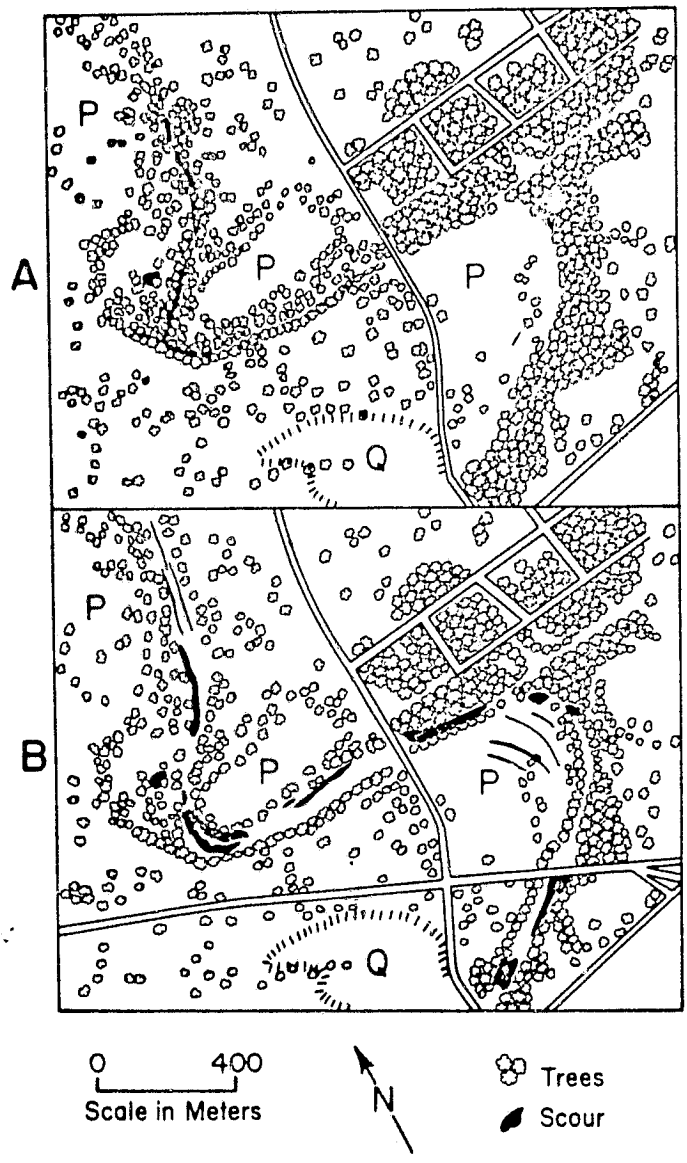

Figure 70, Geomorphic effects of the 1972 flood along Blieders Creek. (A) as mapped from a vertical aerial photograph (U.S.D.A. BQu-2v-161) of Blieders Creek taken in February 1958. The active channel is somewhat obscured by grass and soil. Note the extensive brush and tree vegetation along the stream course. (B) as mapped from a high altitude infrared photograph.

was adjusted to flood discharges that have a recurrence interval between 10 and 50 years. This contrasts to alluvial meanders which are adjusted to much more frequent flows, perhaps wich recurrence intervals between 1 and 3 years (Carlston, 1965; Dury, 1965).

The striking bright response of recently flooded stream bottoms in the New Braunfels area (Figure 71) indicates that many postflood effects remain clearly visible by remote sensing as much as 2 years after a flood event. The coarse, white limestone debris transported by a flood remains as a channel lag and is not appreciably modified by lower discharges. The response of this debris is clear enough to be recognized by orbital imagery (Figure 72).

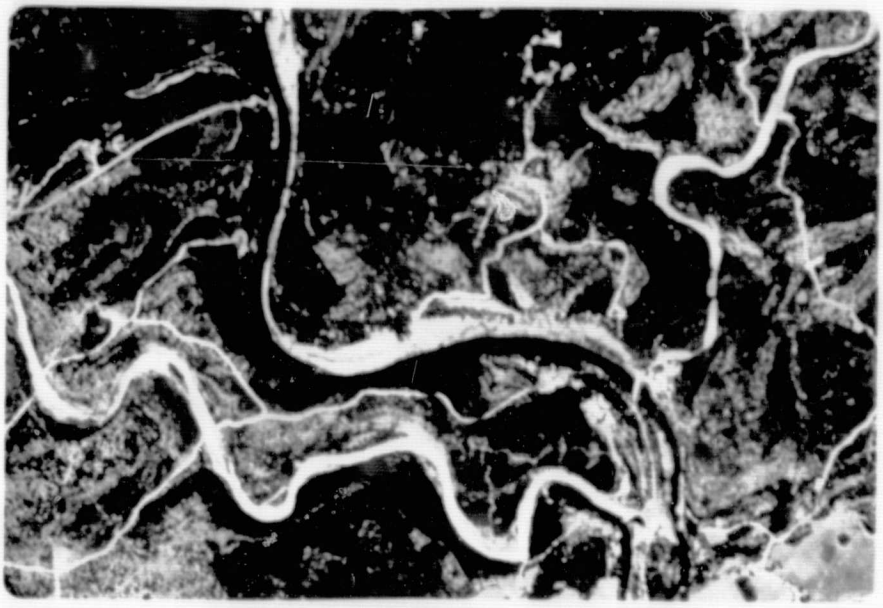

Figure 71. N.A.S.A. infrared aircraft imagery of the Guadalupe River canyon below Canyon Dam and upstream from New Braunfels, Texas. The bright response areas are alluvium and scour in tributary stream valleys resulting from flooding of May 11-12, 1972. Frame depicts a scene 3 x 5 km.

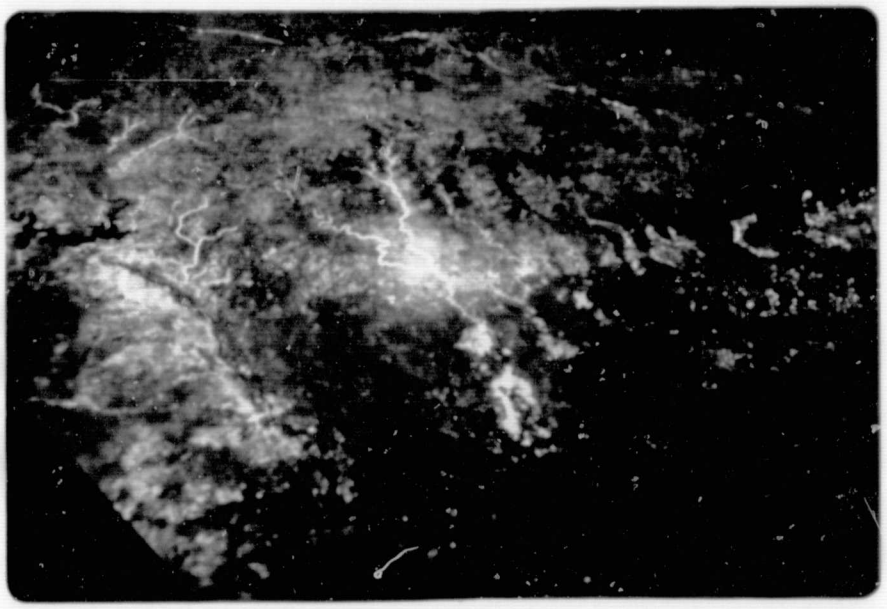

Figure 72. Oblique S-190A photograph of the Balcones Escarpment from Del Rio (left) to San Antonio (right). Bright response of river channels on the Edwards Plateau clearly delineates effects of recent flooding. Frame depicts a scene 200 miles (320 km) across.

COST ASSESSMENT

Previous sections of this report have compared various types of imagery without regard to the economics of surveys by various sensors and platforms. Considerable quantitative information has been presented on the amount of detail that can be resolved by various data formats. However, the economic questions pose many difficulties. Since earth resources surveys are only one by-product of manned orbital platforms, their cost is considerably less than might first be apparent. Moreover, many remote sensing procedures are operating on a high-cost experimental basis. Large-scale continuous monitoring in the future will almost certainly provide several orders of magnitude of more data at a small fraction of present-day costs. For these reasons, the conclusions stated here are tenuous and necessarily subjective.

For the "upstream" flood hazard evaluation problem of drainage network mapping and interpretation of basin characteristics, large-scale suborbital formats have distinct advantages. Expressed as the resolution of first order streams in high relief areas, large-scale stereo pairs resolve 290 percent more detail than topographic maps, which resolve 220 percent more than the best orbital sensors (S-190B). In low relief areas, the disparity in resolution capabilities between orbital and suborbital formats is much less. Thus, an increase in the resolution capabilities of orbital cameras should pay a large dividend for the parametric analysis of drainage basins in areas of high stream density and rugged relief. Even in its present form the S-190B camera is a useful reconaissance tool for areas that (1) lack detailed topographic maps, and (2) are too large for an effective program of suborbital imaging.

An effective philosophy would be to use the synoptic orbital view to focus on local areas of representative terrain types. Detailed suborbital surveys of these areas can then be used to calibrate the orbital imagery by establishing relationships such as that illustrated in Figure 40. This approach would be particularly useful in underdeveloped nations such as in Central and South America and Africa. Terrain factors important in establishing flood hazards there can be quickly evaluated from space in the absence of detailed ground mapping and aerial photography.

Wolman's (1971) evaluation of cost factors for alternative methods of flood plain mapping clearly illustrated the economic advantages small-scale reconaissance surveys for "downstream" flood hazard evaluation. The cost of soils and physiographic approaches to delineating the flood plain can be as little as $1 per mile of channel mapped. In contrast, detailed engineering hydraulic surveys of flood plains cost from $400 to $1,000 per mile of channel mapped. Continuous orbital monitoring even offers certain advantages in this regard. Photographs taken during actual flood events show the detailed extent of inundation without the need for very expensive ground surveys. Moreover, aircraft generation of this information may be severely inhibited by the poor flying weather that often accompanies flood events.

RECOMMENDATIONS

Central Texas is a region of highly variable flood responses that has not yielded to precise evaluation of flood potential by traditional hydrological methods. This paper suggests that a rational model, emphasizing the permanent hydrogeomorphic controls on flood hydrographs, may be a practical alternative. The basis of the approach is the measurement of drainage basin, network, and channel characteristics from various kinds of remote sensing imagery. By the use of machine-assisted measurement and computer processing of data, many of the objections to this hydrogeomorphic approach can be overcome. The most significant hydrogeomorphic controls were found to be drainage density, drainage area, Shreve magnitude, and meander wavelength.

Our study concentrated on the natural geomorphic controls on network and basin properties. Future research should attempt to extend these models to account for man's influence on flood hydrographs in central Texas. A critical factor is land use. Urban hydrological studies (Espey, Morgan, and Masch, 1966) have shown that land use factors alone can increase central Texas peak flood discharges by as much as 300%, all other hydrological factors held constant. Continuous orbital monitoring holds the promise for the most accurate depiction of hydrologically significant land use factors, particularly in areas of rapid change like the Highland Lakes region of central Texas. Other factors which require evaluation in the regional hydrological study include: (1) wavelength of valley and channel meanders; (2) distribution, type and density of vegetation; (3) distribution of exposed bedrock and caliche; (4) estimation of relief; and (5) distribution of roads, fence lines, drainage ditches, and other human disruptions of the

natural drainage geometry.

Schumm (1974a) noted that the relative significance of the large infrequent event versus the small frequent event is one of the crucial questions confronting modern geomorphology, He suggested that the changes induced by major events may be the result of landform instability, The key to resolving the problem appears to be a quantitative definition of thresholds (Schumm, 1974b). In central Texas we have discovered fluvial landform responses, including drainage density, meander wavelength, and flood plain morphology, that are quite distinct from the well-known responses of the rivers in humid regions to relatively frequent flood events (Harvey, 1975). The problem of the frequency of effective discharge requires a world-wide investigation, A solution to the proble is particularly relevant for underdeveloped nations that lack a data base of streamflow records from which to predict extreme hydrologic events. In such areas morphologic-flood process relations offer the only inexpensive means of providing regional flood hazard information. Our study suggests that remote sensing will play a key role in meeting this need in nations that lack large-scale topographic mapping programs.

Orbital satellites offer a powerful potential to aid certain aspects of solving the "map gap" that plagues flood plain management. Specifically, orbital imagery can aid in the following ways: (1) providing a synoptic view of regional floods that have large areal extent, (2) depicting features that indicate flood susceptibility over very large areas, (3) allowing the extension of detailed hydraulic-hydrologic flood plain information from local ground areas into unmapped regions, (4) providing the basic flood hazard information in hydrologically data-sparse, underdeveloped nations, (5) giving multidate, long-term coverage that can be used to develop flood histories

for the rivers of an entire nation, and (6) establishing "upstream" flood-response models.

The true promise of hydrogeomorphic analysis will probably be realized when the output of aircraft and satellite scanning equipment will feed directly into a computer system capable of automatic drainage network recognition and automatic computation of morphometric parameters. This will eliminate the need for operator scanning of imagery, even when assisted by pencil following and digitizing equipment. Before this is feasible, however, we will require considerable manual testing to establish the ground truth for apparent drainage network patterns on the imagery and to evaluate the effects of scale on the hydrological utility of hydrogeomorphic parameters.

SUMMARY OF SIGNIFICANT RESULTS

Central Texas is an example of a high flood-risk area in which certain climatic and hydrologic anomalies complicate the standard hydrologic-engineering approaches to flood-hazard evaluation. The orographic effect of the Balcones Escarpment localizes lift-convective thunderstorms at the topographic rise. Even more spectacular is the effect on the infrequent moisture-laden air mass of tropical origin that moves inland from the Gulf of Mexico. The erratic chance of such high-intensity storm occurrence in central Texas is the major problem for flood prediction. It may be that the average flood experience in this region offers a better basis for establishing predictive hydrologic relations than does the local flood experience at any one location (Benson, 1964). We suggest that the geomorphic character of the local drainage basins, which controls the conversion of storm precipitation to flood flow in stream channels, is the key to evaluating flood potential in this region.

The development of a quantitative hydrogeomorphic approach to flood-hazard evaluation has been hindered by (1) problems of resolution and definition of the morphometric parameters which have hydrologic significance, and (2) mechanical difficulties in creating the necessary volume of data for meaningful analysis. We addressed the first problem by quantitatively comparing the resolution capabilities of (1) small-scale, orbital imagery formats, specifically Skylab, (2) large-scale suborbital imagery, (3) conventional aerial photographs, and (4) topographic maps.

Measures of network resolution such as drainage density and basin Shreve magnitude indicated that large-scale topographic maps (1:24,000) offered greater resolution than small-scale suborbital imagery (1:48,000

and 1:123,000) and orbital imagery. Detailed field surveys of high-relief drainage basins revealed that even networks developed from very large-scale (1:24,000) topographic maps failed to record some second order and many first order streams. Only field surveys and perhaps stereo interpretation of large-scale photography (1:13,000) can resolve vegetation-obscured discontinuous gullies that range from 30 to 100 meters in length.

The disparity in network resolution capabilities between orbital and suborbital imagery formats (including topographic maps) depends on factors such as rock type, vegetation, and land use. However, an overriding factor seems to have been basin relief as measured by the relief ratio. For a given relief ratio drainage network results from Skylab imagery appear to conform proportionately to the topographic map base data. Moreover, in the low relief basins of the inner Coastal Plain, such as Wilbarger Creek orbital network definition is nearly as accurate as topographic map definition.

The remote sensing imagery, especially the high resolution photographs, offered several advantages for measuring data relating to flood potential, including (a) depiction of dynamic drainage basin adjustments to varying hydrologic inputs, (b) evaluation of efficiency of different elements in the network for concentrating flood runoff, and (c) evaluation of vegetation, soil, and land use factors. Although scale is an important factor in extracting stream channels especially from suborbital imagery, it is often less significant than other factors such as sun angle, vegetation, shadow, tone and texture, land use change, pattern and exposures of bedrock, bare alluvium and open water in stream channels. It is sufficient to say that with the exception of photographs generated from space, remote sensing imagery offers the researcher more opportunity for measuring stream networks than do much larger

scale topographic maps. Because of problems of resolution (scale), associated with other variables, imagery generated from space was of lesser value in developing stream networks for small basins.

The problem of morphometric data analysis was approached by developing a computer-assisted method for network analysis. A system of computer programs from Purdue and Toronto Universities was modified for use with a variety of imagery formats and scale. The system allows the rapid identification of network properties which can then be related to measures of flood response.

The most appropriate use of morphometric variables for basin drainage efficiency in flood-response analysis is in a parametric model of peak discharge. Our central Texas model relates peak flood discharge Q_{max}, to Shreve magnitude M_s, and drainage density, Dd as follows:

$$Q_{max} = 5930.3 + 20.7M_s - 616.1Dd.$$

In statistical terms, 86 percent of the variation in maximum discharge was explained by the two variables M_s and Dd.

Additional potential for the use of remote sensing imagery in evaluating flood response exists in the relationship of meander wavelength to a formative discharge. In central Texas, unlike the humid temperate regions studied by others, meander wavelength is related to infrequent flood peak discharges with recurrence intervals of fifty years or greater.

Remote sensing imagery was found to have a broad range of uses in a variety of flood plain mapping approaches. The Skylab S-190B sensor was found to be a useful tool for the rapid generation of geomorphic flood hazard zone maps. Studies of the Colorado River valley near Austin, Texas, easily dis-

tinguished the boundary between upland physiography and active flood plain. In addition, the recognition of paleochannel patterns associated with higher, less active portions of the flood plain allowed a distinction to be made between infrequent (i.e., 100 year recurrence interval), intermediate (10-30 year), and frequent (1-4 year) hazard zones. The significance of the hazard zones was confirmed by field profiles and detailed mapping using aerial infrared imagery and stereopairs of low altitude panchromatic, black and white aerial photography (1:22,000 scale).

N. A. S. A. - generated aerial infrared type 2443 imagery at 1:48,000 scale was found to be useful for botanic, soils, and geomorphic flood hazard mapping both along the deeply entrenched bedrock streams of the Edwards Plateau and for the broad alluvial flood plain of the Colorado River east of the Balcones Fault Zone. These mapping techniques can provide rapid regional evaluation of flood hazards much more quickly than standard engineering-hydraulic approaches. Where a significant economic threat is identified in a local area, the regional remote sensing studies can be supplemented by the time-consuming, but more accurate engineering approaches at cost increase factors that range from 4 to 250 per mile of channel mapped.

REFERENCES CITED

Arbingast, S. A., Kennamer, L. G., and Bonine, M. E., 1973, Atlas of Texas: Bureau of Business Research, The University of Texas at Austin, p. 15.

Atwood, W. W., 1940, The physiographic provinces of North America: New York, Ginn and Company, p. 13.

Baker, V. R., 1974, Geomorphic effects of floods in central Texas and their application in recognizing flood hazards: Geol. Soc. America Abstracts with programs, v. 6, no. 7, p. 640-641.

_____ 1975, Flood hazards along the Balcones Escarpment in central Texas -- alternative approaches to their recognition, mapping and management: Univ. Texas, Bur. Econ. Geology Circular, 40 p.

Baker, V. R., Garner, L. E., Turk, L. J., and Young, K. P., 1973, Urban flooding and slope stability, Austin, Texas: Austin Geological Society Field Trip Guidebook, 31 p.

Baker, V. R., Holz, R. K., and Hulke, S. D., 1974, A hydrogeomorphic approach to evaluating flood potential in central Texas from orbital and suborbital remote sensing imagery: Proc. Ninth Int. Symp. on Remote Sensing of the Environment, Ann Arbor, Michigan, v. 1, p. 629-646.

Baker, V. R., and Penteado, M. M., 1975, River adjustment to late Quaternary hydrologic regimen changes in central Texas: Geol. Soc. America Abstracts with Programs, v. 7, no. 2, p. 144.

Baker, V. R. and Penteado, M. M., in press, Sedimentology and paleohydrology of Quaternary fluvial regime changes, Colorado River, central Texas: Ninth International Congress of Sedimentology, Nice, France, July, 1975.

Beatty, C. B., 1974, Debris flows, alluvial fans, and a revitalized catastrophism: Zeit. Geomorph., Suppl. Bd. 21, p. 39-51.

Benson, M. A., 1962, Factors influencing the occurrence of floods in a humid region of diverse terrain: U. S. Geol. Survey Water Supply Paper 1580-B, 64 p.

Blair, W. F., 1950, Biotic provinces of Texas: Texas Jour. Sci., v. 2, p. 93-117.

Blyth, K., and Rodda, J. C., 1973, A stream length study: Water Resources Research, v. 9, no. 5, p. 1454-1461.

Bodhaine, G. L., and Robinson, W. H., 1952, Floods in western Washington, frequency and magnitude in relation to drainage basin characteristics: U. S. Geol. Survey Circular 191, 124 p.

Breeding, S. D., and Montgomery, J. H., 1954, Floods of September 1952 in the Colorado and Guadalupe River basins, central Texas: U. S. Geol. Survey Water-Supply Paper 1260-A, 47 p.

Brown, L. F., Jr., 1974, Environmental inventory: innovation in geology and geologic presentation, in Wermund, E. G., ed., Approaches to environmental geology: Univ. Texas, Austin, Bur. Econ. Geology Rept. Inv. 81, p. 3-11.

Burgess, L. C. N., 1967, Airphoto interpretation as an aid in flood susceptibility determination, in International conference on water for peace: Washington, D. C., U. S. Government Printing Office, p. 867-881.

Burkham, D. E., 1966, Hydrology of Cornfield Wash area and effects of land-treatment practices, Sandoval County, New Mexico, 1951-60: U. S. Geol. Survey Water-Supply Paper 1831, 87 p.

Cain, J. M., and Beatty, M. T., 1968, The use of soil maps in the delineation of flood plains: Water Resources Research, v. 4, p. 173-182.

Carlston, C. W., 1963, Drainage density and streamflow: U. S. Geol. Survey Prof. Paper 422-C, 8 p.

_____ 1965, The relation of free meander geometry to stream discharge and its geomorphic implications: Amer. Jour. Sci., v. 263, p. 864-865.

Carr, J. T., Jr., 1967, The climate and physiography of Texas: Texas Water Dev. Board Rept. 53, 27 p.

Chorley, R. J., 1957, Climate and morphometry: Jour. Geology, v. 65, p. 628-668.

Chorley, R. J., and Morgan, M. A., 1962, Comparison of morphometric features, Unaka Mountains, Tennessee and North Carolina, and Dartmoor England: Geol. Soc. Am. Bull., v. 73, p. 17-34.

Clark, M. M., 1971, Comparison of SLAR images and small-scale, low-sun aerial photographs: Geol. Soc. America Bull., v. 82, p. 1735-1742.

Coates, D. R., 1971, Hydrogeomorphology of Susquehanna and Delaware basins, in Morisawa, Marie, ed., Quantitative geomorphology: Proc. Second Annual Geomorphology Symposium Series, Binghamton, N. Y., Publications in Geomorphology, Binghamton, N. Y., p. 272-306.

Coffman, D. M., 1971, Parameter measurement in fluvial morphology: Indiana Acad. Sci. Proc., v. 79, p. 333-344.

Coffman, D. M., Turner, A. K., and Melhorn, W. N., 1971, The W.A.T.E.R. system: Computer programs for stream network analysis: Purdue Univ. Water Resources Research Center Tech. Rept. 16, 138 p.

Colwick, A. B., McGill, H. H., and Erichsen, F. P., 1973, Severe floods at New Braunfels, Texas: American Soc. Agricultural Engineers Paper

No. 73-206, 8 p.

Costa, J. E., 1974, Response and recovery of a piedmont watershed from tropical storm Agnes, June 1972: Water Resources Research, v. 10, p. 106-112.

Deussen, Alexander, 1924, Geology of the coastal plain of Texas west of the Brazos River: U. S. Geol. Survey Prof. Paper 126, 139 p.

Deutsch, Morris, and Ruggles, Fred, 1974, Optical data processing and projected applications of the ERTS-1 imagery covering the 1973 Mississippi River valley floods: Water Resources Bull., v. 10, p. 1023-1039.

DeWiest, R. J. M., 1965, Geohydrology: New York, John Wiley and Sons, 366 p.

Dickerson, E. J., 1974, Environmental geologic mapping of flood-prone areas: an alternative to engineering methods, in Wermund, E. G., ed., Approaches to environmental geology: Univ. Texas, Austin, Bur. Econ. Geology Rept. Inv. 81, p. 220-228.

Dorroh, J. A., Jr., 1946, Certain hydrologic and climatic characteristics of the southwest: Publications in Engineering, Albuquerque, New Mexico Univ. Press, 64 p.

Draper, N. R., and Smith, H., 1966, Applied regression analysis: New York, John Wiley and Sons, 407 p.

Dury, G. H., 1964, Principles of underfit streams: U. S. Geol. Survey Prof. Paper 452-A, 67 p.

_____ 1965, Theoretical implications of underfit streams: U. S. Geol. Survey Prof. Paper 452-C, 43 p.

Eyles, R. J., 1966, Stream representation on Malayan maps: Jour. Tropical Geog., v. 22, p. 1-9.

Fisk, H. N., 1944, Geological investigations of the alluvial valley of the lower Mississippi River: Vicksburg, U. S. Army Corps of Engineers, 78 p.

Giusti, E. V., and Schneider, W. J., 1962, Comparison of drainage on topographic maps of the Peidmont province: U. S. Geol. Survey Prof. Paper 450-E, p. E118-E119.

Gregory, K. J., and Walling, D. E., 1973, Drainage basin form and process, a geomorphological approach: London, Edward Arnold, 456 p.

Grevelius, H., 1914, Flusskunde: Berlin, Goschen'sche Verlagshandlung, 176 p.

Gustavson, T. C., and Cannon, P. J., 1974, Preliminary environmental geologic mapping of the inner coastal plain, southwest Texas, in Wermund, E. G., ed., Approaches to environmental geology: Univ. Texas, Austin, Bur. Econ. Geology Rept. Inv. 81, p. 79-100.

Hack, J. T., 1957, Studies of longitudinal stream profiles in Virginia and Maryland: U. S. Geol. Survey Prof. Paper 294-B, p. 45-97.

Hadley, R. F., and Schumm, S. A., 1961, Hydrology of the upper Cheyenne River basin: U. S. Geol. Survey Water-Supply Paper 1531-B, p. 186-198.

Heerdegen, R. G., 1974, The unit hydrograph: a satisfactory model of watershed response: Water Resources Bull., v. 10, p. 1143-1161.

Holz, R. K., and Boyer, R. E., 1972, Patterns from Apollo VI photos: Photogrammetric Eng., v. 38, p. 974-984.

Horton, R. E., 1932, Drainage basin characteristics: Trans. Am. Geophys. Union, v. 13, p. 350-361.

_____ 1945, Erosional development of streams and their drainage basins: hydrophysical approach to quantitative morphology: Geol.

Soc. Am. Bull., v. 56, p. 275-370.

Hoyt, W. G., and Langbein, W. B., 1955, Floods: Princeton, Princeton Univ. Press, 469 p.

Hunt, C. B., 1967, Physiography of the United States: San Francisco, W. H. Freeman and Company, p. 8.

Jahns, R. H., 1947, Geologic features of the Connecticut Valley, Massachusetts, as related to recent floods: U. S. Geol. Survey Water-Supply Paper 996, 158 p.

Jennings, A. H., 1950, World's greatest observed point rainfalls: Monthly Weather Review, v. 78, p. 4-5.

Kilpatrick, F. A., and Barnes, H. H., 1964, Channel geometry of Piedmont streams as related to frequency of floods: U. S. Geol. Survey Prof. Paper 422-E, 10 p.

Langbein, W. B., 1947, Topographic characteristics of drainage basins: U. S. Geol. Survey Water-Supply Paper 968-C, p. 125-157.

Lee, G. B., Parker, O. E., and Milfred, C. J., 1972, Development of new techniques for delineation of flood plain hazard zones: Water Resources Center, Univ. of Wisconsin, Madison, 15 p.

Leopold, L. B., and Langbein, W. B., 1963, Association and indeterminancy in geomorphology, in Albritton, C. C., Jr., ed., The fabric of geology: Stanford, Calif., Freeman, Cooper, and Company, p. 184-192:

Leopold, L. B., and Maddock, T., 1953, The hydraulic geometry of stream channels and some physiographic implications: U. S. Geol. Survey Prof. Paper 252, 57 p.

Leopold, L. B., and Miller, J. P., 1956, Ephemeral streams -- hydraulic factors and their relation to the drainage net: U. S. Geol. Survey

Prof. Paper 282-A, 37 p.

Leopold, L. B., Wolman, M. G., and Miller, J. P., 1964, Fluvial processes in geomorphology: San Francisco, Freeman, 504 p.

Leuder, D. R., 1959, Aerial photographic interpretations: New York, McGraw-Hill Book Company, Inc., 462 p.

Lewin, J., 1970, A note on stream ordering: Area, v. 2, p. 32-35.

Linsley, R. K., Kohler, M. A., and Paulhus, J. L., 1958, Hydrology for Engineers: New York, McGraw-Hill Book Company, 340 p.

Lott, G. A., 1952, Rainstorm of September 9-10, 1952: Monthly Weather Review, v. 80, p. 161-163.

Lyon , R. J. P., Mercado, J., and Campbell, R., Jr., 1970, Pseudo radar: Photogrammetric Eng., v. 36, p. 1257-1261.

Maxwell, J. C., 1960, Quantitative geomorphology of the San Dimas Experimental Forest, California: Tech. Report no. 19, Office of Naval Research, Project NR 389-042, Dept. of Geology, Columbia Univ., New York.

McCoy, R. M., 1969, Drainage networks with K-band radar imagery: Geog. Rev., v. 59, p. 493-512.

_____ 1971, Rapid measurement of drainage density: Geol. Soc. America Bull., v. 82, p. 757-762.

Meier, W. L., Jr., 1964, Analysis of unit hydrographs for small watersheds in Texas: Texas Water Commission Bull. 6414, 58 p.

Melton, M. A., 1957, An analysis of the relations among elements of climate, surface properties, and geomorphology: Tech. Report no. 11, Office of Naval Research, Project NR 389-042, Dept. of Geology, Columbia Univ., New York.

_____ 1958, Correlation structure of morphometric properties of drainage systems and their controlling agents: Jour. Geology, v. 66, p. 442-460.

_____ 1959, A derivation of Strahler's channel-ordering system: Jour. Geology, v. 67, p. 345-346.

Miller, V. C., 1954, A quantitative geomorphic study of drainage basin characteristics in the Clinch Mountain area, Virginia, Tennessee: Tech. Report no. 3, Office of Naval Research, Project NR 271-30, Dept. of Geology, Columbia Univ., New York, 30 p.

Morgan, C. W., 1966, Characteristic meteorology of some large flood-producing storms in Texas - thunderstorms: Texas Water Dev. Board Rept. 33, p. 31-43.

Morisawa, M. E., 1957, Accuracy of determination of stream lengths from topographic maps: Trans. Am. Geophys. Union, v. 33, p. 86-88.

_____ 1959, Relation of quantitative geomorphology to stream flow in representative watersheds of the Appalachian Plateau Province: Columbia Univ. Dept. Geol., Tech. Rept. 20, 94 p.

_____ 1962, Quantitative geomorphology of some watersheds in the Appalachian Plateau: Geol. Soc. America Bull., v. 73, p. 1025-1046.

Morton, R. A., 1974, Delineation and environmental application of active processes mapped in recharge area of the Edwards aquifer, in Wermund, E. G., ed., Approaches to environmental geology: Univ. Texas, Austin, Bur. Econ. Geology Rept. Inv. 81, p. 204-219.

Orton, Robert, 1966, Characteristic meteorology of some large flood-producing storms in Texas - easterly waves: Texas Water Dev. Board Rept. 33,

p. 1-18.

Patton, P. C., and Baker, V. R., 1975, Low frequency high magnitude floods and their relation to the morphology of streams in central Texas: Geol. Soc. Am., Abstracts with programs, 1975 south-central meeting, p. 224-225.

Paulhus, J. L. H., 1965, Indian Ocean and Taiwan set new records: Monthly Weather Review, v. 93, p. 331-335.

Rango, Albert, and Salomonson, V. V., 1974, Regional flood mapping from space: Water Resources Research, v. 10, p. 473-484.

Reckendorf, F. F., 1973, Techniques for identifying flood plains in Oregon: Oregon State Univ., Ph.D. thesis (unpub.), 344 p.

Rodda, J. C., 1967, The significance of characteristics of basin rainfall and morphometry in a study of floods in the United Kingdom: UNESCO Studies and Reports in Hydrology, no. 3, p. 834-843.

_____ 1969, The flood hydrograph, in Chorley, R. J., ed., Water, earth, and man: London, Methuen and Company, p. 405-418.

Ruhe, R. V., 1971, Stream regimen and man's manipulation, in Coates, D. R., ed., Environmental geomorphology: Publications in Geomorphology, State Univ. of New York, Binghamton, p. 9-23.

Salomonson, V. V., 1973, Water resources, in Freden, S. C., and Mercanti, E. P., eds., Symposium on significant results obtained from ERTS-1: NASA Goddard Space Flight Center, Green Belt, Maryland, Report X-650-73-155, p. 57-69.

Scheidegger, A. E., 1965, The algebra of stream-order numbers: U. S. Geol. Survey Prof. Paper 525-B, p. B187-B189.

_____ 1966, Stochastic branching processes and the law of stream orders: Water Resources Research, v. 2, p. 199-203.

_____ 1967, On the topology of river nets: Water Resources Research, v. 3, p. 103-106.

Schick, A. P., 1974, Formation and obliteration of desert stream terraces - a conceptual analysis: Zeit. Geomorph., Suppl. Bd. 21, p. 88-105.

Schumm, S. A., 1956, Evolution of drainage systems and slopes in badlands at Perth Amboy, N. J.: Geol. Soc. America Bull., v. 67, p. 597-646.

Scott, K. M., and Gravlee, G. C., Jr., 1968, Flood surge on the Rubicon River, California -- hydrology, hydraulics and boulder transport: U. S. Geol. Survey Prof. Paper 422-M, 38 p.

Selby, M. J., 1968, Morphometry of drainage basins in areas of pumice lithology: Proc. fifth New Zealand Geog. Conference, New Zealand Geog. Soc., p. 169-174.

Snedecor, G. W., and Cochran, W. G., 1972, Statistical methods: Ames, Iowa, The Iowa State Univ. Press, 593 p.

Sherman, L. K., 1932, The relation of hydrographs of runoff to size and character of drainage basins: Trans. Am. Geophys. Union, v. 13, p. 332-339.

Shreve, R. L., 1966, Statistical law of stream numbers: Jour. Geology, v. 74, p. 17-37.

_____ 1967, Infinite topologically random channel networks: Jour. Geology, v. 75, p. 178-186.

_____ 1969, Stream lengths and basin areas in topologically random channel networks: Jour. Geology, v. 77, p. 397-414.

L-3

Simmonett, D. S., and Henderson, F. M., 1969, On the use of space photography for identifying transportation routes: a summary of problems: Proc. Sixth Intern. Symp. on Remote Sensing of Environ., Ann Arbor, Michigan.

Slaymaker, H. O., 1966, Morphometric analysis of maps: British Geomorphological Research Group, Paper 4.

Smart, J. S., 1969, Topological properties of channel networks: Geol. Soc. America Bull., v. 80, p. 1757-1774.

_____ 1972, Quantitative characterization of channel network structure: Water Resources Research v. 8, p. 1487-1505.

Stall, J. B., and Fok, Y. S., 1967, Discharge as related to stream system morphology: Symposium on River Morphology, Bern; Int. Assoc. Sci. Hyd., p. 224-235.

Stall, J. B., and Yang, C. T., 1970, Hydraulic geometry of 12 selected stream systems of the United States: Univ. of Illinois Water Resources Research Rept. 32, 73 p.

Strahler, A. N., 1952, Dynamic basis of geomorphology: Geol. Soc. America Bull., v. 63, p. 923-938.

_____ 1957, Quantitative analysis of watershed geomorphology: Trans. Am. Geophys. Union, v. 38, p. 913-920.

_____ 1958, Dimensional analysis applied to fluvially eroded landforms: Geol. Soc. America Bull., v. 69, p. 279-300.

_____ 1964, Quantitative geomorphology of drainage basins and channel networks, in Chow, V. T., ed., Handbook of applied hydrology, sec. 4-II: New York, McGraw-Hill Book Company, p. 39-76.

_____ 1965, Physical geography: New York, John Wiley and Sons, p. 192.

Tharp, B. J., 1926, Structure of Texas vegetation east of the 98th meridian: Univ. Texas, Austin, Bull. 2606, 97 p.

Thomas, D. M., and Benson, M. A., 1970, Generalization of stream-flow characteristics from drainage-basin characteristics: U. S. Geol. Survey Water-Supply Paper 1975, 55 p.

Thornbury, W. D., 1965, Geomorphology of the United States: New York, John Wiley and Sons, p. 63.

Tinkler, K. J., 1971, Active valley meanders in south-central Texas and their wider implications: Geol. Soc. America Bull., v. 82, p. 1783-1800.

Trainer, F. W., 1969, Drainage density as an indicator of base-flow in part of the Potomac River: U. S. Geol. Survey Prof. Paper 650-C, p. C177-C-183.

U. S. Army Corps of Engineers, 1964, Survey report on Edwards underground reservoir, Guadalupe, San Antonio, and Nueces Rivers and tributaries, Texas: Fort Worth, Texas District, U. S. Army Corps of Engineers, 3 volume rept.

U. S. Soil Conservation Service, 1954, Special storm report, storm of June 26-28, 1954, Johnson Creek Watershed, tributary to the Devils River, Texas: Temple, Texas, Soil Conservation Service, 10 p.

_____ 1958, Supplement to work plan for watershed protection and flood prevention, Sulfur Creek Watershed, Burnet and Lampasas Counties, Texas: Fort Worth, Texas, Soil Conservation Service, 27 p.

Weeks, A. W., 1945, Balcones, Luling, and Mexia fault zones in Texas: Am. Assoc. Petroleum Geologists Bull., v. 29, p. 1733-1737.

Werchan, L. E., Lowther, A. C., and Ramsey, R. N., 1974, Soil survey of Travis County, Texas: U. S. Dept. Agriculture, Soil Conservation

Service, 123 p.

Wermund, E. G., Cannon, P. J., Deal, D. W., Morton, R. A., and Woodruff, C. M., Jr., 1974, A test of environmental geologic mapping, southern Edwards Plateau, southwest Texas: Geol. Soc. America Bull., v. 85, p. 423-432.

White, G. F., 1964, Choice of adjustment to floods: Univ. Chicago, Dept. Geography Research Paper 93, 150 p.

Wiitala, S. W., Jetter, K. R., and Sommerville, A. J., 1961, Hydraulic and hydrologic aspects of flood-plain planning: U. S. Geol. Survey Water-Supply Paper 1526, 69 p.

Williams, B. F., and Lowry, R. L., Jr., 1929, A study of rainfall in Texas: Texas State Reclamation Dept., Bull. No. 18, 170 p.

Wolman, M. G., 1971, Evaluating alternative techniques of flood plain mapping: Water Resources Research, v. 7, no. 6, p. 1383-1392.

Woodyer, K. D., 1968, Bankfull frequency in rivers: Jour. Hydrology, v. 6, p. 114-142.

Wu, I. P. and others, 1964, Determination of peak discharge and design hydrographs for small watersheds in Indiana: Indiana Highway Research, Rept. 7, 124 p.